

FLAVOR CHANGING NEUTRAL CURRENT PROCESSES IN THE
FRAMEWORK OF THE TWO HIGGS DOUBLET MODEL

A THESIS SUBMITTED TO
THE GRADUATE SCHOOL OF NATURAL AND APPLIED SCIENCES
OF
THE MIDDLE EAST TECHNICAL UNIVERSITY

BY

İSMAİL TURAN

IN PARTIAL FULFILLMENT OF THE REQUIREMENTS FOR THE DEGREE OF

DOCTOR OF PHILOSOPHY

IN

THE DEPARTMENT OF PHYSICS

AUGUST 2003

Approval of the Graduate School of Natural and Applied Sciences.

Prof. Dr. Canan Özgen
Director

I certify that this thesis satisfies all the requirements as a thesis for the degree of Doctor of Philosophy.

Prof. Dr. Sinan Bilikmen
Head of Department

This is to certify that we have read this thesis and that in our opinion it is fully adequate, in scope and quality, as a thesis for the degree of Doctor of Philosophy.

Prof. Dr. Erhan Onur İltan
Supervisor

Examining Committee Members

Prof. Dr. Erhan Onur İltan

Prof. Dr. Tahmasib M. Aliyev

Prof. Dr. Hüseyin Koru

Prof. Dr. Mustafa Savcı

Assoc. Prof. Dr. Sibel Baykal

ABSTRACT

FLAVOR CHANGING NEUTRAL CURRENT PROCESSES IN THE FRAMEWORK OF THE TWO HIGGS DOUBLET MODEL

TURAN, İsmail

Ph.D., Department of Physics

Supervisor: Prof. Dr. Erhan Onur İltan

August 2003, 113 pages.

It is widely believed that the Standard Model (SM) can not be a fundamental theory of the basic interactions. Originated from this fact, many *new physics* models have been proposed. Among them, the two Higgs doublet model (2HDM), the SM enlarged by adding one extra scalar doublet, is considered as the simplest extension of the SM.

In this work, within the framework of the model III version of the 2HDM, the exclusive decay $B \rightarrow K^* \tau^+ \tau^-$ including the neutral Higgs boson effects is investigated by focusing on the physical parameters, such as the CP violating asymmetry, the forward–backward asymmetry of the lepton pair, and the CP asymmetry in the forward–backward asymmetry. Furthermore, the dependencies of these quantities on the parameters of the model considered are analyzed.

Next, in the same model context, lepton flavor violating Z decay, $Z \rightarrow l_1^- l_2^+$ ($l_1, l_2 = e, \mu, \tau$), is studied. The motivation for this decay mode comes from the fact that the predicted branching ratio in the SM, with even massive neutrinos is very far from experimental verification. Thus this decay is a good candidate for searching *new physics* effects. For this decay the branching ratio is calculated

and discussed in various physical regions determined by model parameters. It is observed that it is possible to reach present experimental upper limits in model III.

Finally, the flavor changing top quark decay, $t \rightarrow cl_1^- l_2^+ (l_1, l_2 = e, \mu, \tau)$, is investigated in model III. The branching ratio is computed and the limits of the branching ratio of each decay modes are separately discussed regarding sensitivity of the model parameters.

Keywords: Two Higgs doublet model, Flavor Changing Neutral Current, Lepton Flavor Violation, Decay Rate, CP Asymmetry, Dimensional Regularization.

ÖZ

İKİ HİGGS DUBLET MODELİ ÇERÇEVESİNDE ÇEŞNİ DEĞİŞTİREN NÖTR AKIM BOZUNMALARI

TURAN, İsmail

Doktora, Fizik Bölümü

Tez Yöneticisi: Prof. Dr. Erhan Onur İltan

Agustos 2003, 113 sayfa.

Standart Model'in (SM) basit etkileşimlerin temel teorisi olamayacağına yaygın olarak inanılmaktadır. Bu gerçekten yola çıkarak, birçok *yeni fizik* modelleri önerilegeldi. Bunlar arasında, SM'e yeni bir skaler dublet eklenmesiyle büyütülmüşü olan iki Higgs dublet modeli (2HDM) SM'in genişletilmiş en basit şekli kabul ediliyor.

Bu çalışmada, 2HDM'in model III versiyonu çerçevesinde, nötr Higgs bozon etkilerini içeren $B \rightarrow K^* \tau^+ \tau^-$ bozunumu, CP bozulum asimetrisi, lepton çiftinin ileri-geri asimetrisi, ve ileri-geri asimetride CP bozulumu gibi fiziksel parametrelere odaklanarak araştırıldı. Ek olarak bu büyüklüklerin ele alınan modelin parametrelerine bağımlılıkları incelendi.

Bundan sonra, aynı model çerçevesinde, lepton çeşni bozan Z bozunumu, $Z \rightarrow l_1^- l_2^+$ ($l_1, l_2 = e, \mu, \tau$), çalışıldı. Bu bozunum modu için motivasyon, kütleli nötrinoların olduğu SM'de bile, öngörülen dallanma oranının deneysel doğrulamadan çok uzak olmasıdır. Dolayısıyla $Z \rightarrow l_1^- l_2^+$ yeni fizik etkilerini araştırmak için uygun bir bozunumdur. Bu bozunum için dallanma oranı hesaplandı ve model parametreleri tarafından belirlenen fiziksel bölgede tartışıldı. Model III çerçevesinde

günümüz deneysel limitlerine ulaşmanın mümkün olduğu gözlemlendi.

Son olarak, lepton çeşni bozan top kuvarik bozunumu, $t \rightarrow c l_1^- l_2^+ (l_1, l_2 = e, \mu, \tau)$ model III çerçevesinde çalışıldı. Dallanma oranı heaplanarak, herbir bozunum modunun dallanma oranı sınırlarının model parametrelerine hassasiyeti tartışıldı.

Anahtar Sözcükler: İki Higgs Dublet Modeli, Çeşni Değiştiren Nötr Akımlar, Lepton Çeşni İhlali, Bozunum Genliği, CP Asimetrisi, Boyutsal Düzenleme.

...TO MY FAMILY

ACKNOWLEDGMENTS

It is with great pleasure that I thank Prof. Dr. E. O. İltan very much not only for giving me the privilege of undertaking research in particle physics but also for his continuous guidance and morale throughout my graduate study. I have learned much physics from him.

I am very grateful to Prof. Dr. T. M. Aliyev who made for many inspiring discussions and technical advises during my studies. I owe special thanks to Prof. Dr. M. Savcı for reading this manuscript carefully.

I am thankful to all of my best friends, especially B. Özgür Sarıoğlu, Hakan Cebeci, Barış Akaoglu, İsmet Yurduşen and his wife, Sema Yurduşen, for their warm friendships and continuous morale supports. I am also thankful to my family for constant support and trust in me.

Lastly, I am more than grateful to Ayşe Seyhan who has brought unconditional grace, love and beauty into my life and her presence has been one of my great blessings. Without his immense love this accomplishment would have never been fulfilled.

TABLE OF CONTENTS

ABSTRACT		iii
ÖZ		v
DEDICATION		vii
ACKNOWLEDGMENTS		viii
TABLE OF CONTENTS		ix
LIST OF TABLES		x
LIST OF FIGURES		xi
CHAPTER		
1	INTRODUCTION	1
2	THE GENERAL TWO HIGGS DOUBLET MODEL (2HDM)	4
2.1	The Standard Model (SM)	4
2.2	Two Higgs Doublet Model (2HDM)	9
2.2.1	Motivation for Additional Scalars	9
2.2.2	The Yukawa Lagrangian and the Scalar Potential in 2HDM	11
3	$B \rightarrow K^* \tau^+ \tau^-$ DECAY IN THE GENERAL TWO HIGGS DOUBLET MODEL INCLUDING THE NEUTRAL HIGGS BOSON EFFECTS	16
3.1	Rare $B \rightarrow K^* \tau^+ \tau^-$ Decay Including the NHB Effects	19
3.2	Numerical Analysis and Discussion	35
4	LEPTON FLAVOR VIOLATING $Z \rightarrow l_1^- l_2^+$ DECAY	46
4.1	The One-Loop Calculation for $Z \rightarrow l_1^- l_2^+$	49

4.2	Numerical Analysis and Discussion	59
5	THE FLAVOR CHANGING $t \rightarrow c l_1^- l_2^+$ IN MODEL III	67
5.1	$t \rightarrow c (l_1^- l_2^+ + l_1^+ l_2^-)$ in Model III	69
5.2	Numerical Analysis and Discussion	73
6	CONCLUSION	79
	REFERENCES	82
	APPENDICES	
A	MINIMA CONDITIONS OF THE POTENTIAL AND THE PHYSICAL EIGENSTATES	89
A.1	The Charged Scalar Sector	92
A.2	The Neutral Scalar Sector	93
A.3	For Case a) Set of Solutions	95
A.4	For Case b) Set of Solutions	96
B	AN EQUIVALENT NEW PARAMETRIZATION OF THE DOUBLET AND THE YUKAWA LAGRANGIAN IN THE QUARK MASS BASIS	99
C	THE FEYNMAN PARAMETRIZATION	106
D	DIMENSIONAL REGULARIZATION	109
VITA	113

LIST OF TABLES

TABLES

3.1	The values of parameters existing in Eq. (??) for the various form factors appearing in the $B \rightarrow K^*$ matrix elements.	32
3.2	The values of the input parameters used in the numerical analysis of the exclusive decay $B \rightarrow K^* \tau^+ \tau^-$	37
4.1	The values of the input parameters used in the numerical calculations for the decay $Z \rightarrow l_1^- l_2^+$, $l_{1,2} = e, \mu, \tau$	61

LIST OF FIGURES

FIGURES

3.1	The one-loop Feynman diagrams contributing the decay $b \rightarrow s\tau^+\tau^-$ in the SM.	28
3.2	The additional one-loop diagrams contributing the process $b \rightarrow s\tau^+\tau^-$ obtained within the framework of model III without NHB contributions.	29
3.3	The one-loop diagrams contributing the process $b \rightarrow s\tau^+\tau^-$ within the framework of model III by including NHB contributions . . .	30
3.4	A_{FB} as a function of $\sin\theta$ for $m_{A^0} = 80 \text{ GeV}$ without NHB effects. Here A_{FB} is restricted in the region between solid (dashed) lines for $C_7^{eff} > 0$ ($C_7^{eff} < 0$). Straight line corresponds to the SM prediction.	38
3.5	A_{FB} as a function of $\sin\theta$ for $\bar{\xi}_{N,\tau\tau}^E = 10 m_\tau$ including the NHB effects. Here A_{FB} is restricted in the region between solid (dashed) lines for $C_7^{eff} > 0$ ($C_7^{eff} < 0$). Straight line corresponds to the SM prediction.	39
3.6	A_{FB} as a function of $\bar{\xi}_{N,\tau\tau}^E$ for $\sin\theta = 0.5$ and $m_{A^0} = 80 \text{ GeV}$. Here A_{FB} is restricted in the region between solid (dashed) lines for $C_7^{eff} > 0$ ($C_7^{eff} < 0$). Straight line corresponds to the SM prediction.	40
3.7	A_{FB} as a function of m_{h^0}/m_{A^0} for $\sin\theta = 0.5$ and $\bar{\xi}_{N,\tau\tau}^E = 10 m_\tau$. Here A_{FB} is restricted in the region between solid (dashed) lines for $C_7^{eff} > 0$ ($C_7^{eff} < 0$). Straight line corresponds to the SM prediction.	41
3.8	A_{CP} as a function of $\sin\theta$ for $m_{A^0} = 80 \text{ GeV}$ without the NHB effects. Here A_{FB} is restricted in the region between solid (dashed) lines for $C_7^{eff} > 0$ ($C_7^{eff} < 0$).	42
3.9	A_{CP} as a function of $\sin\theta$ for $\bar{\xi}_{N,\tau\tau}^E = 10 m_\tau$ including the NHB effects. Here A_{FB} is restricted in the region between solid (dashed) lines for $C_7^{eff} > 0$ ($C_7^{eff} < 0$).	42
3.10	A_{CP} as a function of $\bar{\xi}_{N,\tau\tau}^E$ for $\sin\theta = 0.5$ and $m_{A^0} = 80 \text{ GeV}$. Here A_{FB} is restricted in the region between solid (dashed) lines for $C_7^{eff} > 0$ ($C_7^{eff} < 0$).	43

3.11	A_{CP} as a function of m_{h^0}/m_{A^0} for $\sin\theta = 0.5$ and $\bar{\xi}_{N,\tau\tau}^E = 10 m_\tau$. Here A_{FB} is restricted in the region between solid (dashed) lines for $C_7^{eff} > 0$ ($C_7^{eff} < 0$).	43
3.12	$A_{CP}(A_{FB})$ as a function of $\sin\theta$ for $\bar{\xi}_{N,\tau\tau}^E = 10 m_\tau$ including the NHB effects. Here A_{FB} is restricted in the region between solid (dashed) lines for $C_7^{eff} > 0$ ($C_7^{eff} < 0$).	44
3.13	$A_{CP}(A_{FB})$ as a function of $\bar{\xi}_{N,\tau\tau}^E$ for $\sin\theta = 0.5$ and $m_{A^0} = 80 \text{ GeV}$. Here A_{FB} is restricted in the region between solid (dashed) lines for $C_7^{eff} > 0$ ($C_7^{eff} < 0$).	44
3.14	$A_{CP}(A_{FB})$ as a function of m_{h^0}/m_{A^0} for $\sin\theta = 0.5$ and $\bar{\xi}_{N,\tau\tau}^E = 10 m_\tau$. Here A_{FB} is restricted in the region between solid (dashed) lines for $C_7^{eff} > 0$ ($C_7^{eff} < 0$).	45
4.1	One loop diagrams contributing to $Z \rightarrow l_j^- l_k^+$ decay due to the neutral Higgs bosons $S_\alpha = h^0, A^0$ in the 2HDM. l_i represents the internal, l_j (l_k) outgoing (incoming) lepton, wavy lines the vector field Z, and the dashed lines h_0 and A_0 fields.	50
4.2	The leg including one loop of the self energy diagrams in Fig. (??).	52
4.3	The maximum value of $Br(Z \rightarrow \mu^\pm e^\pm)$ as a function of $\sin\theta_{\tau e}$ for $\sin\theta_{\tau\mu} = 0.5$, $m_{h^0} = 70 \text{ GeV}$ and $m_{A^0} = 80 \text{ GeV}$	62
4.4	The minimum value of $Br(Z \rightarrow \mu^\pm e^\pm)$ as a function of $\sin\theta_{\tau e}$ for $\sin\theta_{\tau\mu} = 0.5$, $m_{h^0} = 70 \text{ GeV}$ and $m_{A^0} = 80 \text{ GeV}$	63
4.5	The minimum value of $Br(Z \rightarrow \mu^\pm e^\pm)$ as a function of m_{A^0} for $\sin\theta_{\tau\mu} = 0.5$, $\sin\theta_{\tau e} = 0.5$ and $m_{h^0} = 70 \text{ GeV}$	64
4.6	The maximum value of $Br(Z \rightarrow \tau^\pm e^\pm)$ as a function of $\sin\theta$ for $\bar{\xi}_{N,\tau\tau}^D = 10^3 \text{ GeV}$, $m_{h^0} = 70 \text{ GeV}$ and $m_{A^0} = 80 \text{ GeV}$. Here solid line represents the dependence with respect to $\sin\theta_{\tau\mu}$ for $\sin\theta_{\tau e} = 0.5$ and dashed line to $\sin\theta_{\tau e}$ for $\sin\theta_{\tau\mu} = 0.5$	65
4.7	The minimum value of $Br(Z \rightarrow \tau^\pm e^\pm)$ as a function of $\sin\theta$ for $\bar{\xi}_{N,\tau\tau}^D = 10^3 \text{ GeV}$, $m_{h^0} = 70 \text{ GeV}$ and $m_{A^0} = 80 \text{ GeV}$. Here solid line represents the dependence with respect to $\sin\theta_{\tau\mu}$ for $\sin\theta_{\tau e} = 0.5$ and dashed line to $\sin\theta_{\tau e}$ for $\sin\theta_{\tau\mu} = 0.5$	65
4.8	The maximum value of $Br(Z \rightarrow \tau^\pm e^\pm)$ as a function of $\bar{\xi}_{N,\tau\tau}^D$ for $\sin\theta_{\tau\mu} = 0.5$, $\sin\theta_{\tau e} = 0.5$, $m_{h^0} = 70 \text{ GeV}$ and $m_{A^0} = 80 \text{ GeV}$	66
4.9	The minimum value of $Br(Z \rightarrow \tau^\pm e^\pm)$ as a function of $\bar{\xi}_{N,\tau\tau}^D$ for $\sin\theta_{\tau\mu} = 0.5$, $\sin\theta_{\tau e} = 0.5$, $m_{h^0} = 70 \text{ GeV}$ and $m_{A^0} = 80 \text{ GeV}$	66

5.1	Tree level and one loop level diagrams contributing to the decay $t \rightarrow c l_1^- l_2^+$. The dashed lines represent the Higgs bosons h^0, A^0 . In Figs. (b), (c), (d) the wavy lines represent both W^\pm, ϕ^\pm, H^\pm and h^0, A^0 at the same time.	69
5.2	dBr ($t \rightarrow c (\tau^- \mu^+ + \tau^+ \mu^-)$) as a function of $ \bar{\xi}_{N,\tau\mu}^E $ for $\sin \theta_{\tau\mu} = 0.5$, real $\bar{\xi}_{N,tc}^D$ and $\Gamma_{tot}^{h^0} = \Gamma_{tot}^{A^0} = 0.1 \text{ GeV}$. The solid (dashed, dash-dotted) line represents the case for $s = (10/175)^2((50/175)^2, (150/175)^2)$	74
5.3	dBr ($t \rightarrow c (\tau^- \mu^+ + \tau^+ \mu^-)$) as a function of $ \bar{\xi}_{N,\tau\mu}^E $ for $\sin \theta_{\tau\mu} = 0.5$, real $\bar{\xi}_{N,tc}^D$ and $\Gamma_{tot}^{h^0} = \Gamma_{tot}^{A^0} = 0.1 \text{ GeV}$. The solid (dashed) line represents the case for $s = (80/175)^2((90/175)^2)$	75
5.4	dBr ($t \rightarrow c (\tau^- \mu^+ + \tau^+ \mu^-)$) as a function of s for $ \bar{\xi}_{N,\tau\mu}^E = 10 \text{ GeV}$, $\sin \theta_{\tau\mu} = 0.5$, real $\bar{\xi}_{N,tc}^D$ and $\Gamma_{tot}^{h^0} = \Gamma_{tot}^{A^0} = 0.1 \text{ GeV}$	76
5.5	BR ($t \rightarrow c (\tau^- \mu^+ + \tau^+ \mu^-)$) as a function of $ \bar{\xi}_{N,\tau\mu}^E $ for $\sin \theta_{\tau\mu} = 0.5$, real $\bar{\xi}_{N,tc}^D$ and $\Gamma_{tot}^{h^0} = \Gamma_{tot}^{A^0} = 0.1 \text{ GeV}$	77

CHAPTER 1

INTRODUCTION

The Glashow–Weinberg–Salam [1]–[4] theory of electroweak interactions, combined with the Quantum Chromodynamics (QCD) is called the Standard Model (SM) in which all of the known non-gravitational interactions are fundamentally described. So far it is universally accepted that the SM has been very successful in explaining beautifully all the experimental data in the energy range available at present¹.

The SM is based on the gauge group $SU(3)_C \otimes SU(2)_L \otimes U(1)_Y$. The gauge sector of the SM is composed of eight gluons, G_i , which are the gauge bosons of $SU(3)_C$ and mediating the strong interactions among quarks, and the photon, γ , which is one of the four gauge bosons of $SU(2)_L \otimes U(1)_Y$ and responsible for the electromagnetic interactions, and the remaining three weak bosons, W^\pm, Z which are the corresponding intermediate bosons of the weak interactions.

Although the SM is extraordinarily robust, there is a general consensus about the fact that it can not be the final theory of elementary particles. Instead it could be considered as an effective form of a more fundamental theory at low energies. There are indeed strong conceptual indications and phenomenological hints which motivates us to look physics beyond the SM. The hierarchy problem, existence of many arbitrary fundamental parameters, and the mysterious pattern of fermion masses are some examples for the conceptual problems of the SM. Measurements

¹ there are strong indications in favor of both the atmospheric and solar neutrino oscillation between different flavors. This implies nonzero neutrino masses which are not considered in the SM. Another crucial test for the SM which worths mentioning is the most recent measurement on the muon anomalous magnetic moment which shows a deviation as large as 3σ from the SM predictions.

of flavor changing neutral current (FCNC) processes, which are very suppressed or zero, including lepton flavor violating (LFV) processes which differ from the SM predictions can be taken as phenomenological hints from experiments for both testing the quantum structure of the SM and for searching new physics beyond the SM.

There are various alternative extended models proposed for solving the problems of the SM. Some of the more representative ones are the two Higgs doublet models (2HDM), left–right (super)symmetric models, the minimal supersymmetric model (MSSM), the Zee model, the see–saw model, the SM enlarged with massive neutrinos, and universal top color assisted technicolor models. Among them, the most conservative extensions of the SM are, apparently, the 2HDM. Since it is just a mild extension of the SM with one additional scalar $SU(2)_L$ doublet –an extension of the Higgs sector about which we have no direct experimental information. Furthermore it adds the fewest new arbitrary parameters into the play and such a Higgs structure is also required in low energy supersymmetric models.

The 2HDM, obtained by introducing another doublet, would automatically lead to FCNC problem in its Yukawa coupling sector –representing interactions between the Higgs fields and fermions. FCNC problem simply means that the additional doublet makes the FCNCs at tree level possible, in general. The FCNC processes can be identified as rare decays. They are in fact rare in a sense that they appear at least at one loop level in the SM, which leads to a high suppression. Hence rare processes offer an ideal place both to test the quantum structure of the SM and to search new physics effects beyond the SM. Therefore, any positive observation of FCNC couplings deviated from that in SM would certainly signal the presence of new physics.

In this thesis, we will first investigate within the framework of the general 2HDM the rare exclusive $B \rightarrow K^* \tau^+ \tau^-$ decay including neutral Higgs boson (NHB) effects [5]. After giving the expression for the matrix element for the decay including NHB effects, the CP asymmetry (A_{CP}) and the forward–backward

asymmetry (A_{FB}) of the lepton pair, and the CP asymmetry in A_{FB} ($A_{CP}(A_{FB})$), dependencies of these physically observable quantities on various model parameters such as the CP parameter $\sin\theta$, Yukawa coupling parameter $\bar{\xi}_{N,\tau\tau}^E$, and the mass ratio of the neutral Higgs bosons, m_{h^0}/m_{A^0} will be discussed in detail.

Next, in Chapter 4, LFV $Z \rightarrow l_1^- l_2^+$ decay [6] will be investigated in the same framework of the 2HDM. This decay mode is important since even in the context of the SM extended by allowing massive neutrinos the predicted branching ratio (Br) is really very far from experimental verification. The limits of the Br 's of the decay modes will be discussed as regards to sensitivity of the model parameters.

In the final chapter of this thesis, we analyzed the flavor changing (FC) top decay, $t \rightarrow cl_1^- l_2^+$, in the same model [7]. Since it can exist at tree level, the flavor changing couplings both in the quark and the lepton sectors play the main role in this decay.

Before presenting the investigations outlined above, we will pause and present a brief review of the SM and then the 2HDM, pointing out the theoretical ground which will be the basis for the calculations in the subsequent chapters.

CHAPTER 2

THE GENERAL TWO HIGGS DOUBLET MODEL (2HDM)

In this chapter, as a preliminary basis to all subsequent chapters, I will provide an overview of the notion of two Higgs doublet model (2HDM), in the framework of which all our studies available in the thesis have been carried out. The model is indeed the minimal extension of the Standard model (SM) and can be formulated by modifying the experimentally less known part of the SM, the Higgs sector, by adding an extra scalar doublet to the SM scalar sector. Therefore the customary way of introducing 2HDM is to make available initially the basic ingredients over which the SM is constructed and then 2HDM is to be considered basically as a SM with two scalar doublets. Furthermore the consequences of this modification can be obtained without much more effort. Along this line, having given a brief introduction of the basic aspects of the SM, we mainly focus on 2HDM in the rest of the chapter.

2.1 The Standard Model (SM)

The current view of elementary particle physics is based on a gauge theory of quarks and leptons and three fundamental interactions of the nature are described as a $SU(3)_C \otimes SU(2)_L \otimes U(1)_Y$ gauge theory in which the SM is based on as a quantum field theory. In order to define the SM the following three basic ingredients are needed:

1. The symmetries of the Lagrangian;
2. The representation of fermions and scalars;

3. The pattern of Spontaneous Symmetry Breaking (SSB).

The SM can be then defined as follows:

1. As is stated above, the gauge symmetry under which the Lagrangian is invariant is

$$G_{SM} \equiv SU(3)_C \otimes SU(2)_L \otimes U(1)_Y. \quad (2.1)$$

2. There are three fermion families, each consisting of five representations. These can be expressed in a very compact way of the form

$$Q_{Li}(\mathbf{3}, \mathbf{2})_{1/3}, U_{Ri}(\mathbf{3}, \mathbf{1})_{4/3}, D_{Ri}(\mathbf{3}, \mathbf{1})_{-2/3}, \ell_{Li}(\mathbf{1}, \mathbf{2})_{-1}, E_{Ri}(\mathbf{1}, \mathbf{1})_{-2}, \quad (2.2)$$

where the left-handed (right-handed up (down)) quarks denoted as Q_L (U_{Ri} (D_{Ri})). ℓ_{Li} (E_{Ri}) similarly represents left-handed (right-handed) lepton. Our notation meant that, for example, $Q_L(\mathbf{3}, \mathbf{2})_{1/3}$ are in a triplet ($\mathbf{3}$) of the $SU(3)_C$ group, a doublet ($\mathbf{2}$) of $SU(2)_L$ and carry hypercharge $Y = 1/3$, obtained using the Gell-Mann-Nishijima relation [8] $Q = T_3 + Y/2$. There is merely a single scalar multiplet represented in our notation as $\Phi(\mathbf{1}, \mathbf{2})_{+1}$.

3. One of the crucial ingredients of the SM that is worth mentioning is the existence of SSB of gauge symmetries, giving rise to Goldstone excitations [9] which in turn can be related to gauge boson mass terms [10]. In general, the phenomenon of SSB is simply stated as follows. *A system is said to possess a symmetry that is spontaneously broken if the Lagrangian describing the dynamics of the system is invariant under these symmetry transformations, but the vacuum of the theory is not.* Here the vacuum is the state in which expectation value of the Hamiltonian of the system becomes minimum. The discovery of the W^\pm and Z gauge bosons at CERN in 1983 [11] may be considered as the first experimental evidence of the SSB phenomenon in weak interactions. The physical implication of the SSB phenomenon is twofold. One way is the realization of SSB for theories having global symmetries,

the ones which imply space–time independent continuous parameters of the symmetry transformation, and it is described by the Goldstone theorem [9]. The second way is the case for the theories with spontaneously broken local (gauge) symmetries like the SM, the ones which imply space–time dependent continuous parameters of the transformation. There is a mechanism, the so–called Higgs Mechanism [12] operating in the Electroweak theory in order to generate a mass for the weak gauge bosons, W^\pm and Z , and to the fermions. The operation indeed leaves as a consequence the prediction of a new particle, the Higgs particle, which has not been seen in experiments so far [10]. The minimum formulation, the SM, requires a single complex scalar field (Higgs field) denoted as $\Phi(\mathbf{1}, \mathbf{2})_{+1}$. Additionally the scalar should interact with the gauge sector in a G_{SM} gauge invariant manner and its self–interactions, being introduced *ad hoc*, must produce the desired breaking,

$$G_{SM} \rightarrow SU(3)_C \otimes U(1)_{em}, \quad (2.3)$$

which is characterized by non zero vacuum expectation value (VEV) of the scalar field Φ of the form

$$\langle \Phi \rangle = \frac{1}{\sqrt{2}} \begin{pmatrix} 0 \\ v \end{pmatrix}. \quad (2.4)$$

Let us say a few words about why that type of breaking occurs. The reason for this is as follows. Having massive weak gauge bosons W^\pm , Z indicates that $SU(2)_L \otimes U(1)_Y$ is not a symmetry of the vacuum. In contrast the photon being massless reflects that $U(1)_{em}$, a subgroup of $SU(2)_L \otimes U(1)_Y$, is a good symmetry of the vacuum. Thus, we should eventually get the above SSB pattern.

Having discussed three ingredients giving the route for defining the SM, let us turn our attention to the SM Lagrangian, \mathcal{L}_{SM} , the most general renormalizable Lagrangian consistent with the gauge symmetry G_{SM} in Eq. (2.1). It can be, in

principle, divided into to five parts:

$$\mathcal{L}_{\mathcal{SM}} = \mathcal{L}_{kinetic}^f + \mathcal{L}_{kinetic}^\Phi + \mathcal{L}_{kinetic}^{Gaugefields} + \mathcal{L}_{Higgs}^{SM} + \mathcal{L}_Y^{SM}. \quad (2.5)$$

As concerns the kinetic terms, to maintain gauge invariance, one has to replace the derivative with a covariant derivative defined as

$$D^\mu = \partial^\mu + ig_s G_a^\mu L_a + ig W_b^\mu T_b + ig' B^\mu Y, \quad (2.6)$$

where G_a^μ are the gluon fields, W_b^μ the three weak interaction bosons and B^μ the single hypercharge boson and L_a are $SU(3)_C$ generators, the T_b 's are $SU(2)$ generators (the 2×2 Pauli matrices $\sigma_b/2$ for doublets, 0 for singlets), Y are the $U(1)_Y$ charges. As an example, for the left-handed quarks Q_L we have

$$\mathcal{L}_{kinetic}(Q_L) = i\bar{Q}_{Li}\gamma^\mu D_\mu Q_{Li}, \quad (2.7)$$

with

$$D^\mu Q_{Li} = (\partial^\mu + ig_s G_a^\mu L_a + ig W_b^\mu T_b + ig' B^\mu Y)Q_{Li}, \quad (2.8)$$

and the other kinetic terms for Higgs and Gauge fields are given

$$\begin{aligned} \mathcal{L}_{kinetic}^\Phi &= (D_\mu \Phi)^\dagger (D^\mu \Phi), \\ \mathcal{L}_{kinetic}^{Gaugefields} &= -\frac{1}{4} \sum_{a=1}^3 F_{\mu\nu}^a F^{a\mu\nu} - \frac{1}{4} B_{\mu\nu} B^{\mu\nu}, \end{aligned} \quad (2.9)$$

where $F_{\mu\nu}^a = \partial_\mu W_\nu^a - \partial_\nu W_\mu^a - g\epsilon_{abc}W_\mu^b W_\nu^c$ and $B_{\mu\nu} = \partial_\mu B_\nu - \partial_\nu B_\mu$ are the gauge antisymmetric tensors with ϵ_{abc} as the group structure constant. After diagonalizing the mass matrix of the gauge bosons the mass fields are

$$\begin{aligned} A_\mu &= \frac{1}{\sqrt{g^2 + g'^2}}(g'W_\mu^3 + gB_\mu), \\ Z_\mu &= \frac{1}{\sqrt{g^2 + g'^2}}(gW_\mu^3 - g'B_\mu), \\ W_\mu^\pm &= \frac{1}{\sqrt{2}}(W_\mu^1 \mp iW_\mu^2). \end{aligned} \quad (2.10)$$

Note that kinetic parts of the Lagrangian, $\mathcal{L}_{kinetic}^{f,\Phi,Gf}$, are further invariant under CP transformation.

The second part of \mathcal{L}_{SM} consists of the Higgs potential describing the scalar self-interactions and is given by

$$\mathcal{L}_{Higgs}^{SM} = \mu^2 \Phi^\dagger \Phi - \lambda (\Phi^\dagger \Phi)^2. \quad (2.11)$$

For $\mu^2 > 0$, the scalar field Φ develops a non zero VEV given in Eq. (2.4) where the vacuum value is $v = \mu/\sqrt{2\lambda}$ ($\simeq 246 \text{ GeV}$) and the physical Higgs mass to be yielded as a consequence of the Higgs mechanism is given by $m_H = \sqrt{2\lambda} v$ and after the SSB, at the tree level, the masses of the weak gauge bosons can also be given as $m_W = gv/2$ and $m_Z = \sqrt{g^2 + g'^2} v$. This part of the Lagrangian is also CP conserving for the scalar doublet Φ in the SM¹.

The final piece of the Lagrangian, called Yukawa Lagrangian, describes the interaction among the fermions and the Higgs field. The general form can be expressed as follows

$$\mathcal{L}_Y^{SM} = \eta_{ij}^D \bar{Q}_{iL} \Phi D_{jR} + \eta_{ij}^U \bar{Q}_{iL} \tilde{\Phi} U_{jR} + \eta_{ij}^E \bar{\ell}_{iL} \Phi E_{jR} + h.c., \quad (2.12)$$

where η_{ij} 's are the complex Yukawa couplings.

As is pointed out earlier, the 2HDM is constructed by modifying the Higgs sector of the SM, which is directly related to the modification of \mathcal{L}_Y^{SM} . That's why I want to say a few words about the behavior of the \mathcal{L}_Y^{SM} under CP transformation. If one looks the structure of the Eq. (2.12) it is, in general, CP violating due to *complex* Yukawa couplings. An intuitive explanation of why this is related to the complex Yukawa couplings goes as follows. From the Hermiticity of the Lagrangian one can write each term in \mathcal{L}_Y^{SM} as pairs of the form

$$\eta_{ij} \bar{\psi}_{iL} \Phi \psi_{jR} + \eta_{ij}^* \bar{\psi}_{iR} \Phi^\dagger \psi_{jL}. \quad (2.13)$$

Under CP transformation there is an exchange of the operators in Eq. (2.13) of the form

$$\bar{\psi}_{iL} \Phi \psi_{jR} \leftrightarrow \bar{\psi}_{iR} \Phi^\dagger \psi_{jL}, \quad (2.14)$$

while leaving the Yukawa coefficients, η_{ij} and η_{ij}^* , unchanged. This, in fact, means that CP is a symmetry of the Yukawa Lagrangian, \mathcal{L}_Y^{SM} , if $\eta_{ij} = \eta_{ij}^*$.

¹ For extended scalar sector, such as that of 2HDM, \mathcal{L}_{Higgs}^{SM} can be CP conserving. Even in this case, it may lead to spontaneous CP violation.

2.2 Two Higgs Doublet Model (2HDM)

2.2.1 Motivation for Additional Scalars

We first present the motivation for examining alternatives to the usual Higgs (scalar) sector in otherwise conventional gauge theories of weak and electromagnetic interactions. Then 2HDM can be pinned down by just merely mentioning what kinds of modifications result in the SM due to additional scalar doublet.

Although the experimental evidence in support of the gauge boson and of the fermion sector of the SM is very strong, experimental information concerning the scalar sector is very weak. The ρ -parameter, defined through the relation $\mathcal{L}_z^{eff} = (4G_F/\sqrt{2})\rho J_z^\mu J_{z\mu}$, where \mathcal{L}_z^{eff} is the effective low-energy neutral current Lagrangian and $J_{z\mu}$ is the standard weak neutral current, is determined by the Higgs structure of the theory. Thus the most important piece of evidence providing information about this sector comes from that parameter. It is in fact a measure of the ratio of the neutral current to charged current strength in effective low energy lagrangian. In the SM, at tree level, $\rho = m_W^2/(m_Z^2 \cos^2 \theta_W)$ is equal to unity². The general formula in the case of having N scalar multiplets, Φ_i , with VEV v_i , isospin T_i and hypercharge Y_i is [14]

$$\rho = \frac{\sum_{i=1}^N [T_i(T_i + 1) - \frac{1}{4}Y_i^2]v_i}{\sum_{i=1}^N \frac{1}{2}Y_i^2 v_i}. \quad (2.15)$$

The simplest method of satisfying the constraint, $\rho = 1$ at the tree level, is to choose only representations such that $T(T + 1) = 3Y^2/4$, clear from Eq. (2.15). There are in fact an infinite number of complicated Higgs representations satisfying the constraint. The simplest choice among them are $SU(2)$ doublets with $Y = \pm 1$. Consequently the minimal extension of the scalar sector of the SM is a model with two scalar doublet of $Y = \pm 1$.

We may state further motivations for extending the scalar sector to models with at least two doublets as follows. The first motivation is supersymmetry. Whereas, in the SM, only one Higgs doublet is required to give mass to the

² Experimentally [13], the value of ρ is 0.992 ± 0.02 .

quarks and leptons, in the supersymmetric model, two Higgs doublets are needed to give mass to both up-type and down-type quarks (and the corresponding leptons) [15]. Another motivation arises in axion models [16]. The QCD violating parameter $\bar{\theta}$. However, Peccei and Quinn [17] stated that $\bar{\theta}$ can be rotated away if the Lagrangian contains a global $U(1)$ symmetry whose implementation requires two Higgs doublet. Yet another motivation for additional doublets stems from models of CP violation. As already noted, the only source of CP violation in the SM is the phase in the Cabbibo–Kobayashi–Maskawa matrix (CKM). If there exist additional scalars and , in particular $SU(2)$ doublets, then not only there are new sources of CP violation, but also the Yukawa couplings in the mass basis as well as the scalar self-interactions may violate CP. Therefore once enough independent observations of CP violating effects are made, we will find that there is no single choice of CKM parameters that is consistent with all measurements. Lee [18] showed that a model with two scalar doublets could spontaneously violate CP. That is, the Lagrangian could be CP invariant, but the minimum could occur for complex values of the scalar fields, thus violating CP. His model in fact had FCNCs forcing a very large scalar mass of the value about $10 TeV$. Then any *ad hoc* discrete symmetry which eliminates these currents also eliminates the CP violation. Later Weinberg [19] showed that with three doublets, CP could be violated spontaneously in the presence of a discrete symmetry eliminating FCNC. Branco and Rebelo [20] showed that the discrete symmetry which eliminates FCNC could be softly broken, giving CP violation in a 2HDM. As a final motivation for additional doublets, grand unified theories can be considered. It can be shown that models with only one $SU(2)$ doublet do not generate sufficient baryon number and at least two such doublets are needed [21]. Having stated the motivations for additional scalar doublets, our next task is to analyze the points differing from those of the *minimal* SM.

2.2.2 The Yukawa Lagrangian and the Scalar Potential in 2HDM

The Yukawa Lagrangian involving two scalar fields is the first piece differentiating that of the one Higgs doublet SM. The other is, naturally, Higgs (scalar) potential describing interactions of scalar fields. Therefore discussing only the Yukawa couplings and the scalar potential in the presence of two Higgs doublets are enough to construct 2HDM over the SM.

As is stated in the previous subsection, a potential problem with 2HDM is the possibility of FCNCs at the tree level. The reason for this is the fact that with unrestricted Yukawa couplings diagonalization of the up-type and down-type quarks do not diagonalize the Yukawa couplings with each single scalar doublet. To avoid FCNC problem, one can impose an *ad hoc* discrete symmetry [22] and then Yukawa couplings are restricted such a way that there is no FCNC at the tree level. Let us first write the general form of the Yukawa Lagrangian in the presence of two scalar doublets, denoted as \mathcal{L}_Y^{2HDM} , of the form

$$\begin{aligned} \mathcal{L}_Y^{2HDM} = & \eta_{ij}^U \bar{Q}_{iL} \tilde{\Phi}_1 U_{jR} + \eta_{ij}^D \bar{Q}_{iL} \Phi_1 D_{jR} + \xi_{ij}^{U\dagger} \bar{Q}_{iL} \tilde{\Phi}_2 U_{jR} + \xi_{ij}^D \bar{Q}_{iL} \Phi_2 D_{jR} \\ & + \eta_{kl}^E \bar{l}_{kL} \Phi_1 E_{lR} + \xi_{kl}^E \bar{l}_{kL} \Phi_2 E_{lR} + h.c. , \end{aligned} \quad (2.16)$$

where Φ_i , for $i = 1, 2$ are two scalar doublet of a 2HDM, while $\eta_{ij}^{U,D,E}$ and $\xi_{ij}^{U,D,E}$ are the non-diagonal matrices of Yukawa couplings and \bar{l}_{kL} and E_{lR} represent left-handed $SU(2)$ lepton doublet, right-handed $SU(2)$ singlet, respectively. Then it is possible that 2HDM can be categorized into three types by explicitly imposing the following discrete symmetry sets,

$$\begin{aligned} (I) \quad & \Phi_1 \rightarrow -\Phi_1, \Phi_2 \rightarrow \Phi_2, D_i \rightarrow -D_i, U_i \rightarrow -U_i, \\ (II) \quad & \Phi_1 \rightarrow -\Phi_1, \Phi_2 \rightarrow \Phi_2, D_i \rightarrow -D_i, U_i \rightarrow +U_i. \end{aligned} \quad (2.17)$$

Clearly imposing set (I) into the Yukawa Lagrangian \mathcal{L}_Y^{2HDM} forces all the quarks, both the up-type and down-types, to couple only to Φ_1 doublet, which is so called model I and the set (II) apparently forces the quarks of different charges to couple to the separate scalar doublets, namely the down-types are coupled to Φ_1 and the up-types are coupled to Φ_2 only. This kind is so called model II version of

2HDM. Finally, the third class which is formed by just relaxing these discrete symmetry sets is the general 2HDM with FCNCs at tree level, which is so called model III [23]. Indeed the form of the Yukawa Lagrangian given in Eq. (2.16) describes the most general Yukawa couplings between the Higgs scalar fields and fermions, i.e., those that are possible only in model III.

Having presented the form of the Yukawa couplings within three versions of 2HDM, there remains to explore the allowed scalar self-interactions named scalar potential. The most general $SU(2)_L \otimes U(1)_Y$ gauge-invariant, renormalizable scalar potential³ for two $SU(2)$ doublets of hypercharge $Y = +1$ can be written as [24]

$$\begin{aligned}
V(\Phi_1, \Phi_2) = & \mu_1^2 \Phi_1^\dagger \Phi_1 + \mu_2^2 \Phi_2^\dagger \Phi_2 + \mu_{12} \Phi_1^\dagger \Phi_2 + \mu_{12}^* \Phi_2^\dagger \Phi_1 + \lambda_1 (\Phi_1^\dagger \Phi_1)^2 \\
& + \lambda_2 (\Phi_2^\dagger \Phi_2)^2 + \lambda_3 (\Phi_1^\dagger \Phi_1) (\Phi_2^\dagger \Phi_2) + \lambda_4 (\Phi_1^\dagger \Phi_2) (\Phi_2^\dagger \Phi_1) \\
& + \frac{1}{2} \lambda_5 [(\Phi_1^\dagger \Phi_2)^2 + (\Phi_2^\dagger \Phi_1)^2] ,
\end{aligned} \tag{2.18}$$

where all coupling constants are taken real by Hermiticity requirement of the potential V (without restricting μ_{12}). The details about the scalar potential are discussed in appendix A. Implementation of discrete symmetry of Eq. (2.17) corresponds to taking $\mu_{12} = \mu_{12}^* = 0$. For computational simplicity, I will assume here that the potential doesn't include the μ_{12} and μ_{12}^* terms, which indeed represent the soft breaking terms. If this assumption is relaxed, analysis of the potential is straightforward. We observed that its qualitative features are unchanged.

In the following we summarize the results obtained in appendix A for the case that scalar potential does not include the soft breaking part, i.e., $\mu_{12} = \mu_{12}^* = 0$. In order to break the original $SU(2)_L \otimes U(1)_Y$ gauge symmetry down to $U(1)_{em}$

³ Even though the discrete symmetry given in Eq. (2.17) is violated only softly by mass-dimension-two-terms, this breaking would not affect the Yukawa couplings.

the vacuum expectation values of the scalar fields must have the form⁴

$$\langle \Phi_1 \rangle = \frac{1}{\sqrt{2}} \begin{pmatrix} 0 \\ v_1 \end{pmatrix} ; \quad \langle \Phi_2 \rangle = \frac{1}{\sqrt{2}} \begin{pmatrix} 0 \\ v_2 \end{pmatrix} . \quad (2.19)$$

The minima conditions for the potential, in fact, lead to two linearly independent solutions for v_1^2 and v_2^2 (see appendix A). For the Case a) we have assumed that both VEVs are non-zero. For the Case b) v_2 is assumed to be zero.

The mass squared matrix described explicitly in appendix A is properly diagonalized, since the mass squared matrix for the physical Higgs fields decouples in a direct product of 2×2 sub-matrices. As a consequence we get the Higgs masses and eigenstates (see appendix A for details). We recall here a summary of the results for the potential without soft breaking term:

For the Case a) where v_1^2 and v_2^2 are given in terms of the coupling constants in the potential, Eq. (A.5).

- From the part of the mass squared matrix spanned by the gauge fields $\{\phi_1, \phi_2, \phi_5, \phi_6\}$ the charged components of Φ_1 and Φ_2 mix to give a charged Goldstone boson χ^\pm and a physical charged Higgs H^\pm with masses

$$\{m_{\chi^\pm}, m_{H^\pm}\} = \{0, -(v_1^2 + v_2^2)\lambda_{45}\} . \quad (2.20)$$

with mass eigenstates in terms of gauge eigenstates

$$\begin{pmatrix} \chi^{+(-)} \\ H^{+(-)} \end{pmatrix} = \begin{pmatrix} \cos \beta & \sin \beta \\ -\sin \beta & \cos \beta \end{pmatrix} \begin{pmatrix} \phi_{1(2)} \\ \phi_{5(6)} \end{pmatrix} , \quad (2.21)$$

where $\lambda_{45} = 2(\lambda_4 + \lambda_5)$ and the mixing angle is defined as $\tan \beta = v_2/v_1$ ($0 \leq \beta \leq \pi/2$).

- The imaginary parts of the neutral components, $\{\phi_4, \phi_8\}$, mix to give a neutral Goldstone boson χ^0 and a neutral pseudoscalar (CP-odd) A^0 with masses

$$\{m_{\chi^0}, m_{A^0}^2\} = \{0, -(v_1^2 + v_2^2)\lambda_5\} , \quad (2.22)$$

⁴ The unobservable phase difference between these two expectation values will be nonzero, which indeed leads to spontaneous CP violation, unless soft breaking terms included are real and non-zero (and $\lambda_4 = \lambda_5$). In this case, the phase can be rotated away by a redefinition of one of the fields, leaving other terms in the potential unchanged.

with the mass eigenstates

$$\begin{pmatrix} \chi^0 \\ A^0 \end{pmatrix} = \begin{pmatrix} \cos \beta & \sin \beta \\ -\sin \beta & \cos \beta \end{pmatrix} \begin{pmatrix} \phi_4 \\ \phi_8 \end{pmatrix}. \quad (2.23)$$

- The real parts, $\{\phi_3, \phi_7\}$, mix to give two neutral scalars (CP-even) H^0, h^0 with masses

$$m_{H^0, h^0}^2 = A + B \pm \sqrt{(A - B)^2 + C^2}. \quad (2.24)$$

with the mass eigenstates

$$\begin{pmatrix} H^0 \\ h^0 \end{pmatrix} = \begin{pmatrix} \cos \alpha & \sin \alpha \\ -\sin \alpha & \cos \alpha \end{pmatrix} \begin{pmatrix} \phi_3 \\ \phi_7 \end{pmatrix}, \quad (2.25)$$

where

$$A = v_1^2 \lambda_1, \quad B = v_2^2 \lambda_2, \quad C = 2 v_1 v_2 \lambda_{345}, \quad (2.26)$$

and subindexes (H^0, h^0) refer respectively to $(+, -)$, $\lambda_{345} \equiv 2(\lambda_3 + \lambda_4 + \lambda_5)$ and the mixing angle is $\tan 2\alpha = C/(A - B)$ ($0 \leq \alpha \leq \pi/2$). As is obvious from the condition $m_{H^0} \geq m_{h^0}$ and from $m_{h^0}^2 \geq 0$ that the constraint $|C| \leq 2\sqrt{AB}$ ($|\lambda_{345}| \leq \sqrt{\lambda_1 \lambda_2}$) is induced.

For the Case b) where v_2 vanishes, the Higgs masses and eigenstates are given as follows:

- The charged sector has four fields with masses

$$\{m_{\chi^\pm}, m_{H^\pm}\} = \{0, \mu_2^2 + \frac{\lambda_3}{2} v_1^2\}, \quad (2.27)$$

and the eigenstates are identical to the gauge eigenstates such that (from Eq. (A.32)) $\chi^\pm = \phi_1 \pm i\phi_2$ and $H^\pm = \phi_5 \pm i\phi_6$.

- The imaginary parts of the neutral components are now identical to a neutral Goldstone boson χ^0 and a neutral pseudoscalar Higgs boson A^0 with masses

$$\{m_{\chi^0}, m_{A^0}\} = \{0, \mu_2^2 + (\lambda_{345} - \lambda_5) v_1^2\}, \quad (2.28)$$

and the mass eigenstates are identical to the gauge eigenstates, $\chi^0 = \phi_4, A^0 = \phi_8$.

- The real parts of the neutral components are the same as the neutral Higgs bosons (H^0, h^0) with masses

$$\{m_{H^0}, m_{h^0}\} = \{2\lambda_1 v_1^2, \mu_2^2 + \lambda_{345} v_1^2\}, \quad (2.29)$$

and again there is no mixing, i.e., $H^0 = \phi_3, h^0 = \phi_7$.

To aid the interpretation of the fields present, it is instructive to introduce a new basis due to Georgi [24] related to the original ones as (see appendix B for details)

$$\begin{aligned} \Phi'_1 &\equiv \Phi_1 \cos \beta + \Phi_2 \sin \beta, \\ \Phi'_2 &\equiv -\Phi_1 \sin \beta + \Phi_2 \cos \beta. \end{aligned} \quad (2.30)$$

Then we get

$$\Phi'_1 \equiv \frac{1}{\sqrt{2}} \left[\begin{pmatrix} 0 \\ v + \bar{H}^0 \end{pmatrix} + \begin{pmatrix} \sqrt{2}\chi^+ \\ i\chi^0 \end{pmatrix} \right]; \quad \Phi'_2 \equiv \frac{1}{\sqrt{2}} \begin{pmatrix} \sqrt{2}H^+ \\ H_1 + iH_2 \end{pmatrix}. \quad (2.31)$$

where $v^2 = v_1^2 + v_2^2$ and the weak eigenstates in terms of mass eigenstates are of the form

$$\begin{aligned} \bar{H}^0 &\equiv H^0 \cos(\beta - \alpha) + h^0 \sin(\beta - \alpha), \\ H_1 &\equiv -H^0 \sin(\beta - \alpha) + h^0 \cos(\beta - \alpha), \\ H_2 &\equiv A^0. \end{aligned} \quad (2.32)$$

Therefore Φ'_1 can be identified with the scalar doublet of the SM and the mass of the W and Z bosons are given at the tree level by $m_W = m_Z \cos \theta_W = gv/\sqrt{2}$, where g is the $SU(2)$ coupling constant and then all the new scalar fields belong to the Φ'_2 .

Final remark before finishing the chapter is about our choices of the VEVs of the Φ_1 and Φ_2 doublets in subsequent chapters. For convenience, in all our calculations, we choose for Φ_1 and Φ_2 a suitable basis such that merely $\eta_{ij}^{U,D,E}$ Yukawa couplings generate the fermion masses. This in fact means $v_2 = 0$. Then from Eq. (2.26) and the relations $\tan \beta = v_2/v_1$ and $\tan 2\alpha = C/(A - B)$, the mixing angles simply become $\alpha = \beta = 0$. As a consequence from Eq. (2.32), (\bar{H}^0, H^1, H^2) coincide with the mass eigenstates (H^0, h^0, A^0) .

CHAPTER 3

$B \rightarrow K^* \tau^+ \tau^-$ DECAY IN THE GENERAL TWO HIGGS DOUBLET MODEL INCLUDING THE NEUTRAL HIGGS BOSON EFFECTS

The rare dileptonic decays of B mesons have been the subject of much recent interest. This is since the operators responsible for these rare decays are absent in the SM, and only appear at the one-loop level. Therefore the study of these rare B meson decays can provide sensitive tests of many issues, both within and beyond the SM, such as the 2HDM, the MSSM [25], etc. The mass of the Higgs boson, the existence or non existence of other Higgs multiplets, extracting the values of the CKM matrix elements are just some of the issues to which these decays are sensitive. The experimental work for rare B meson decays continue at SLAC (BaBar), KEK (BELLE), B-Factories, DESY (HERA-B) and this stimulates the theoretical effort on them.

Currently, the main interest on rare B meson decays is focused on decays having “large” SM predicted Br 's which have the potential to be measured in the near future. The rare exclusive $B \rightarrow K^* l^+ l^-$ decay process is one of such decays. The experimental situation for this decay is very promising [26], with e^+e^- and hadron colliders focusing merely on the observation of exclusive channels with $l = e, \mu$ and τ final states, respectively.

The inclusive decay inducing $B \rightarrow K^* l^+ l^-$ process is $b \rightarrow s l^+ l^-$ transition occurring at quark level and it is extensively studied in the literature in the framework of the SM, the 2HDM and the MSSM [27]–[40]. In these references

$b \rightarrow sl^+l^-$ process is studied for light lepton pairs, namely $l = e, \mu$. This is because the NHB effects can be negligible due to having contributions proportional to the light lepton masses or corresponding Yukawa couplings. Having a heavier lepton pair final state however changes the situation and the NHB effects give sizable contributions. In [41]–[42] the inclusive decay $B \rightarrow X_s \tau^+ \tau^-$ decay was studied in the framework of model I and model II versions of the 2HDM. It was there shown that the contributions of the NB are significant when $\tan\beta$ is large. Furthermore the inclusive decay $b \rightarrow sl^+l^-$ was studied in the model II version of the 2HDM [43] and it was concluded that the NHB effects can give considerable contributions when the Yukawa interaction between τ lepton and neutral Higgs bosons is large.

There are some advantages and disadvantages of analyzing the exclusive decays differing from inclusive ones. From the theoretical point of view, in calculating the Br 's and other observables at hadron level, i.e., for $B \rightarrow K^*l^+l^-$ decay, we have the problem of computing the matrix element of the effective weak Hamiltonian \mathcal{H}_{eff} between the states B and K^* . The matrix elements are described in terms of a number of a priori unknown, incalculable, non-perturbative form factors. The dependence of these form factors on the appropriate kinematical variable may be modelled and this brings some model dependencies in the extraction of information from the measured quantities. These hadronic form factors also bring substantial uncertainty in the calculations. These matrix elements have been investigated in the framework of different approaches such as relativistic quark model by light-front formalism [40], chiral theory [44], three point QCD sum rules method [45], effective heavy quark theory [46] and light cone QCD sum rules [47, 48].

From the experimental point of view, however, it is well known that the experimental investigation of exclusive decays is much more easier compared to those of inclusive ones. This is one of the motivations for studying exclusive decays such as $B \rightarrow K^*l^+l^-$. Additionally, with the measured upper limit 5.2×10^{-6} (4.0×10^{-6}) for the Br of the decay $B^+ \rightarrow K^+\mu^+\mu^-$ ($B^0 \rightarrow K^{0*}\mu^+\mu^-$) [49], the decay $B \rightarrow K^*l^+l^-$ has received great interest. There are extensive studies

on these decays in the SM, the SM with fourth generation, multi Higgs doublet models, the MSSM, and in a model independent way in the literature [27]–[40] and [44]–[60].

CP violation plays also a privileged role in our quest for new physics beyond the SM and generally represents a major constraint on any attempt at model building beyond the SM. The CP violation for $B \rightarrow K^* l^+ l^-$ decay almost vanishes in the SM. This is because for $b \rightarrow s l^+ l^-$ induced process the matrix element contains a term proportional to $V_{tb} V_{ts}^*$, $V_{cb} V_{cs}^*$ and $V_{ub} V_{us}^*$ coming from $t\bar{t}$, $c\bar{c}$ and $u\bar{u}$ quark loops, respectively. The unitarity of the CKM matrix elements, $\sum_i V_{ib} V_{is}^* = 0$ ($i = u, c, t$), causes this term to be proportional merely to $V_{tb} V_{ts}^*$ since $V_{ub} V_{us}^*$ is smaller compared to $V_{tb} V_{ts}^*$. This leads eventually to the suppression of CP violating effects in the SM. Therefore it is clear that by searching the CP violating effects we may have a good chance to manifest some departure from the SM in particularly challenging class of rare phenomena. Moreover, experiments have just begun to have sensitivity to CP asymmetries at a nontrivial level. Like most extensions of the SM, there is a new source for CP violation, namely complex Yukawa couplings, in the model III version of the 2HDM. In [51]–[52], CP violating effects due to new phases in the model III and three Higgs doublet model, $3HDM(O_2)$, were studied and it was observed that a considerable CP asymmetry was obtained.

In this chapter we study the exclusive $B \rightarrow K^* \tau^+ \tau^-$ decay in model III by including the NHB effects. To get the matrix element for $B \rightarrow K^* \tau^+ \tau^-$ decay the quark level effective weak Hamiltonian calculated in [43] is used and we will investigate A_{CP} and A_{FB} of the lepton pair for the process under consideration. We further calculate $A_{CP}(A_{FB})$ and observed that it is possible to be measured in the forthcoming experiments.

The rest of this work is organized as follows. In the next section we discuss the leading order (LO) QCD corrected effective Hamiltonian and the corresponding matrix element for the inclusive decay including the NHB effects. We also give the explicit forms of the operators appearing in the effective Hamiltonian, the

corresponding Wilson coefficients and the form factors existing in the hadronic matrix elements. Further we present the matrix element for the exclusive $B \rightarrow K^* \tau^+ \tau^-$ decay and the explicit expressions for A_{CP} , A_{FB} and $A_{CP}(A_{FB})$. The analysis of the dependencies of A_{CP} , A_{FB} and $A_{CP}(A_{FB})$ on the CP parameter $\sin \theta$, Yukawa coupling $\bar{\xi}_{N,\tau\tau}^E$ and the mass ratio m_{h^0}/m_{A^0} and the discussion of our results are presented in the last section of this chapter.

3.1 Rare $B \rightarrow K^* \tau^+ \tau^-$ Decay Including the NHB Effects

As we have discussed in the previous chapter, in the model III, FCNCs at tree level are permitted and various new parameters, such as Yukawa couplings, masses of new Higgs bosons exist. Our starting point is the inclusive $b \rightarrow s \tau^+ \tau^-$ decay process inducing exclusive $B \rightarrow K^* \tau^+ \tau^-$ decay and the corresponding Yukawa Lagrangian, responsible for interactions between fermions and Higgs fields, is given in Eq. (2.17). As already presented in Chapter 2, FC part of the Yukawa Lagrangian at tree level is

$$\mathcal{L}_{Y,FC}^{III} = \xi_{ij}^D \bar{Q}_{iL} \Phi_2 D_{jR} + \xi_{ij}^{U\dagger} \bar{Q}_{iL} \tilde{\Phi}_2 U_{jR} + \xi_{kl}^E \bar{l}_{kL} \Phi_2 E_{lR} + h.c. , \quad (3.1)$$

The neutral FC couplings $\xi_{Neutral}^{U,D,E}$ ¹ are (see appendix B for details)

$$\xi_N^{U(D)} = \left(V_{R(L)}^{U(D)} \right)^{-1} \xi^{U(D)} V_{L(R)}^{U(D)} , \quad \xi_N^E = (V_L^E)^{-1} \xi^E V_R^E . \quad (3.2)$$

On the other hand for the charged FC couplings we have

$$\begin{aligned} \xi_{Ch}^U &= \xi_N^U V_{CKM} , \\ \xi_{Ch}^D &= V_{CKM} \xi_N^D . \end{aligned} \quad (3.3)$$

The charged couplings appear as a linear combination of neutral FC couplings multiplied by some CKM matrix elements which is indeed a particular form peculiar to model III (see [61] for details).

It is now better to summarize the basic steps for the calculation of the matrix element for the inclusive $b \rightarrow s \tau^+ \tau^-$ decay process in the following steps:

¹ In the rest of all discussions we denote $\xi_{Neutral}^{U,D,E}$ as $\xi_N^{U,D,E}$.

- The calculation of the full theory including the NHB effects which comes from the interactions of neutral Higgs bosons H^0 , h^0 and A^0 with τ lepton.
- Overcoming the logarithmic divergences by using the on-shell renormalization scheme. The renormalized vertex function is taken as

$$\Gamma_N^R(p^2) = \Gamma_N^0(p^2) + \Gamma_N^C, \quad (3.4)$$

with the renormalization condition

$$\Gamma_N^R(p^2 = m_N^2) = 0, \quad (3.5)$$

and from Eq. (3.4) and Eq. (3.5) we get the counter terms. Here the suffix N denotes the neutral Higgs bosons, H^0 , h^0 and A^0 and p is the momentum transfer. Note that the self energy diagrams do not contribute in this scheme.

- Integrating out the heavy degrees of freedom, namely in this case t quark, W^\pm , H^\pm , H^0 , h^0 , and A^0 bosons and getting the effective theory.
- Performing the QCD corrections through matching the full theory with the effective low energy one at the high scale $\mu = m_W$ and by evaluating the Wilson coefficients from m_W down to the lower scale $\mu \sim O(m_b)^2$.
- Obtaining the effective Hamiltonian relevant for the considered process $b \rightarrow s \tau^+ \tau^-$ given by

$$\mathcal{H}_{eff} = -4 \frac{G_F}{\sqrt{2}} V_{tb} V_{ts}^* \left\{ \sum_i C_i(\mu) O_i(\mu) + \sum_i C_{Q_i}(\mu) Q_i(\mu) \right\}, \quad (3.6)$$

where O_i are current–current ($i = 1, 2$), penguin ($i = 3, \dots, 6$), magnetic penguin ($i = 7, 8$) and semileptonic ($i = 9, 10$) operators. Here $C_i(\mu)$ are the Wilson coefficients renormalized at the scale μ . The additional operators Q_i ($i = 1, \dots, 10$) are due to the NHB exchange diagrams and $C_{Q_i}(\mu)$ are their Wilson coefficients.

² We choose the higher scale as $\mu = m_W$ since the evaluation from the scale $\mu = m_{H^\pm}$ to $\mu = m_W$ give negligible contribution to the Wilson coefficients ($\sim 5\%$).

The explicit form of the operator basis in the 2HDM (model III) for the process is [41, 62, 63]

$$\begin{aligned}
O_1 &= (\bar{s}_{L\alpha}\gamma_\mu c_{L\beta})(\bar{c}_{L\beta}\gamma^\mu b_{L\alpha}), \\
O_2 &= (\bar{s}_{L\alpha}\gamma_\mu c_{L\alpha})(\bar{c}_{L\beta}\gamma^\mu b_{L\beta}), \\
O_3 &= (\bar{s}_{L\alpha}\gamma_\mu b_{L\alpha}) \sum_{q=u,d,s,c,b} (\bar{q}_{L\beta}\gamma^\mu q_{L\beta}), \\
O_4 &= (\bar{s}_{L\alpha}\gamma_\mu b_{L\beta}) \sum_{q=u,d,s,c,b} (\bar{q}_{L\beta}\gamma^\mu q_{L\alpha}), \\
O_5 &= (\bar{s}_{L\alpha}\gamma_\mu b_{L\alpha}) \sum_{q=u,d,s,c,b} (\bar{q}_{R\beta}\gamma^\mu q_{R\beta}), \\
O_6 &= (\bar{s}_{L\alpha}\gamma_\mu b_{L\beta}) \sum_{q=u,d,s,c,b} (\bar{q}_{R\beta}\gamma^\mu q_{R\alpha}), \\
O_7 &= \frac{e}{16\pi^2} \bar{s}_\alpha \sigma_{\mu\nu} (m_b R + m_s L) b_\alpha \mathcal{F}^{\mu\nu}, \\
O_8 &= \frac{g}{16\pi^2} \bar{s}_\alpha T_{\alpha\beta}^a \sigma_{\mu\nu} (m_b R + m_s L) b_\beta \mathcal{G}^{a\mu\nu}, \\
O_9 &= \frac{e}{16\pi^2} (\bar{s}_{L\alpha}\gamma_\mu b_{L\alpha})(\bar{\tau}\gamma^\mu \tau), \\
O_{10} &= \frac{e}{16\pi^2} (\bar{s}_{L\alpha}\gamma_\mu b_{L\alpha})(\bar{\tau}\gamma^\mu \gamma_5 \tau), \\
Q_1 &= \frac{e^2}{16\pi^2} (\bar{s}_L^\alpha b_R^\alpha) (\bar{\tau}\tau), \\
Q_2 &= \frac{e^2}{16\pi^2} (\bar{s}_L^\alpha b_R^\alpha) (\bar{\tau}\gamma_5 \tau), \\
Q_3 &= \frac{g^2}{16\pi^2} (\bar{s}_L^\alpha b_R^\alpha) \sum_{q=u,d,s,c,b} (\bar{q}_L^\beta q_R^\beta), \\
Q_4 &= \frac{g^2}{16\pi^2} (\bar{s}_L^\alpha b_R^\alpha) \sum_{q=u,d,s,c,b} (\bar{q}_R^\beta q_L^\beta), \\
Q_5 &= \frac{g^2}{16\pi^2} (\bar{s}_L^\alpha b_R^\beta) \sum_{q=u,d,s,c,b} (\bar{q}_L^\beta q_R^\alpha), \\
Q_6 &= \frac{g^2}{16\pi^2} (\bar{s}_L^\alpha b_R^\beta) \sum_{q=u,d,s,c,b} (\bar{q}_R^\beta q_L^\alpha), \\
Q_7 &= \frac{g^2}{16\pi^2} (\bar{s}_L^\alpha \sigma^{\mu\nu} b_R^\alpha) \sum_{q=u,d,s,c,b} (\bar{q}_L^\beta \sigma_{\mu\nu} q_R^\beta), \\
Q_8 &= \frac{g^2}{16\pi^2} (\bar{s}_L^\alpha \sigma^{\mu\nu} b_R^\alpha) \sum_{q=u,d,s,c,b} (\bar{q}_R^\beta \sigma_{\mu\nu} q_L^\beta), \\
Q_9 &= \frac{g^2}{16\pi^2} (\bar{s}_L^\alpha \sigma^{\mu\nu} b_R^\beta) \sum_{q=u,d,s,c,b} (\bar{q}_L^\beta \sigma_{\mu\nu} q_R^\alpha),
\end{aligned}$$

$$Q_{10} = \frac{g^2}{16\pi^2} (\bar{s}_L^\alpha \sigma^{\mu\nu} b_R^\beta) \sum_{q=u,d,s,c,b} (\bar{q}_R^\beta \sigma_{\mu\nu} q_L^\alpha), \quad (3.7)$$

where α and β are $SU(3)$ color indices and $\mathcal{F}^{\mu\nu}$ and $\mathcal{G}^{\mu\nu}$ are the field strength tensors of the electromagnetic and strong interactions, respectively. Note that there are also flipped chirality partners of these operators, which can be obtained by interchanging L and R in the basis given above in model III. However, we do not present them here since the corresponding Wilson coefficients are negligible.

Additionally the initial values of the Wilson coefficients for the relevant process in the SM are [62]

$$\begin{aligned} C_{1,3,\dots,6}^{SM}(m_W) &= 0, \\ C_2^{SM}(m_W) &= 1, \\ C_7^{SM}(m_W) &= \frac{3x_t^3 - 2x_t^2}{4(x_t - 1)^4} \ln x_t + \frac{-8x_t^3 - 5x_t^2 + 7x_t}{24(x_t - 1)^3}, \\ C_8^{SM}(m_W) &= -\frac{3x_t^2}{4(x_t - 1)^4} \ln x_t + \frac{-x_t^3 + 5x_t^2 + 2x_t}{8(x_t - 1)^3}, \\ C_9^{SM}(m_W) &= -\frac{1}{\sin^2 \theta_W} B(x_t) + \frac{1 - 4 \sin^2 \theta_W}{\sin^2 \theta_W} C(x_t) - D(x_t) + \frac{4}{9}, \\ C_{10}^{SM}(m_W) &= \frac{1}{\sin^2 \theta_W} (B(x_t) - C(x_t)), \\ C_{Q_i}^{SM}(m_W) &= 0 \quad i = 1, \dots, 10, \end{aligned} \quad (3.8)$$

where $x_t = m_t^2/m_W^2$ and the implicit functions $B(x_t)$, $C(x_t)$ and $D(x_t)$ are

$$\begin{aligned} B(x_t) &= \frac{x_t}{4(x_t - 1)} - \frac{x_t \ln x_t}{4(x_t - 1)^2}, \\ C(x_t) &= \frac{-x_t(x_t - 6)}{8(x_t - 1)} - \frac{x_t(3x_t + 2)}{8(x_t - 1)^2} \ln x_t, \\ D(x_t) &= \frac{19x_t^3 - 25x_t^2}{36(x_t - 1)^3} + \frac{6x_t^4 - 60x_t^3 + 108x_t^2 - 64x_t + 16}{36(x_t - 1)^4} \ln x_t, \end{aligned} \quad (3.9)$$

and for the additional part due to charged Higgs bosons are

$$\begin{aligned} C_{1,\dots,6}^H(m_W) &= 0, \\ C_7^H(m_W) &= Y^2 F_1(y_t) + XY F_2(y_t), \\ C_8^H(m_W) &= Y^2 G_1(y_t) + XY G_2(y_t), \\ C_9^H(m_W) &= Y^2 H_1(y_t), \\ C_{10}^H(m_W) &= Y^2 L_1(y_t), \end{aligned} \quad (3.10)$$

where

$$\begin{aligned} X &= \frac{1}{m_b} \left(\bar{\xi}_{N,bb}^D + \bar{\xi}_{N,sb}^D \frac{V_{ts}}{V_{tb}} \right), \\ Y &= \frac{1}{m_t} \left(\bar{\xi}_{N,tt}^U + \bar{\xi}_{N,tc}^U \frac{V_{cs}^*}{V_{ts}^*} \right). \end{aligned} \quad (3.11)$$

The inclusion of the NHB effects brings new operators as stated before and the corresponding Wilson coefficients read as

$$\begin{aligned} C_{Q_2}^{A^0}((\bar{\xi}_{N,tt}^U)^3) &= \frac{\bar{\xi}_{N,\tau\tau}^D (\bar{\xi}_{N,tt}^U)^3 m_b y_t (\Theta_5(y_t) z_A - \Theta_1(z_A, y_t))}{32\pi^2 m_{A^0}^2 m_t \Theta_1(z_A, y_t) \Theta_5(y_t)}, \\ C_{Q_2}^{A^0}((\bar{\xi}_{N,tt}^U)^2) &= \frac{\bar{\xi}_{N,\tau\tau}^D (\bar{\xi}_{N,tt}^U)^2 \bar{\xi}_{N,bb}^D}{32\pi^2 m_{A^0}^2 \Theta_1(z_A, y_t) \Theta_5(y_t)} \left(y_t (\Theta_1(z_A, y_t) - \Theta_5(y_t)(xy + z_A)) \right. \\ &\quad \left. - 2\Theta_1(z_A, y_t) \Theta_5(y_t) \ln \left[\frac{z_A \Theta_5(y_t)}{\Theta_1(z_A, y_t)} \right] \right), \\ C_{Q_2}^{A^0}(\bar{\xi}_{N,tt}^U) &= \frac{g^2 \bar{\xi}_{N,\tau\tau}^D \bar{\xi}_{N,tt}^U m_b x_t}{64\pi^2 m_{A^0}^2 m_t} \left(\frac{2}{\Theta_5(x_t)} - \frac{xyx_t + 2z_A}{\Theta_1(z_A, x_t)} - 2 \ln \left[\frac{z_A \Theta_5(x_t)}{\Theta_1(z_A, x_t)} \right] \right. \\ &\quad \left. - \frac{(x-1)x_t(y_t/z_A - 1) - (1+x)y_t}{(\Theta_6 - (x-y)(x_t - y_t))(\Theta_3(z_A) + (x-y)(x_t - y_t)z_A)} \right. \\ &\quad \left. - \frac{x(y_t + x_t(1 - y_t/z_A)) - 2y_t}{\Theta_6 \Theta_3(z_A)} \right), \\ C_{Q_2}^{A^0}(\bar{\xi}_{N,bb}^D) &= \frac{g^2 \bar{\xi}_{N,\tau\tau}^D \bar{\xi}_{N,bb}^D}{64\pi^2 m_{A^0}^2} \left(1 - \frac{x_t^2 y_t + 2y(x-1)x_t y_t - z_A(x_t^2 + \Theta_6)}{\Theta_3(z_A)} \right. \\ &\quad \left. + \frac{x_t^2(1 - y_t/z_A)}{\Theta_6} + 2 \ln \left[\frac{z_A \Theta_6}{\Theta_2(z_A, x)} \right] \right), \\ C_{Q_1}^{H^0}((\bar{\xi}_{N,tt}^U)^2) &= \frac{g^2 (\bar{\xi}_{N,tt}^U)^2 m_b m_\tau}{64\pi^2 m_{H^0}^2 m_t^2} \left(\frac{x_t(1-2y)y_t}{\Theta_5(y_t)} \right. \\ &\quad + \frac{(-1 + 2\cos^2 \theta_W)(-1+x+y)y_t}{\cos^2 \theta_W \Theta_4(y_t)} + \frac{z_H \Theta_1(z_H, y_t) xy_t}{\cos^2 \theta_W \Theta_1(z_H, y_t) \Theta_7} \\ &\quad \left. + \frac{z_H \cos^2 \theta_W (-2x^2(-1+x_t)yy_t^2 + xx_t yy_t^2 - \Theta_8 z_H)}{\cos^2 \theta_W \Theta_1(z_H, y_t) \Theta_7} \right), \\ C_{Q_1}^{H^0}(\bar{\xi}_{N,tt}^U) &= \frac{g^2 \bar{\xi}_{N,tt}^U \bar{\xi}_{N,bb}^D m_\tau}{64\pi^2 m_{H^0}^2 m_t} \left(\frac{(-1 + 2\cos^2 \theta_W) y_t}{\cos^2 \theta_W \Theta_4(y_t)} - \frac{x_t y_t}{\Theta_5(y_t)} + \frac{x_t y_t (xy - z_H)}{\Theta_1(z_H, y_t)} \right. \\ &\quad \left. + \frac{(-1 + 2\cos^2 \theta_W) y_t z_H}{\cos^2 \theta_W \Theta_7} - 2x_t \ln \left[\frac{\Theta_5(y_t) z_H}{\Theta_1(z_H, y_t)} \right] \right), \\ C_{Q_1}^{H^0}(g^4) &= -\frac{g^4 m_b m_\tau x_t}{128\pi^2 m_{H^0}^2 m_t^2} \left(-1 + \frac{(-1+2x)x_t}{\Theta_5(x_t) + y(1-x_t)} + \frac{2x_t(-1+(2+x_t)y)}{\Theta_5(x_t)} \right) \end{aligned}$$

$$\begin{aligned}
& -\frac{4\cos^2\theta_W(-1+x+y)+x_t(x+y)}{\cos^2\theta_W\Theta_4(x_t)} + \frac{x_t(x(x_t(y-2z_H)-4z_H)+2z_H)}{\Theta_1(z_H, x_t)} \\
& + \frac{y_t((-1+x)x_tz_H + \cos^2\theta_W((3x-y)z_H + x_t(2y(x-1)-z_H(2-3x-y))))}{\cos^2\theta_W(\Theta_3(z_H) + x(x_t-y_t)z_H)} \\
& + 2\left(x_t \ln \left[\frac{\Theta_5(x_t)z_H}{\Theta_1(z_H, x_t)} \right] + \ln \left[\frac{x(y_t-x_t)z_H - \Theta_3(z_H)}{(\Theta_5(x_t) + y(1-x_t))y_tz_H} \right] \right), \tag{3.12}
\end{aligned}$$

$$C_{Q_1}^{h_0}((\bar{\xi}_{N,tt}^U)^3) = -\frac{\bar{\xi}_{N,\tau\tau}^D(\bar{\xi}_{N,tt}^U)^3 m_b y_t (\Theta_1(z_h, y_t)(2y-1) + \Theta_5(y_t)(2x-1)z_h)}{32\pi^2 m_{h_0}^2 m_t \Theta_1(z_h, y_t) \Theta_5(y_t)}$$

$$\begin{aligned}
C_{Q_1}^{h_0}((\bar{\xi}_{N,tt}^U)^2) &= \frac{\bar{\xi}_{N,\tau\tau}^D(\bar{\xi}_{N,tt}^U)^2}{32\pi^2 m_{h_0}^2} \left(\frac{\Theta_5(y_t)z_h(y_t-1)(x+y-1)}{\Theta_1(z_h)\Theta_5(y_t)} \right. \\
&\quad \left. - \frac{\Theta_1(z_h, y_t)(\Theta_5(y_t) + y_t)}{\Theta_1(z_h)\Theta_5(y_t)} - 2 \ln \left[\frac{z_h\Theta_5(y_t)}{\Theta_1(z_h)} \right] \right)
\end{aligned}$$

$$\begin{aligned}
C_{Q_1}^{h_0}(\bar{\xi}_{N,tt}^U) &= -\frac{g^2 \bar{\xi}_{N,\tau\tau}^D \bar{\xi}_{N,tt}^U m_b x_t}{64\pi^2 m_{h_0}^2 m_t} \left(\frac{2(-1+(2+x_t)y)}{\Theta_5(x_t)} - \frac{x_t(x-1)(y_t-z_h)}{\Theta_2'(z_h)} \right. \\
&\quad + 2 \ln \left[\frac{z_h\Theta_5(x_t)}{\Theta_1(z_h, x_t)} \right] + \frac{x(x_t(y-2z_h)-4z_h)+2z_h}{\Theta_1(z_h, x_t)} \\
&\quad - \frac{(1+x)y_tz_h}{xyx_t y_t + z_h((x-y)(x_t-y_t)-\Theta_6)} \\
&\quad + \frac{\Theta_9 + y_tz_h((x-y)(x_t-y_t)-\Theta_6)(2x-1)}{z_h\Theta_6(\Theta_6-(x-y)(x_t-y_t))} \\
&\quad \left. + \frac{x(y_tz_h + x_t(z_h-y_t)) - 2y_tz_h}{\Theta_2(z_h)} \right),
\end{aligned}$$

$$\begin{aligned}
C_{Q_1}^{h_0}(\bar{\xi}_{N,bb}^D) &= -\frac{g^2 \bar{\xi}_{N,\tau\tau}^D \bar{\xi}_{N,bb}^D}{64\pi^2 m_{h_0}^2} \left(\frac{yx_t y_t (xx_t^2(y_t-z_h) + \Theta_6 z_h(x-2))}{z_h\Theta_2(z_h)\Theta_6} \right. \\
&\quad \left. + 2 \ln \left[\frac{\Theta_6}{x_t y_t} \right] + 2 \ln \left[\frac{x_t y_t z_h}{\Theta_2(z_h)} \right] \right),
\end{aligned}$$

where

$$\begin{aligned}
\Theta_1(\omega, \lambda) &= -(-1+y-y\lambda)\omega - x(y\lambda + \omega - \omega\lambda), \\
\Theta_2(\omega) &= (x_t + y(1-x_t))y_t\omega - xx_t(yy_t + (y_t-1)\omega), \\
\Theta_2'(\omega) &= \Theta_2(\omega, x_t \leftrightarrow y_t), \\
\Theta_3(\omega) &= (x_t(-1+y)-y)y_t\omega + xx_t(yy_t + \omega(-1+y_t)), \\
\Theta_4(\omega) &= 1 - x + x\omega,
\end{aligned}$$

$$\begin{aligned}
\Theta_5(\lambda) &= x + \lambda(1 - x), \\
\Theta_6 &= (x_t + y(1 - x_t))y_t + xx_t(1 - y_t), \\
\Theta_7 &= (y(y_t - 1) - y_t)z_H + x(yy_t + (y_t - 1)z_H), \\
\Theta_8 &= y_t(2x^2(1 + x_t)(y_t - 1) + x_t(y(1 - y_t) + y_t) + x(2(1 - y + y_t) \\
&\quad + x_t(1 - 2y(1 - y_t) - 3y_t))), \\
\Theta_9 &= -x_t^2(-1 + x + y)(-y_t + x(2y_t - 1))(y_t - z_h), \\
&\quad - x_t y_t z_h(x(1 + 2x) - 2y) + y_t^2(x_t(x^2 - y(1 - x)) + (1 + x)(x - y)z_h),
\end{aligned} \tag{3.13}$$

and

$$x_t = \frac{m_t^2}{m_W^2}, \quad y_t = \frac{m_t^2}{m_{H^\pm}^2}, \quad z_H = \frac{m_t^2}{m_{H^0}^2}, \quad z_h = \frac{m_t^2}{m_{h^0}^2}, \quad z_A = \frac{m_t^2}{m_{A^0}^2}.$$

The explicit forms of the functions $F_{1(2)}(y_t)$, $G_{1(2)}(y_t)$, $H_1(y_t)$ and $L_1(y_t)$ appeared in Eq. (3.10) are given as

$$\begin{aligned}
F_1(y_t) &= \frac{y_t(7 - 5y_t - 8y_t^2)}{72(y_t - 1)^3} + \frac{y_t^2(3y_t - 2)}{12(y_t - 1)^4} \ln y_t, \\
F_2(y_t) &= \frac{y_t(5y_t - 3)}{12(y_t - 1)^2} + \frac{y_t(-3y_t + 2)}{6(y_t - 1)^3} \ln y_t, \\
G_1(y_t) &= \frac{y_t(-y_t^2 + 5y_t + 2)}{24(y_t - 1)^3} + \frac{-y_t^2}{4(y_t - 1)^4} \ln y_t, \\
G_2(y_t) &= \frac{y_t(y_t - 3)}{4(y_t - 1)^2} + \frac{y_t}{2(y_t - 1)^3} \ln y_t, \\
H_1(y_t) &= \frac{1 - 4\sin^2\theta_W}{\sin^2\theta_W} \frac{xy_t}{8} \left[\frac{1}{y_t - 1} - \frac{1}{(y_t - 1)^2} \ln y_t \right] \\
&\quad - y_t \left[\frac{47y_t^2 - 79y_t + 38}{108(y_t - 1)^3} - \frac{3y_t^3 - 6y_t + 4}{18(y_t - 1)^4} \ln y_t \right], \\
L_1(y_t) &= \frac{1}{\sin^2\theta_W} \frac{xy_t}{8} \left[-\frac{1}{y_t - 1} + \frac{1}{(y_t - 1)^2} \ln y_t \right].
\end{aligned} \tag{3.14}$$

Finally, the initial values of the coefficients in the model III are

$$\begin{aligned}
C_i^{2HDM}(m_W) &= C_i^{SM}(m_W) + C_i^H(m_W), \\
C_{Q_1}^{2HDM}(m_W) &= \int_0^1 dx \int_0^{1-x} dy (C_{Q_1}^{H^0}((\bar{\xi}_{N,tt}^U)^2) + C_{Q_1}^{H^0}(\bar{\xi}_{N,tt}^U) + C_{Q_1}^{H^0}(g^4) \\
&\quad + C_{Q_1}^{h^0}((\bar{\xi}_{N,tt}^U)^3) + C_{Q_1}^{h^0}((\bar{\xi}_{N,tt}^U)^2) + C_{Q_1}^{h^0}(\bar{\xi}_{N,tt}^U) + C_{Q_1}^{h^0}(\bar{\xi}_{N,b\bar{b}}^D)), \\
C_{Q_2}^{2HDM}(m_W) &= \int_0^1 dx \int_0^{1-x} dy (C_{Q_2}^{A^0}((\bar{\xi}_{N,tt}^U)^3) + C_{Q_2}^{A^0}((\bar{\xi}_{N,tt}^U)^2)
\end{aligned}$$

$$\begin{aligned}
& + C_{Q_2}^{A^0}(\bar{\xi}_{N,tt}^U) + C_{Q_2}^{A^0}(\bar{\xi}_{N,b\bar{b}}^D), \\
C_{Q_3}^{2HDM}(m_W) &= \frac{m_b}{m_\tau \sin^2 \theta_W} (C_{Q_1}^{2HDM}(m_W) + C_{Q_2}^{2HDM}(m_W)), \\
C_{Q_4}^{2HDM}(m_W) &= \frac{m_b}{m_\tau \sin^2 \theta_W} (C_{Q_1}^{2HDM}(m_W) - C_{Q_2}^{2HDM}(m_W)), \\
C_{Q_i}^{2HDM}(m_W) &= 0, \quad i = 5, \dots, 10.
\end{aligned} \tag{3.15}$$

Here we present C_{Q_1} and C_{Q_2} in terms of the Feynman parameters x and y since the integrated results are extremely large and are not suitable to be explicitly included. Using these initial values, we can calculate the coefficients $C_i^{2HDM}(\mu)$ and $C_{Q_i}^{2HDM}(\mu)$ at any lower scale in the effective theory with five quarks, namely u, c, d, s, b and use the renormalization group to sum the large logarithms and their evaluations are similar to the SM case [38, 58, 63, 64].

The Wilson coefficients playing the essential role in this process are $C_7^{2HDM}(\mu)$, $C_9^{2HDM}(\mu)$, $C_{10}^{2HDM}(\mu)$, $C_{Q_1}^{2HDM}(\mu)$ and $C_{Q_2}^{2HDM}(\mu)$ and the others merely enter into expressions due to operator mixing. The operators O_5, O_6 give a contribution to the leading order matrix element of $b \rightarrow s\gamma$ and the magnetic moment type coefficient $C_7^{eff}(\mu)$ is redefined in the naive dimensional reduction (NDR) scheme as [65]

$$C_7^{eff}(\mu) = C_7^{2HDM}(\mu) + Q_d (C_5^{2HDM}(\mu) + N_c C_6^{2HDM}(\mu)),$$

where N_c is the number of colors and Q_d is the charge for down-type quarks. Furthermore the next to leading order (NLO) corrected coefficient $C_7^{2HDM}(\mu)$ is expressed as

$$C_7^{2HDM}(\mu) = C_7^{LO,2HDM}(\mu) + \frac{\alpha_s(\mu)}{4\pi} C_7^{(1),2HDM}(\mu),$$

where the leading order (LO) QCD corrected Wilson coefficient $C_7^{LO,2HDM}(\mu)$ is

$$\begin{aligned}
C_7^{LO,2HDM}(\mu) &= \eta^{16/23} C_7^{2HDM}(m_W) + (8/3)(\eta^{14/23} - \eta^{16/23}) C_8^{2HDM}(m_W) \\
&+ C_2^{2HDM}(m_W) \sum_{i=1}^8 h_i \eta^{a_i},
\end{aligned} \tag{3.16}$$

and $\eta = \alpha_s(m_W)/\alpha_s(\mu)$, h_i and a_i are the numbers which appear during the evaluation [38] and $C_7^{(1),2HDM}(\mu)$ is the α_s correction to the LO result, the explicit form of which can be found in [66, 67].

Since $O_2 = (\bar{s}_{L\alpha}\gamma_\mu c_{L\alpha})(\bar{c}_{L\beta}\gamma^\mu b_{L\beta})$ produce dilepton via virtual photon, the corresponding Wilson coefficient $C_2(\mu)$ and the Wilson coefficients $C_1(\mu), C_3(\mu), \dots, C_6(\mu)$ induced by the operator mixing give contributions to the Wilson coefficient C_9^{eff} . The perturbative part of $C_9^{eff}(\mu)$ is defined as

$$\begin{aligned}
C_9^{pert}(\mu) &= C_9^{2HDM}(\mu) \\
&+ h(z, s) (3C_1(\mu) + C_2(\mu) + 3C_3(\mu) + C_4(\mu) + 3C_5(\mu) + C_6(\mu)) \\
&- \frac{1}{2}h(1, s) (4C_3(\mu) + 4C_4(\mu) + 3C_5(\mu) + C_6(\mu)) \\
&- \frac{1}{2}h(0, s) (C_3(\mu) + 3C_4(\mu)) + \frac{2}{9}(3C_3(\mu) \\
&+ C_4(\mu) + 3C_5(\mu) + C_6(\mu)), \tag{3.17}
\end{aligned}$$

where $z = m_c/m_b$, $s = q^2/m_b^2$, and the function $h(z, s)$ arises from the one loop contribution of the four quark operators O_1, \dots, O_6 and can be given by

$$h(u, s) = -\frac{8}{9}\ln\frac{m_b}{\mu} - \frac{8}{9}\ln u + \frac{8}{27} + \frac{4}{9}x \tag{3.18}$$

$$\begin{aligned}
&- \frac{2}{9}(2+x)|1-x|^{1/2} \begin{cases} \left(\ln\left|\frac{\sqrt{1-x}+1}{\sqrt{1-x}-1}\right| - i\pi\right), & \text{for } x \equiv \frac{4u^2}{s} < 1 \\ 2 \arctan \frac{1}{\sqrt{x-1}}, & \text{for } x \equiv \frac{4u^2}{s} > 1, \end{cases} \\
h(0, s) &= \frac{8}{27} - \frac{8}{9}\ln\frac{m_b}{\mu} - \frac{4}{9}\ln s + \frac{4}{9}i\pi, \tag{3.19}
\end{aligned}$$

with $u = m_c/m_b$. In addition to the short distance part there also exist long distance (LD) effects due to the real $\bar{c}c$ in the intermediate states, i.e. the cascade process $B \rightarrow K^*\psi_i \rightarrow K^*\tau^+\tau^-$ where $i = 1, \dots, 6$. AMM approach [68] is one of the way of taking these intermediate states into account. In this method the resonance $\bar{c}c$ contribution is parameterized using a Breit-Wigner form of the resonance propagator and this contribution is added to the perturbative one to form LO QCD corrected $C_9^{eff}(\mu)$ as

$$C_9^{eff}(\mu) = C_9^{pert}(\mu) + Y_{reson}(s), \tag{3.20}$$

where $Y_{reson}(\mu, s)$ contains both real and imaginary parts³ and is of the form in the NDR scheme

$$Y_{reson}(\mu, s) = -\frac{3}{\alpha_{em}^2}\kappa \sum_{V_i=\psi_i} \frac{\pi\Gamma(V_i \rightarrow \tau^+\tau^-)m_{V_i}}{q^2 - m_{V_i}^2 + im_{V_i}\Gamma_{V_i}} (3C_1(\mu) + C_2(\mu))$$

³ The imaginary part arises when the c-quark in the loop is on the mass shell.

$$+ 3C_3(\mu) + C_4(\mu) + 3C_5(\mu) + C_6(\mu)), \quad (3.21)$$

where the phenomenological parameter $\kappa = 2.3$ is chosen to be able to reproduce the correct value of the branching ratio $Br(B \rightarrow J/\psi X \rightarrow X l \bar{l}) = Br(B \rightarrow J/\psi X) Br(J/\psi \rightarrow l \bar{l})$ [35]. Finally the Wilson coefficients $C_{Q_i}(\mu)$ at any scale can be related to the ones at the scale $\mu = m_W$ as [41]

$$C_{Q_i}(\mu) = \eta^{-12/23} C_{Q_i}(m_W), \quad i = 1, 2. \quad (3.22)$$

The relevant one-loop diagrams contributing to this decay in the SM are given in Fig. (3.1) and additional contributions from 2HDM are shown in Fig. (3.2). Finally if we take into account the contributions coming from NHB we get the diagrams depicted in Fig. (3.3).

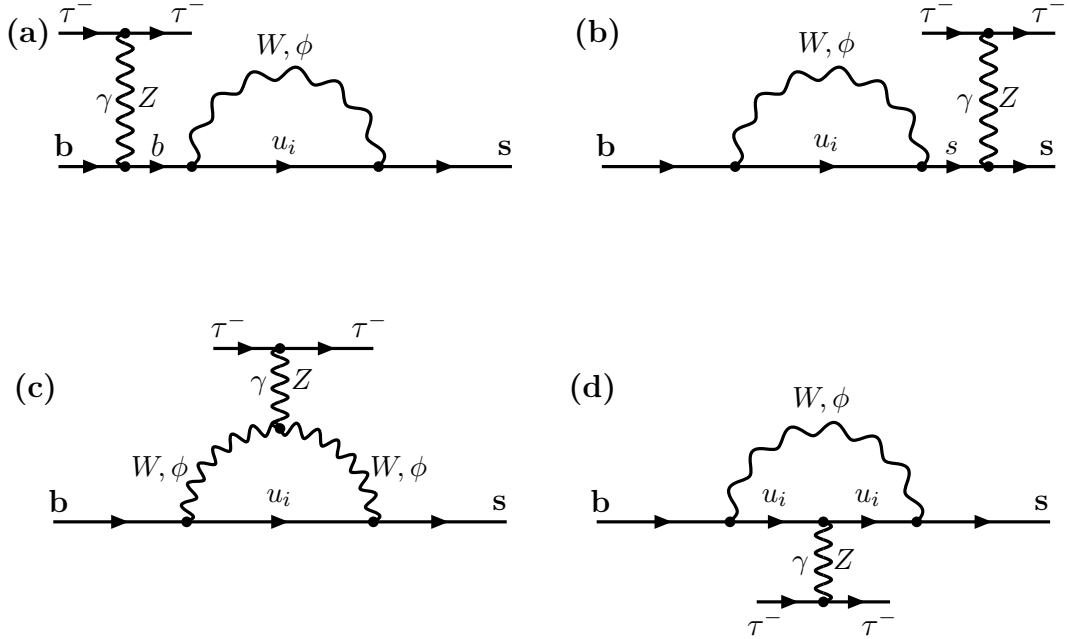


Figure 3.1: The one-loop Feynman diagrams contributing the decay $b \rightarrow s \tau^+ \tau^-$ in the SM.

We now turn our attention back to the decay amplitude of the decay $b \rightarrow s \tau^+ \tau^-$. Neglecting the strange quark mass the effective Hamiltonian Eq. (3.6)

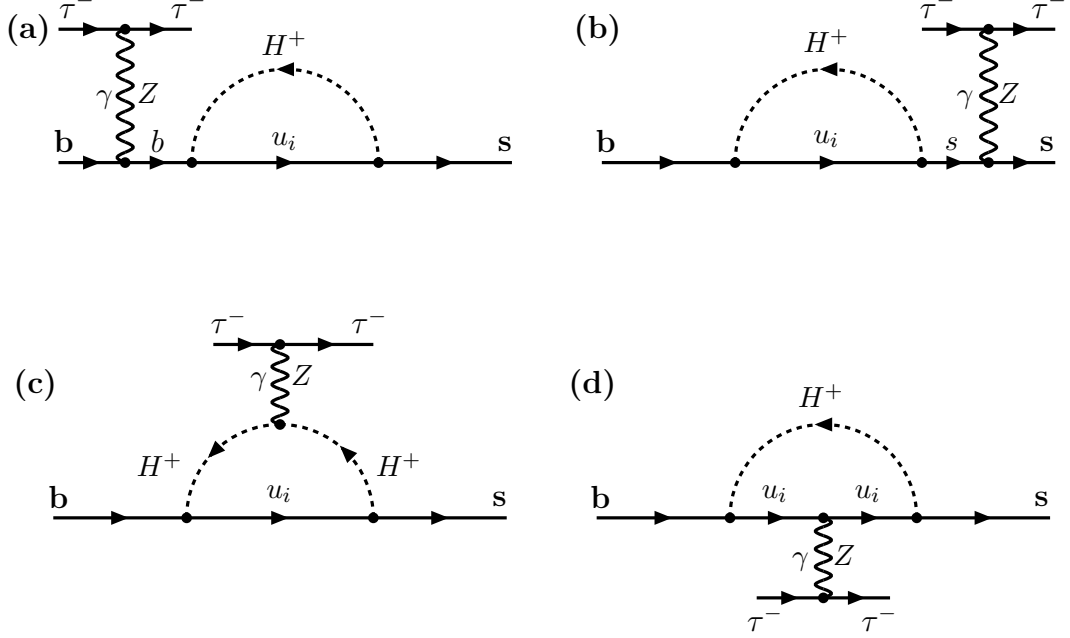


Figure 3.2: The additional one-loop diagrams contributing the process $b \rightarrow s \tau^+ \tau^-$ obtained within the framework of model III without NHB contributions.

leads to the following QCD corrected amplitude for the inclusive $b \rightarrow s \tau^+ \tau^-$ decay in the model III

$$\mathcal{M} = \frac{\alpha_{em} G_F}{\sqrt{2} \pi} V_{tb} V_{ts}^* \left\{ C_9^{eff} (\bar{s} \gamma_\mu P_L b) \bar{\tau} \gamma_\mu \tau + C_{10} (\bar{s} \gamma_\mu P_L b) \bar{\tau} \gamma_\mu \gamma_5 \tau \right. \\ \left. - 2C_7^{eff} \frac{m_b}{q^2} (\bar{s} i \sigma_{\mu\nu} q_\nu P_R b) \bar{\tau} \gamma_\mu \tau + C_{Q_1} (\bar{s} P_R b) \bar{\tau} \tau + C_{Q_2} (\bar{s} P_R b) \bar{\tau} \gamma_5 \tau \right\}. \quad (3.23)$$

Now our aim is to look at the decay in the hadronic level. To calculate the decay width, branching ratio, and some more physical quantities for the exclusive $B \rightarrow K^* \tau^+ \tau^-$ decay, we need the matrix element of the decay which can be obtained by inserting the inclusive level effective Hamiltonian in Eq. (3.6) between initial, B, and final, K^* , hadronic states. The needed matrix element structures are of the form $\langle K^* | \bar{s} \gamma_\mu (1 \pm \gamma_5) b | B \rangle$, $\langle K^* | \bar{s} i \sigma_{\mu\nu} q^\nu (1 + \gamma_5) b | B \rangle$, and

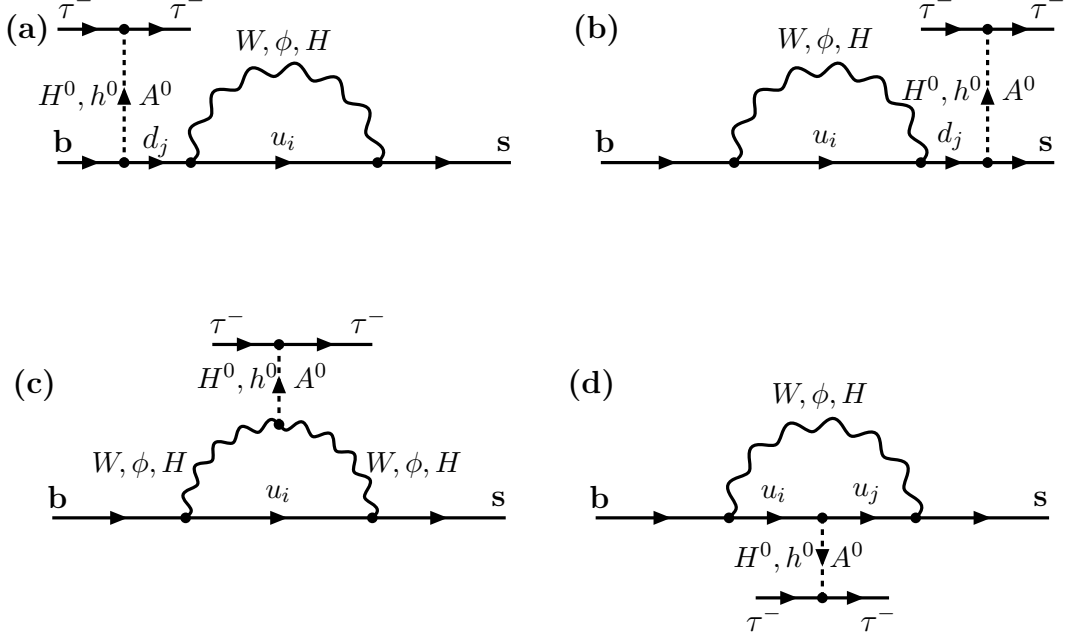


Figure 3.3: The one-loop diagrams contributing the process $b \rightarrow s\tau^+\tau^-$ within the framework of model III by including NHB contributions

$\langle K^* | \bar{s}(1 \pm \gamma_5)b | B \rangle$. These are calculated by using some non-perturbative methods such as QCD sum rules, light-cone QCD sum rules, etc., These matrix elements can be parameterized in terms of the form factors as follows (see [45])

$$\begin{aligned}
\langle K^*(p_{K^*}, \epsilon^*) | \bar{s}\gamma_\mu(1 - \gamma_5)q | B(p_B) \rangle &= -\epsilon_{\mu\nu\rho\sigma} \epsilon^{*\nu} p^\rho q^\sigma \frac{2V(q^2)}{m_B + m_{K^*}} \\
&\quad -i\epsilon_\mu^* (m_B + m_{K^*}) A_1(q^2) + i(\epsilon^* \cdot q)(p_B + p_{K^*})_\mu \frac{A_2(q^2)}{m_B + m_{K^*}} \\
&\quad +i(\epsilon^* \cdot q) \frac{2m_{K^*}}{q^2} [A_3(q^2) - A_0(q^2)] q_\mu,
\end{aligned} \tag{3.24}$$

$$\begin{aligned}
\langle K^*(p_{K^*}, \epsilon^*) | \bar{s}i\sigma_{\mu\nu}q^\nu(1 + \gamma_5)b | B(p_B) \rangle &= 4\epsilon_{\mu\nu\rho\sigma} \epsilon^{*\nu} p_{K^*}^\rho q^\sigma T_1(q^2) \\
&\quad + 2i \left[\epsilon_\mu^* ((p_B + p_{K^*}) \cdot q) - (\epsilon^* \cdot q)(p_B + p_{K^*})_\mu \right] T_2(q^2) \\
&\quad + 2i(\epsilon^* \cdot q) \left[q_\mu - \frac{q^2}{p_B q + p_{K^*} q} (p_B + p_{K^*})_\mu \right] T_3(q^2),
\end{aligned} \tag{3.25}$$

$$\langle K^*(p_{K^*}, \epsilon^*) | \bar{s}(1 \pm \gamma_5)b | B(p_B) \rangle = \mp i \frac{2m_{K^*}}{m_b} A_0(q^2) (\epsilon^* \cdot q), \tag{3.26}$$

where ϵ_μ^* is the polarization vector of K^* , p_B and p_{K^*} are four momentum of B and K^* mesons, respectively. V , A_i and T_i ($i = 1, 2, 3$) are the relevant form factors and $q = p_B - p_{K^*}$. The form factor $A_3(q^2)$ can in fact be written as a linear combination of the form factors A_1 and A_2 of the form (see [47])

$$A_3(q^2) = \frac{m_B + m_{K^*}}{2m_{K^*}} A_1(q^2) - \frac{m_B - m_{K^*}}{2m_{K^*}} A_2(q^2) , \quad (3.27)$$

with the condition $A_3(0) = A_0(0)$. Therefore, the matrix element of the $B \rightarrow K^* \tau^+ \tau^-$ decay can be written in a compact form as

$$\begin{aligned} \mathcal{M} = & -\frac{G\alpha_{em}}{2\sqrt{2}\pi} V_{tb} V_{ts}^* \left\{ \bar{\tau} \gamma^\mu \tau \left[2A \epsilon_{\mu\nu\rho\sigma} \epsilon^{*\nu} p_{K^*}^\rho q^\sigma + iB_1 \epsilon_\mu^* - iB_2 (\epsilon^* \cdot q) (p_B + p_{K^*})_\mu \right. \right. \\ & - iB_3 (\epsilon^* \cdot q) q_\mu \left. \right] + \bar{\tau} \gamma^\mu \gamma_5 \tau \left[2C \epsilon_{\mu\nu\rho\sigma} \epsilon^{*\nu} p_{K^*}^\rho q^\sigma + iD_1 \epsilon_\mu^* - iD_2 (\epsilon^* \cdot q) (p_B + p_{K^*})_\mu \right. \\ & \left. \left. - iD_3 (\epsilon^* \cdot q) q_\mu \right] + i \bar{\tau} \tau F(\epsilon^* \cdot q) + i \bar{\tau} \gamma_5 \tau G(\epsilon^* \cdot q) \right\} , \end{aligned} \quad (3.28)$$

where A , C , F and G , B_i and D_i , $i = 1, 2, 3$ are functions of Wilson coefficients and form factors of the relevant process. Their explicit forms are

$$\begin{aligned} A &= -C_9^{eff} \frac{V}{m_B + m_{K^*}} - 4C_7^{eff} \frac{m_b}{q^2} T_1, \\ B_1 &= -C_9^{eff} (m_B + m_{K^*}) A_1 - 4C_7^{eff} \frac{m_b}{q^2} (m_B^2 - m_{K^*}^2) T_2, \\ B_2 &= -C_9^{eff} \frac{A_2}{m_B + m_{K^*}} - 4C_7^{eff} \frac{m_b}{q^2} \left(T_2 + \frac{q^2}{m_B^2 - m_{K^*}^2} T_3 \right), \\ B_3 &= -C_9^{eff} \frac{2m_{K^*}}{q^2} (A_3 - A_0) + 4C_7^{eff} \frac{m_b}{q^2} T_3, \\ C &= -C_{10} \frac{V}{m_B + m_{K^*}}, \\ D_1 &= -C_{10} (m_B + m_{K^*}) A_1, \\ D_2 &= -C_{10} \frac{A_2}{m_B + m_{K^*}}, \\ D_3 &= -C_{10} \frac{2m_{K^*}}{q^2} (A_3 - A_0), \\ F &= C_{Q1} \frac{2m_{K^*}}{m_b} A_0, \\ G &= C_{Q2} \frac{2m_{K^*}}{m_b} A_0, \end{aligned} \quad (3.29)$$

We use the following q^2 dependent parametrization which is calculated in the framework of light-cone QCD sum rules in [48] to calculate the hadronic form

factors V , A_1 , A_2 , A_0 , T_1 , T_2 and T_3 :

$$F(q^2) = \frac{F(0)}{1 - a_F \frac{q^2}{m_B^2} + b_F \left(\frac{q^2}{m_B^2}\right)^2}, \quad (3.30)$$

where the values of parameters $F(0)$, a_F and b_F are listed in Table (3.1).

Table 3.1: The values of parameters existing in Eq. (3.30) for the various form factors appearing in the $B \rightarrow K^*$ matrix elements.

	$F(0)$	a_F	b_F
A_1	0.34 ± 0.05	0.60	-0.023
A_2	0.28 ± 0.04	1.18	0.281
V	0.46 ± 0.07	1.55	0.575
T_1	0.19 ± 0.03	1.59	0.615
T_2	0.19 ± 0.03	0.49	-0.241
T_3	0.13 ± 0.02	1.20	0.098

After getting the matrix element of the relevant decay process we are ready to calculate the forward-backward asymmetry of the lepton pair and CP violating asymmetry in forward-backward asymmetry for $B \rightarrow K^* \tau^+ \tau^-$ decay.

The forward-backward asymmetry A_{FB} of the lepton pair is a measurable physical quantity providing important clues to test the theoretical models used. The differential A_{FB} is defined as:

$$A_{FB} = \frac{\int_0^1 dz \frac{d\Gamma}{dz} - \int_{-1}^0 dz \frac{d\Gamma}{dz}}{\int_0^1 dz \frac{d\Gamma}{dz} + \int_{-1}^0 dz \frac{d\Gamma}{dz}}, \quad (3.31)$$

with $z = \cos \theta$, where θ is the angle between the momentum of B meson and that of τ^- in the center of mass frame of the dileptons $\tau^+ \tau^-$. With the help of the well-known equation for the differential decay width

$$d\Gamma = \frac{(2\pi)^4}{2M} |\mathcal{M}|^2 \delta^4(P - \sum_{i=1}^n p_i) \prod_{i=1}^n \frac{d^3 p_i}{(2\pi)^3 2E_i}, \quad (3.32)$$

where M is the mass of the decaying particle, P is its momentum, and p_i and E_i are the momenta and the energies of the final particles, and by using the

matrix element in Eq. (3.28) together with Eqs. (3.31) and (3.32) we can get the differential A_{FB} as of the form

$$A_{FB} = \frac{\int ds E(s)}{\int ds D(s)}, \quad (3.33)$$

where

$$\begin{aligned} E(s) = & 6 m_B \lambda v^2 \left\{ \frac{1}{m_b r (r-1)} \left(4 m_B m_\tau \text{Re}(C_7^{eff*} C_{Q_1}) (m_b(\sqrt{r}-1) A_2(q^2) \right. \right. \\ & + m_b(\sqrt{r}+1) A_1(q^2) - 2 m_B s T_3(q^2)) ((r-1)(3r-s+1) T_2(q^2) \\ & + (r^2 + (s-1)^2 - 2r(s+1)) T_3(q^2)) \Big) \\ & - \frac{1}{m_b^2 r (1+\sqrt{r})} \left(m_B^2 m_\tau \text{Re}(C_9^{eff*} C_{Q_1}) (m_b(\sqrt{r}-1) A_2(q^2) \right. \\ & + m_b(\sqrt{r}+1) A_1(q^2) - 2 m_B s T_3(q^2)) ((1+\sqrt{r})^2 (r+s-1) A_1(q^2) \\ & + \lambda A_2(q^2)) \Big) + 8 C_{10} \left(-2 m_B m_b (\sqrt{r}-1) \text{Re}(C_7^{eff}) T_2(q^2) V(q^2) \right. \\ & + A_1(q^2) (2 m_b m_B (\sqrt{r}+1) \text{Re}(C_7^{eff}) T_1(q^2) \\ & + m_B^2 s \text{Re}(C_9^{eff}) V(q^2)) \Big) \Big\}, \quad (3.34) \end{aligned}$$

$$\begin{aligned} D(s) = & \sqrt{\lambda} v \left\{ \frac{32}{m_B s^2} m_b^2 |C_7|^2 (2 m_\tau^2 + m_{B_s}^2 s) \left(\frac{2s}{r(r-1)} (1+3r-s) (T_2(q^2) \right. \right. \\ & T_3(q^2) \lambda) + 8 T_1^2(q^2) \lambda + \frac{T_3^2(q^2) s \lambda^2}{r(r-1)^2} + \frac{1}{r} T_2^2(q^2) (12(r-1)^2 r \\ & - (4r-s) \lambda) \Big) + \frac{2}{(1+\sqrt{r})^2 r s} m_B |C_9^{eff}|^2 (2 m_\tau^2 + m_{B_s}^2 s) \\ & \left(2 A_1(q^2) A_2(q^2) (1+\sqrt{r})^2 (r+s-1) \lambda + A_1^2(q^2) (1+\sqrt{r})^4 \right. \\ & (12rs + \lambda) + \lambda (8rs V^2(q^2) + A_2^2(q^2) \lambda) \Big) + 2 C_{10}^2 m_B \left(\frac{1}{rs} \left(2 A_1(q^2) \right. \right. \\ & A_2(q^2) (2 m_\tau^2 (r-2s-1) + m_{B_s}^2 s (r+s-1)) \lambda) \\ & - \frac{1}{m_b r} \left(24 m_B m_\tau^2 (A_2(q^2) (-1+\sqrt{r}) + A_1(q^2) (1+\sqrt{r})) T_3(q^2) \lambda \right) \\ & + \frac{24}{m_b^2 r} m_{B_s}^2 m_\tau^2 \lambda s T_3(q^2) + \frac{8}{(1+\sqrt{r})^2} (m_{B_s}^2 s - 4 m_\tau^2) V^2(q^2) \lambda \\ & + \frac{\lambda}{(1+\sqrt{r})^2 r s} A_2^2(q^2) (m_{B_s}^2 s \lambda + 2 m_\tau^2 (6s(1+r) - 3s^2 + \lambda)) \Big) \end{aligned}$$

$$\begin{aligned}
& + \frac{1}{r s} \left((1 + \sqrt{r})^2 A_1^2(q^2) (m_{B_s}^2 s (12 r s + \lambda) + m_\tau^2 (-48 r s + 2 \lambda)) \right) \\
& + \frac{3 m_B^3 \lambda}{m_b^4 r} |C_{Q_1}|^2 \left(m_{B_s}^2 s - 4 m_\tau^2 \right) \left(A_2(q^2) m_b (\sqrt{r} - 1) \right. \\
& + \left. A_1(q^2) m_b (\sqrt{r} + 1) - 2 T_3(q^2) m_B s \right)^2 \\
& + \frac{3 m_B^5 \lambda}{m_b^4 r} |C_{Q_2}|^2 s \left(A_2(q^2) (\sqrt{r} - 1) + A_1(q^2) (\sqrt{r} + 1) \right. \\
& - \left. 2 T_3(q^2) m_{B_s}^2 \sqrt{r} s \right)^2 + \frac{1}{(1 + \sqrt{r})^2 s} \text{Re}(C_7^{eff*} C_9^{eff}) 16 m_b (2 m_\tau^2 + m_{B_s}^2 s) \\
& \left(8(1 + \sqrt{r}) T_1(q^2) V(q^2) \lambda - \frac{1}{(-1 + \sqrt{r}) r} \left(A_2(q^2) (\lambda(r - 1)(1 + 3 r - s) \right. \right. \\
& T_2(q^2) + \lambda T_3(q^2)) + A_1(q^2) (1 + \sqrt{r})^2 ((r - 1) T_2(q^2) (12(r - 1) r - \lambda) \\
& + (r + s - 1) T_3(q^2) \lambda)) \right) - \frac{12}{m_b^2 r} C_{10} \text{Re}(C_{Q_2}) m_{B_s}^3 m_\tau \left(m_b ((-1 + \sqrt{r}) \right. \\
& A_2(q^2) + (1 + \sqrt{r}) A_1(q^2)) - 2 m_B T_3(q^2) \left. \right) \left(A_2(q^2) (1 - \sqrt{r}) \right. \\
& - \left. A_1(q^2) (1 + \sqrt{r}) + 2 m_{B_s}^2 \sqrt{r} s T_3(q^2) \right) \lambda \Big\} , \tag{3.35}
\end{aligned}$$

where $\lambda(1, r, s) = 1 + r^2 + s^2 - 2r - 2s - 2rs$, $r = m_{K^*}^2/m_B^2$ and $s = q^2/m_B^2$. The NHB effects bring new contributions to A_{FB} and those are examined in the Numerical analysis and Discussion part.

Another measurable physical quantity to be extracted from the decay is the CP violating asymmetry in the decay. The complex Yukawa couplings are a possible source of CP violation in model III. In our theoretical calculations we neglect all the Yukawa couplings except $\bar{\xi}_{N,tt}^U$, $\bar{\xi}_{N,b\bar{b}}^D$ and $\bar{\xi}_{N,\tau\tau}^D$ and choose $\bar{\xi}_{N,b\bar{b}}^D$ complex, i.e., $\bar{\xi}_{N,b\bar{b}}^D = |\bar{\xi}_{N,b\bar{b}}^D| e^{i\theta}$ (see Numerical Analysis and Discussion part). Therefore the CP violation stems from the Wilson coefficients C_7^{eff} , C_{Q_1} , and C_{Q_2} . The CP violating asymmetry can be defined as

$$A_{CP} = \frac{\Gamma(B \rightarrow K^* \tau^+ \tau^-) - \Gamma(\bar{B} \rightarrow \bar{K}^* \tau^+ \tau^-)}{\Gamma(B \rightarrow K^* \tau^+ \tau^-) + \Gamma(\bar{B} \rightarrow \bar{K}^* \tau^+ \tau^-)} . \tag{3.36}$$

Total decay width can be computed for both $B \rightarrow K^* \tau^+ \tau^-$ and its CP conjugate decay mode and then we eventually get

$$A_{CP} = \frac{\int ds \Omega(s)}{\int ds \Lambda(s)} , \tag{3.37}$$

where

$$\begin{aligned} \Omega(s) = & \frac{m_b \alpha_e^2 G_F^2 \lambda_t^2}{384 \pi^5 s (1 + \sqrt{r})^2} v \sqrt{\lambda} \text{Im}(C_7^{eff}) \text{Im}(C_9^{eff}) (2 m_\tau^2 + m_{B_s}^2 s) \\ & \left\{ 8 (\sqrt{r} + 1) \lambda T_1(q^2) V(q^2) - \frac{1}{r (\sqrt{r} - 1)} \left(\lambda A_2(q^2) \right. \right. \\ & \left. \left((r - 1)(3r - s + 1) T_2(q^2) + \lambda T_3(q^2) \right) + (\sqrt{r} + 1)^2 A_1(q^2) \right. \\ & \left. \left. \left((r - 1) T_2(q^2)(12(r - 1)r - \lambda) + (r + s - 1) \lambda T_3(q^2) \right) \right) \right\}, \end{aligned} \quad (3.38)$$

and

$$\Lambda(s) = D(s) + D_{CP}(s) . \quad (3.39)$$

Here $D_{CP}(s)$ is the CP conjugate of $D(s)$ which is defined as

$$D_{CP}(s) = D(s) (\bar{\xi}_{N,bb}^D \rightarrow \bar{\xi}_{N,bb}^{D*}) . \quad (3.40)$$

The last physical quantity which might be considered is the CP violating asymmetry in $A_{FB}(A_{CP}(A_{FB}))$ and this can also give strong clues for physics beyond the SM. This is directly defined as

$$A_{CP}(A_{FB}) = \frac{A_{FB} - \bar{A}_{FB}}{A_{FB} + \bar{A}_{FB}} , \quad (3.41)$$

where \bar{A}_{FB} is the CP conjugate of A_{FB} and it is, under chosen conditions, given as

$$\bar{A}_{FB} = A_{FB} (\bar{\xi}_{N,bb}^D \rightarrow \bar{\xi}_{N,bb}^{D*}) . \quad (3.42)$$

Note that during the calculations of A_{CP} , A_{FB} and $A_{CP}(A_{FB})$ we take into account merely the second resonance for the LD effects coming from the reaction $b \rightarrow s \psi_i \rightarrow s \tau^+ \tau^-$, where $i = 1, \dots, 6$ and divide the integration region for s into two parts : $4m_\tau^2/m_B^2 \leq s \leq (m_{\psi_2} - 0.02)^2/m_B^2$ and $(m_{\psi_2} + 0.02)^2/m_B^2 \leq s \leq 1$, where $m_{\psi_2} = 3.686 \text{ GeV}$ is the mass of the second resonance.

3.2 Numerical Analysis and Discussion

Unlike the cases in the SM and model I(II) version of the 2HDM there are more free parameters in the general 2HDM. These are the masses of charged and neutral

Higgs bosons and complex Yukawa couplings ($\xi_{ij}^{U,D,E}$). The restrictions coming from the experimental measurements put some constraints on the arbitrariness of the numerical values of those parameters. The physical regions for these have become more controlled as time goes on. Let us first discuss the consequences and conditions imposed on the Yukawa couplings by the CLEO measurement for the decay $B \rightarrow X_s \gamma$ [69]

$$Br(B \rightarrow X_s \gamma) = (3.15 \pm 0.35 \pm 0.32) \times 10^{-4} , \quad (3.43)$$

The contributions to C_7^{eff} coming from the neutral Higgs bosons, namely scalar h^0 and pseudoscalar A^0 , can be calculated at m_W level as [64]

$$\begin{aligned} C_7^{h^0}(m_W) &= (V_{tb}V_{ts}^*)^{-1} \sum_{i=d,s,b} \bar{\xi}_{N,bi}^D \bar{\xi}_{N,is}^D \frac{Q_i}{8m_i m_b} , \\ C_7^{A^0}(m_W) &= (V_{tb}V_{ts}^*)^{-1} \sum_{i=d,s,b} \bar{\xi}_{N,bi}^D \bar{\xi}_{N,is}^D \frac{Q_i}{8m_i m_b} , \end{aligned} \quad (3.44)$$

where m_i and Q_i are the masses and charges of the down type quarks ($i = d, s, b$) respectively and we used the redefinition

$$\xi^{U,D,E} = \sqrt{\frac{4G_F}{\sqrt{2}}} \bar{\xi}^{U,D,E} . \quad (3.45)$$

The explicit expressions in Eq. (3.44) show that the neutral Higgs bosons can give a large contribution to the coefficient C_7^{eff} and this is in contradiction with the CLEO measurement given in Eq. (5.11). To fit the theoretical result with experiment we make the assumption that the couplings $\bar{\xi}_{N,is}^D$ ($i = d, s, b$) and $\bar{\xi}_{N,db}^D$ are negligible which enable us to reach the conditions $\bar{\xi}_{N,bb}^D \bar{\xi}_{N,bs}^D \ll 1$ and $\bar{\xi}_{N,db}^D \bar{\xi}_{N,ds}^D \ll 1$. By further using the constraints [61] coming from the ratio $R_b^{exp} = \Gamma(Z \rightarrow b\bar{b})/\Gamma(Z \rightarrow hadrons)$, namely $\bar{\xi}_{N,bb}^D > 60 m_b/v$, the restrictions due to the $\Delta F = 2$ mixing, the ρ parameter [23], and the CLEO measurement leads also to following restrictions on the Yukawa couplings as $\bar{\xi}_{N,tc} < \bar{\xi}_{N,tt}^U$, $\bar{\xi}_{N,bb}^D$ and $\bar{\xi}_{N,ib}^D \sim 0$, $\bar{\xi}_{N,ij}^D$ where the indices i, j denote d and s quarks. Thus we merely take into account the Yukawa couplings of quarks $\bar{\xi}_{N,tt}^U$ and $\bar{\xi}_{N,bb}^D$ and keep the Yukawa coupling $\bar{\xi}_{N,\tau\tau}^E$ free and increase this parameter to enhance the effects of neutral Higgs bosons.

In this section, we indeed study the CP parameter $\sin\theta$, the Yukawa coupling $\bar{\xi}_{N,\tau\tau}^E$ and the mass ratio m_{h^0}/m_{A^0} dependencies of the A_{FB} , A_{CP} and $A_{CP}(A_{FB})$ of the exclusive decay $B \rightarrow K^*\tau^+\tau^-$, restricting $|C_7^{eff}|$ in the region $0.257 \leq |C_7^{eff}| \leq 0.439$ due to the CLEO measurement, Eq. (5.11) (see [61] for details). Our numerical analysis is based on this restriction. We also take $|\bar{\xi}_{N,tt}^U/\bar{\xi}_{N,bb}^D| < 1$ and choose the scale $\mu = m_b$ to include the LD effects and use the input values given in Table (4.1).

Table 3.2: The values of the input parameters used in the numerical analysis of the exclusive decay $B \rightarrow K^*\tau^+\tau^-$.

Parameter	Value
m_τ	1.78 (GeV)
m_c	1.4 (GeV)
m_b	4.8 (GeV)
$\bar{\xi}_{N,bb}^D$	$40 m_b$
α_{em}^{-1}	129
λ_t	0.04
m_t	175 (GeV)
m_W	80.26 (GeV)
m_Z	91.19 (GeV)
m_{H^0}	150 (GeV)
m_{h^0}	70 (GeV)
m_{H^\pm}	400 (GeV)
Λ_{QCD}	0.225 (GeV)
$\alpha_s(m_Z)$	0.117
$\sin\theta_W$	0.2325

In Fig. (3.4) $\sin\theta$ dependency of A_{FB} without the NHB effects is presented for $m_{A^0} = 80 \text{ GeV}$. A_{FB} lies here in the region bounded by solid (dashed) lines for $C_7^{eff} > 0$ ($C_7^{eff} < 0$). There is a straight line indicating the SM contribution. In the model III without the NHB effects, $|A_{FB}|$ is smaller compared to the one in the SM (0.195) for the case $C_7^{eff} > 0$, but there is a possibility to make an enhancement in it, at the order of the magnitude 2%, by increasing $\sin\theta$. For $C_7^{eff} < 0$, A_{FB} is not sensitive to $\sin\theta$ and the restriction region is narrow. However in this case $|A_{FB}|$ can have slightly greater values compared to the SM

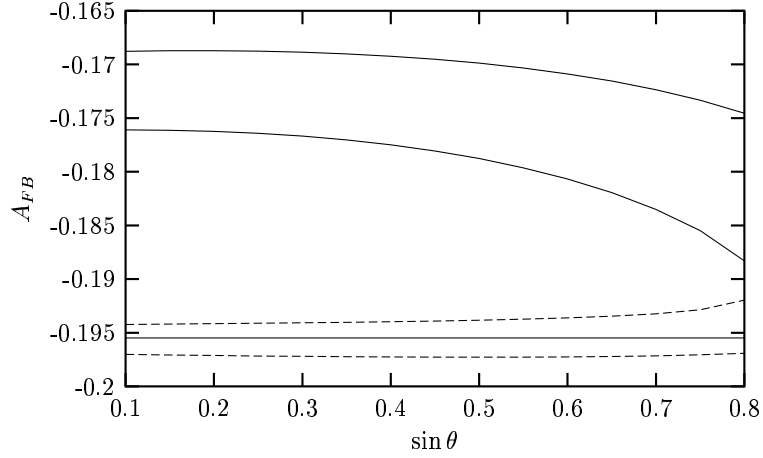


Figure 3.4: A_{FB} as a function of $\sin\theta$ for $m_{A^0} = 80 \text{ GeV}$ without NHB effects. Here A_{FB} is restricted in the region between solid (dashed) lines for $C_7^{eff} > 0$ ($C_7^{eff} < 0$). Straight line corresponds to the SM prediction.

one. Taking into account of the NHB effects (see Fig. (3.5)) reduces $|A_{FB}|$ for $C_7^{eff} > 0$ almost 30% compared to the one without the NHB effects. For $C_7^{eff} < 0$, the restriction region becomes narrow and A_{FB} reaches the SM predicted value for small $\sin\theta$.

Fig. (3.6) represents $\bar{\xi}_{N,\tau\tau}^E$ dependence of A_{FB} for $\sin\theta = 0.5$ and $m_{A^0} = 80 \text{ GeV}$. $|A_{FB}|$ vanishes with increasing $\bar{\xi}_{N,\tau\tau}^E$ for $C_7^{eff} > 0$. But for $C_7^{eff} < 0$, $|A_{FB}|$ does not vanish in the given region of $\bar{\xi}_{N,\tau\tau}^E$ and it stands less than the SM result. Fig. (3.7) is devoted to the ratio m_{h^0}/m_{A^0} dependence of A_{FB} for $\sin\theta = 0.5$ and $\bar{\xi}_{N,\tau\tau}^E = 10 m_\tau$. Increasing values of the ratio causes to increase $|A_{FB}|$ for both $C_7^{eff} > 0$ and $C_7^{eff} < 0$. If the masses of h^0 and A^0 are far from the degeneracy, $|A_{FB}|$ becomes small especially for the case $C_7^{eff} > 0$.

Figs. (3.8)–(3.9) represent A_{CP} of the process $B \rightarrow K^* \tau^+ \tau^-$. In Fig. (3.8) we present $\sin\theta$ dependence of A_{CP} without the NHB effects, for $m_{A^0} = 80 \text{ GeV}$. Here A_{CP} lies in the region bounded by solid (dashed) lines for $C_7^{eff} > 0$ ($C_7^{eff} < 0$). For $C_7^{eff} > 0$, A_{CP} is at the order of the magnitude of 1% for the intermediate values of $\sin\theta$ and its sign does not change in the restriction region. However A_{CP} can have both signs, even vanish for $C_7^{eff} < 0$. With the addition of the

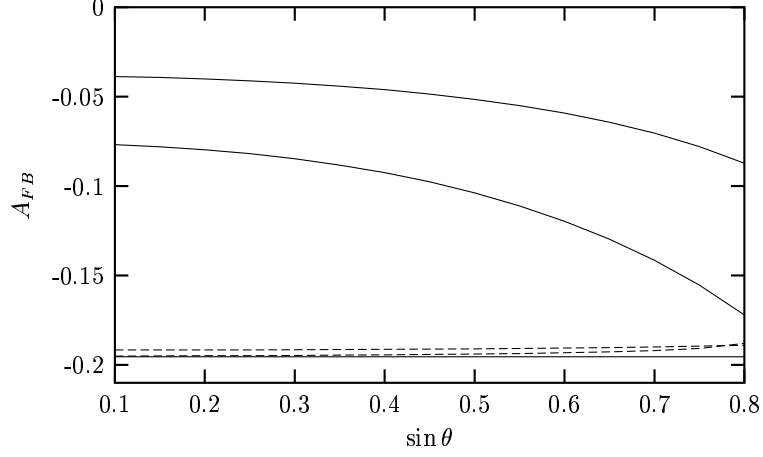


Figure 3.5: A_{FB} as a function of $\sin\theta$ for $\bar{\xi}_{N,\tau\tau}^E = 10 m_\tau$ including the NHB effects. Here A_{FB} is restricted in the region between solid (dashed) lines for $C_7^{eff} > 0$ ($C_7^{eff} < 0$). Straight line corresponds to the SM prediction.

NHB effects (see Fig. (3.9)) A_{CP} for $C_7^{eff} > 0$ decreases to almost one half of what we get in the case without the NHB effects. For $C_7^{eff} < 0$ there is still a decrease in A_{CP} . This behavior can be seen from the expression Eq. (3.38) since the numerator of the A_{CP} ratio is free from the NHB effects and their additional contributions enter into the expression in the denominator part. Further, the restriction regions become narrow.

Fig. (3.10) represents $\bar{\xi}_{N,\tau\tau}^E$ dependence of A_{CP} for $\sin\theta = 0.5$ and $m_{A^0} = 80 \text{ GeV}$. A_{CP} is sensitive to the parameter $\bar{\xi}_{N,\tau\tau}^E$ and it decreases with increasing $\bar{\xi}_{N,\tau\tau}^E$ for $C_7^{eff} > 0$. However, for $C_7^{eff} < 0$, the dependence of A_{CP} to $\bar{\xi}_{N,\tau\tau}^E$ is weak.

The ratio m_{h^0}/m_{A^0} dependence of A_{CP} for $\sin\theta = 0.5$ and $\bar{\xi}_{N,\tau\tau}^E = 10 m_\tau$ is presented in Fig. (3.11). As seen from the figure the sensitivity A_{CP} to the ratio is small, especially for $C_7^{eff} < 0$.

Finally, we present the CP violating asymmetry in A_{FB} in a series of figures (Figs. (3.12)–(3.14)). Fig. (3.12) represent $\sin\theta$ dependence of $A_{CP}(A_{FB})$ with NHB effects, for $m_{A^0} = 80 \text{ GeV}$ and $\bar{\xi}_{N,\tau\tau}^E = 10 m_\tau$. $A_{CP}(A_{FB})$ is at the order of the magnitude of 1% for the intermediate values of $\sin\theta$ for $C_7^{eff} > 0$. Its sign does not change in the restriction region similar to the A_{CP} of the process under consideration. However $A_{CP}(A_{FB})$ can have both signs, even vanish for $C_7^{eff} < 0$.

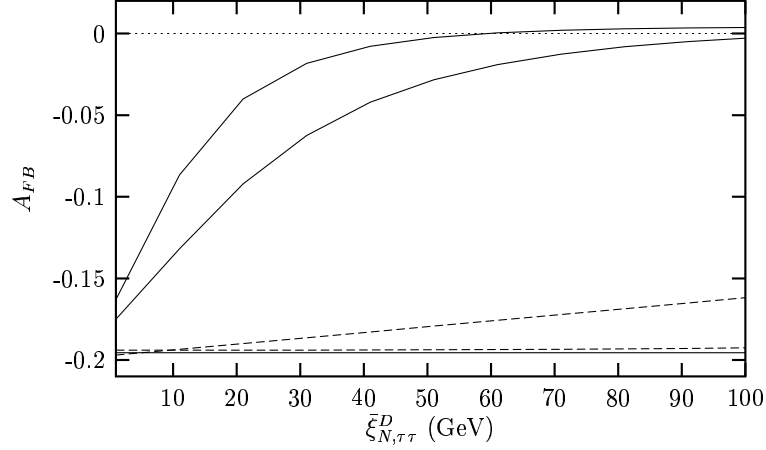


Figure 3.6: A_{FB} as a function of $\bar{\xi}_{N,\tau\tau}^E$ for $\sin\theta = 0.5$ and $m_{A^0} = 80 \text{ GeV}$. Here A_{FB} is restricted in the region between solid (dashed) lines for $C_7^{eff} > 0$ ($C_7^{eff} < 0$). Straight line corresponds to the SM prediction.

$A_{CP}(A_{FB})$ is sensitive to the parameter $\bar{\xi}_{N,\tau\tau}^E$ especially for the large values of $\bar{\xi}_{N,\tau\tau}^E$ and $C_7^{eff} > 0$ (see Fig. (3.13)). It can reach 10% for $\bar{\xi}_{N,\tau\tau}^E = 50 \text{ GeV}$. In the case $C_7^{eff} < 0$, $A_{CP}(A_{FB})$ is not sensitive to $\bar{\xi}_{N,\tau\tau}^E$ and it almost vanishes.

Fig. (3.14) is devoted to the ratio m_{h^0}/m_{A^0} dependence of $A_{CP}(A_{FB})$ for $\sin\theta = 0.5$ and $\bar{\xi}_{N,\tau\tau}^E = 10 m_\tau$. Increasing values of the ratio causes to increase $|A_{CP}(A_{FB})|$ for $C_7^{eff} > 0$. With the increasing mass ratio of h^0 and A^0 , $|A_{CP}(A_{FB})|$ can take large values. For $C_7^{eff} < 0$, $A_{CP}(A_{FB})$ is not sensitive to the mass ratio.

What follows from all these discussions can be briefly summarized as follows:

- $|A_{FB}|$ for the process under consideration is of the order of 10^{-2} and smaller compared to the SM one, for $C_7^{eff} > 0$. It can exceed the SM value (0.195) for $C_7^{eff} < 0$. Addition of the NHB effects decreases its magnitude by 30% (slightly) for $C_7^{eff} > 0$ ($C_7^{eff} < 0$). A_{FB} is sensitive to the parameters $\sin\theta$, $\bar{\xi}_{N,\tau\tau}^E$ and m_{h^0}/m_{A^0} especially for $C_7^{eff} > 0$. Its magnitude decreases (increases) with increasing values of $\bar{\xi}_{N,\tau\tau}^E$ (m_{h^0}/m_{A^0}).
- $|A_{CP}|$ is of the order of 10^{-2} . Addition of the NHB effects decreases its magnitude by 50% (slightly) for $C_7^{eff} > 0$ ($C_7^{eff} < 0$). It has the same sign in the restriction region $C_7^{eff} > 0$ and it can take both signs for $C_7^{eff} < 0$.

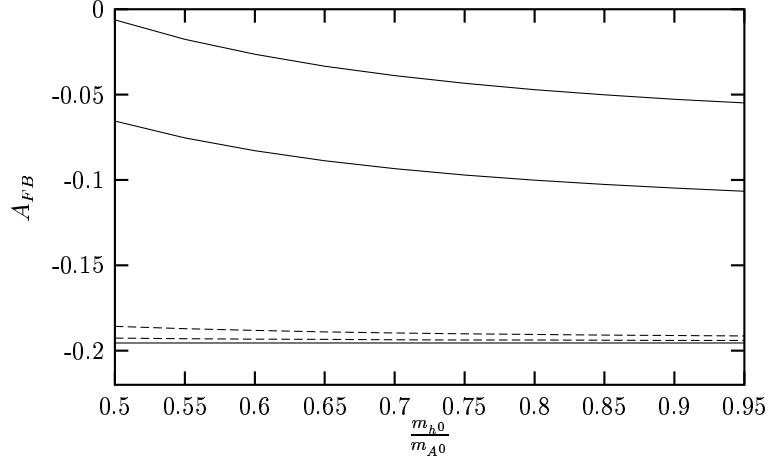


Figure 3.7: A_{FB} as a function of m_{h^0}/m_{A^0} for $\sin\theta = 0.5$ and $\bar{\xi}_{N,\tau\tau}^E = 10 m_\tau$. Here A_{FB} is restricted in the region between solid (dashed) lines for $C_7^{eff} > 0$ ($C_7^{eff} < 0$). Straight line corresponds to the SM prediction.

A_{CP} is sensitive to the parameters $\sin\theta$, $\bar{\xi}_{N,\tau\tau}^E$ especially for $C_7^{eff} > 0$. It decreases with increasing values of $\bar{\xi}_{N,\tau\tau}^E$. The sensitivity of A_{CP} to the ratio m_{h^0}/m_{A^0} is weak.

- $A_{CP}(A_{FB})$ is of the order of the magnitude of 1% for the intermediate values of $\sin\theta$ parameter for $C_7^{eff} > 0$. It has the same sign in the restriction region $C_7^{eff} > 0$ and it can take both signs for $C_7^{eff} < 0$. $A_{CP}(A_{FB})$ is sensitive to the parameters $\bar{\xi}_{N,\tau\tau}^E$ and $\frac{m_{h^0}}{m_{A^0}}$ for $C_7^{eff} > 0$. It increases with increasing values of $\bar{\xi}_{N,\tau\tau}^E$, even reach to 10%. Further increasing the values of the ratio m_{h^0}/m_{A^0} causes to increase $|A_{CP}(A_{FB})|$.

Therefore, the experimental investigations of the physical quantities A_{FB} and A_{CP} and $A_{CP}(A_{FB})$ ensure a crucial test for new physics effects beyond the SM and also for the sign of C_7^{eff} .

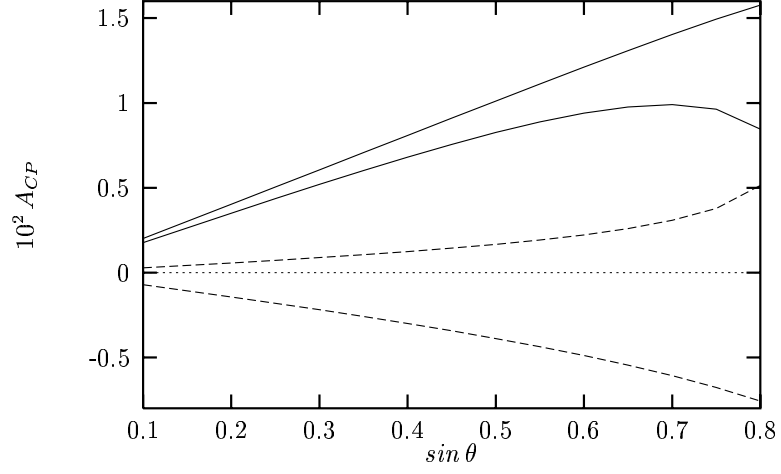


Figure 3.8: A_{CP} as a function of $\sin\theta$ for $m_{A^0} = 80 \text{ GeV}$ without the NHB effects. Here A_{FB} is restricted in the region between solid (dashed) lines for $C_7^{eff} > 0$ ($C_7^{eff} < 0$).

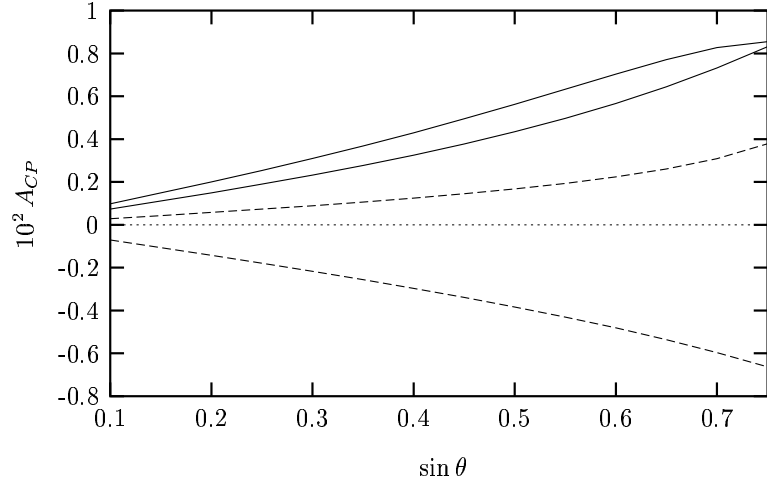


Figure 3.9: A_{CP} as a function of $\sin\theta$ for $\bar{\xi}_{N,\tau\tau}^E = 10 m_\tau$ including the NHB effects. Here A_{FB} is restricted in the region between solid (dashed) lines for $C_7^{eff} > 0$ ($C_7^{eff} < 0$).

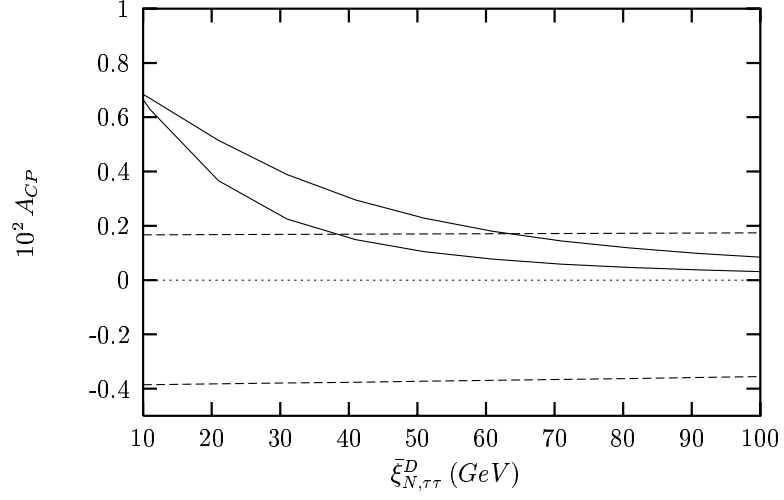


Figure 3.10: A_{CP} as a function of $\bar{\xi}_{N,\tau\tau}^E$ for $\sin\theta = 0.5$ and $m_{A^0} = 80 \text{ GeV}$. Here A_{FB} is restricted in the region between solid (dashed) lines for $C_7^{eff} > 0$ ($C_7^{eff} < 0$).

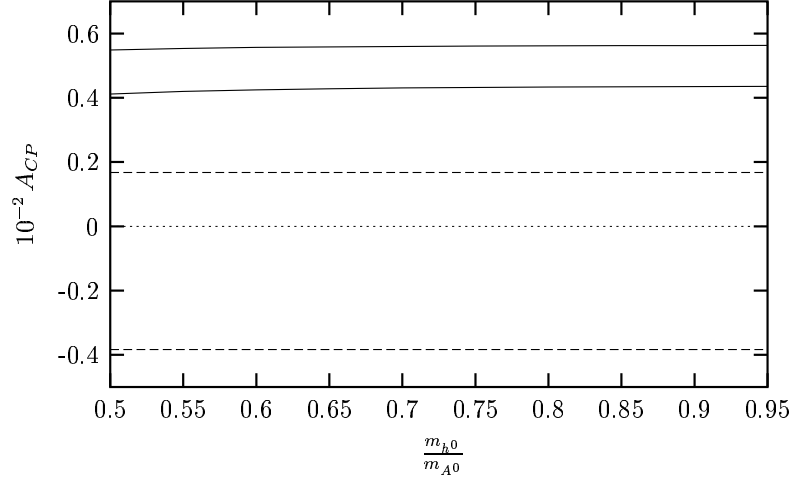


Figure 3.11: A_{CP} as a function of m_{h^0}/m_{A^0} for $\sin\theta = 0.5$ and $\bar{\xi}_{N,\tau\tau}^E = 10 m_\tau$. Here A_{FB} is restricted in the region between solid (dashed) lines for $C_7^{eff} > 0$ ($C_7^{eff} < 0$).

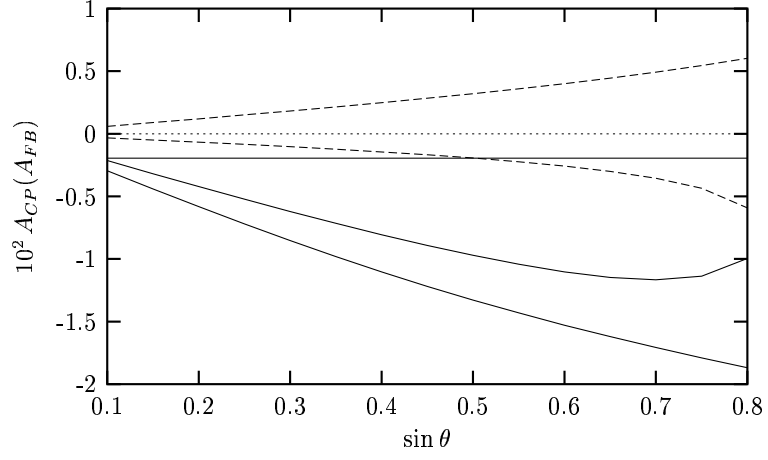


Figure 3.12: $A_{CP}(A_{FB})$ as a function of $\sin\theta$ for $\bar{\xi}_{N,\tau\tau}^E = 10 m_\tau$ including the NHB effects. Here A_{FB} is restricted in the region between solid (dashed) lines for $C_7^{eff} > 0$ ($C_7^{eff} < 0$).

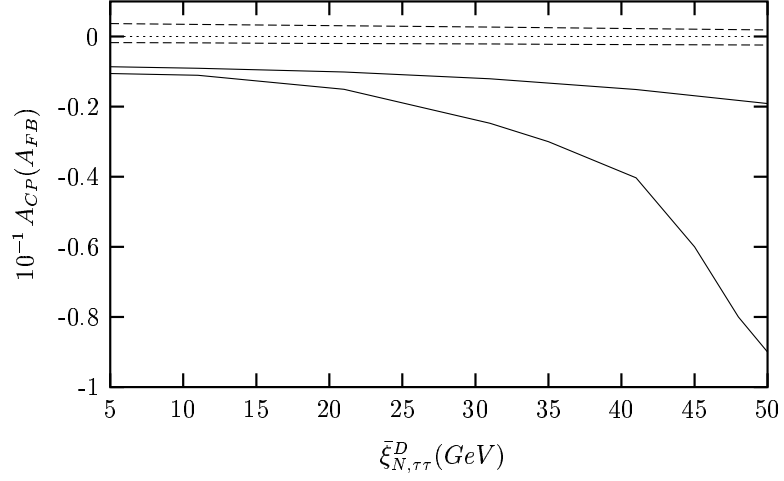


Figure 3.13: $A_{CP}(A_{FB})$ as a function of $\bar{\xi}_{N,\tau\tau}^E$ for $\sin\theta = 0.5$ and $m_{A^0} = 80 \text{ GeV}$. Here A_{FB} is restricted in the region between solid (dashed) lines for $C_7^{eff} > 0$ ($C_7^{eff} < 0$).

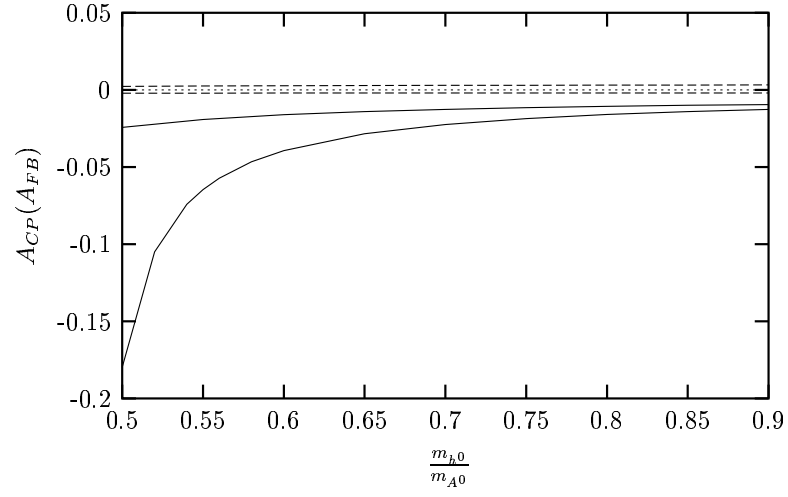


Figure 3.14: $A_{CP}(A_{FB})$ as a function of m_{h^0}/m_{A^0} for $\sin\theta=0.5$ and $\bar{\xi}_{N,\tau\tau}^E=10\,m_\tau$. Here A_{FB} is restricted in the region between solid (dashed) lines for $C_7^{eff} > 0$ ($C_7^{eff} < 0$).

CHAPTER 4

LEPTON FLAVOR VIOLATING $Z \rightarrow l_1^- l_2^+$ DECAY

It is well known that processes involving FCNC, like the one described in the previous chapter are severely suppressed by experimental data even though they seem not to violate any known fundamental law of nature. On the other hand, experimental constraints on FCNC are perfectly consistent with SM issues so far, with the impressive exception of neutrino oscillations [70]. In the case of the leptonic sector this can be achieved by the implementation of the lepton flavor conservation (LFC), a new symmetry which protects the possible phenomenology from these dangerous processes.

However, the high statistic results of the superkamiokande atmospheric neutrino experiment and the solar neutrino experiment [70] have made one to believe that LFC is not exact and we than expect to find out LFV processes in near future experiments. Since the predictions for these processes in the framework of the SM are by far out of the scope of next generation colliders, any signal for this kind of events would imply the existence of the physics beyond the SM. Among these, LFV leptonic Z-decays, such as $Z \rightarrow e\mu$, $Z \rightarrow e\tau$ and $Z \rightarrow \mu\tau$ have recently received great attention for the search of neutrinos, their mixing and possible masses and the physics beyond the SM. This is because that the Giga-Z option of the DESY TeV energy superconducting linear accelerator (TESLA) project will work at the Z resonance and increase the production rate of Z boson at resonance [71].

There are many theories which appear in the literature as an extension of the SM to describe the LFV Z decays. Before discussing, on the theoretical side, the

studies and their predictions for LFV Z decays in the literature, it is suitable to present the current experimental upper bounds for decays under consideration. The first best measurements of the Br 's for $Z \rightarrow e\mu$, $Z \rightarrow e\tau$ and $Z \rightarrow \mu\tau$ obtained at the CERN e^+e^- collider LEP I [72] were¹

$$\begin{aligned} Br(Z \rightarrow e^\mp \mu^\pm) &< 1.7 \times 10^{-6} \quad [73], \\ Br(Z \rightarrow e^\mp \tau^\pm) &< 9.8 \times 10^{-6} \quad [73, 74], \\ Br(Z \rightarrow \mu^\mp \tau^\pm) &< 1.2 \times 10^{-5} \quad [73, 75], \end{aligned} \tag{4.1}$$

and with the improved sensitivity at Giga- Z these numbers could be pulled down to [76]

$$\begin{aligned} Br(Z \rightarrow e^\mp \mu^\pm) &< 2 \times 10^{-9}, \\ Br(Z \rightarrow e^\mp \tau^\pm) &< f \times 6.5 \times 10^{-8}, \\ Br(Z \rightarrow \mu^\mp \tau^\pm) &< f \times 2.2 \times 10^{-8}. \end{aligned} \tag{4.2}$$

On the theoretical side, one of the extended SM permitting lepton mixing mechanism [77] is the so called νSM which consists of massive and mixing neutrinos. In this framework the structure in the lepton sector is similar to the one in the quark sector and the first predictions for such Z decays were given in [78, 79]. In the context of the νSM with light neutrinos the predicted Br 's are indeed extremely small [78, 80], i.e., $Br(Z \rightarrow e^\mp \mu^\pm) \sim Br(Z \rightarrow e^\mp \tau^\pm) \sim 10^{-54}$ and $Br(Z \rightarrow \mu^\mp \tau^\pm) < 4 \times 10^{-60}$. Another way of enhancing the Br 's of Z decays is achieved by further extending the νSM with one heavy ordinary Dirac neutrino [80]. String inspired models [81] and most grand unified theories [82] introduce that kind of heavy neutrinos into picture. In this context the Br 's for Z decays comparable with the current experimental limits can only be possible within a mass range of several hundred GeV for neutrinos. A further variation of the νSM is the one which is extended with two heavy right-handed Majorana neutrinos [80]. Large neutrino mass region is again needed for reaching sizable Br 's for Z

¹ The Br is taken, by summing the CP conjugated final states, of the form $Br(Z \rightarrow l_1^\mp l_2^\pm) = \frac{\Gamma(Z \rightarrow \bar{l}_1 l_2 + l_1 \bar{l}_2)}{\Gamma_Z}$.

decays. Recently the LFV Z decays are also studied in the context of the Zee model [83]. In this framework, among the decay modes of Z considered here, the $Z \rightarrow e\tau$ decay channel receives the largest contribution, even being smaller than the present limits. For the other two decay modes within this context they are far from experimental verification in the next colliders.

Our task in this chapter is to work out the Br 's of LFV Z decay modes $Z \rightarrow e\mu$, $Z \rightarrow e\tau$ and $Z \rightarrow \mu\tau$ in the model III version of 2HDM and to analyze their dependencies on free parameters of the model. By assumption, in the leptonic sector, no charged flavor changing interaction exists due to the absence of a CKM type matrix. Thus the neutral Higgs bosons h^0 and A^0 with tree level FCNC allowed Yukawa couplings are the only source for getting LFV Z decays. From the computational point of view the Yukawa couplings appearing in these decay modes as a free parameter can be constrained in the following manner. Experimental upper limits for the electric dipole moments (EDMs) of leptons put the Yukawa couplings into a restricted region. Theoretically we know that non-zero EDMs are merely possible if the Yukawa couplings are chosen to be complex. The Br of the LFV decay $\mu \rightarrow e\gamma$ which also exists in this model can further be used for predicting the upper bounds of the Yukawa couplings. These are all discussed in the numerical analysis section. We carry out the calculations at one loop level and find that in the context of model III it is possible to reach the present experimental upper limits for the Br 's of the decays considered by adjusting the free parameters of the model respecting the bounds coming from experimental side.

The rest of the chapter is organized as follows. In Section 2, we present the explicit expressions for the Branching ratios of $Z \rightarrow e^-\mu^+$, $Z \rightarrow e^-\tau^+$ and $Z \rightarrow \mu^-\tau^+$ in the framework of the model III. Section 3 is devoted to numerical analysis and our conclusions.

4.1 The One-Loop Calculation for $Z \rightarrow l_1^- l_2^+$

In this section, we outline the basic steps for calculating the one-loop LFV amplitude \mathcal{M} for $Z \rightarrow l_1^- l_2^+$ decay due to contributions coming from neutral Higgs bosons h_0 and A_0 in model III. To this aim, let us first present part of the Lagrangian responsible for this LFV decay. The flavor changing part of the Yukawa Lagrangian in the leptonic sector can be read from Eq. (2.16) as

$$\mathcal{L}_{Y,FC} = \xi_{ij}^E \bar{l}_{iL} \Phi_2 E_{jR} + h.c. . \quad (4.3)$$

This is clear from the fact that by choosing the representation of Φ_1 and Φ_2 doublets of the form in Eq. (2.31), we are able to collect all new particles appearing beyond the SM in the Φ_2 doublet. Therefore FCNCs at tree level can only be produced by the terms being Φ_2 dependent in Eq. (2.31), which is the one depicted above².

The diagrams that modify (at one-loop) the $Z l_j \bar{l}_k$ coupling due to neutral scalar exchanges are depicted in Fig. (4.1). There are four separate diagrams, first two of which are called self-energy diagrams and the others are called triangular vertex diagrams. From Fig. (4.1) it is evident that we have only three types of interaction vertices to consider. These are defined as follows:

- $Z - l_j - \bar{l}_i$ interaction

$$i\gamma^\mu (a_{L(Zi)}L + a_{R(Zi)}R) \delta_{ij} = V_{ij}^\mu(Z) \quad (4.4)$$

² As already noted that only neutral scalars contributes, we then replace ξ_N^E with ξ_N^E where N denotes the word *neutral* and define $\bar{\xi}_N^E$ which satisfies the equation $\xi_N^E = \sqrt{4G_F/\sqrt{2}} \bar{\xi}_N^E$.

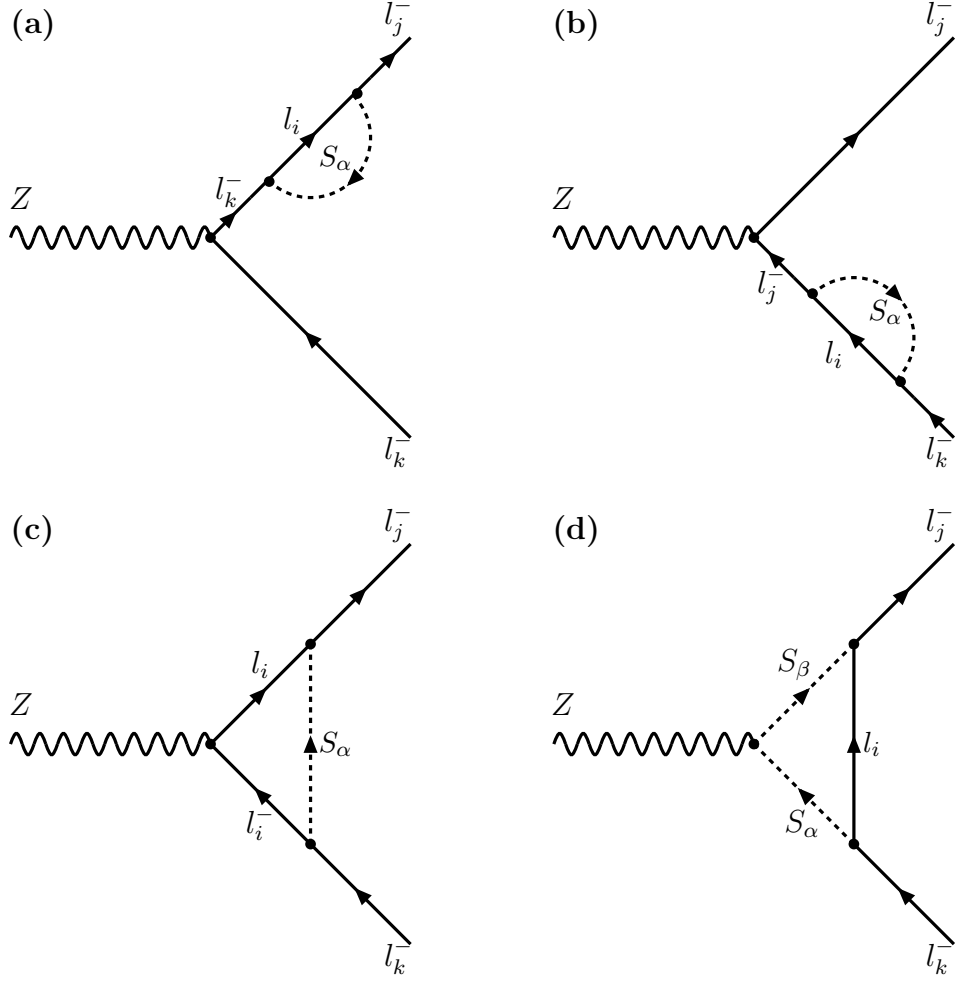


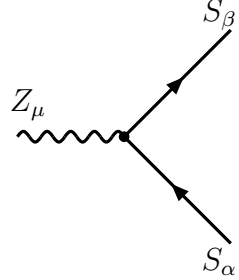
Figure 4.1: One loop diagrams contributing to $Z \rightarrow l_j^- l_k^+$ decay due to the neutral Higgs bosons $S_\alpha = h^0, A^0$ in the 2HDM. l_i represents the internal, l_j (l_k) outgoing (incoming) lepton, wavy lines the vector field Z , and the dashed lines h_0 and A_0 fields.

where $L(R) = (1 - (+)\gamma_5)/2$. For the case of the SM couplings a vector field Z to a pair of leptons, there are only flavor diagonal couplings and the explicit forms of the coefficients are given as

$$a_{L,R}(Zi) = -g_W (T_{L,R}^{3(i)} - \sin^2 \theta_W Q_i), \quad (4.5)$$

where $T_L^{3(i)} = -\frac{1}{2}$, $T_R^{3(i)} = 0$ and Q_i is the charge of the lepton i (-1) and the coupling constants are defined as $g_W = g/\cos \theta_W$, $g = e/\sin \theta_W$.

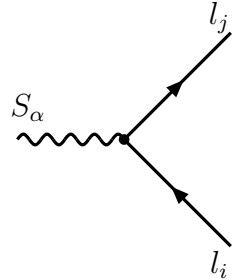
- $Z - S_\alpha - S_\beta$ interaction



$$\frac{g_W}{2}(p_\beta - p_\alpha)^\mu(1 - \delta_{\alpha\beta}) = V_\beta^\mu \quad (4.6)$$

where p_α and p_β are the incoming 4-momenta of the neutral Higgs bosons ($S_{\alpha,\beta} = h^0, A^0$). In this case, scalar diagonal vertex vanishes which can be justified from the kinetic term for the Higgs fields in the Lagrangian. Here this is implemented with the factor $(1 - \delta_{\alpha\beta})$.

- $S_\alpha - l_j - \bar{l}_i$ interaction



$$-\frac{i}{\sqrt{2}}[b_{L(\alpha)}^{ij}L + b_{L(\alpha)}^{ij}R] = V_{ij}^{(\alpha)} \quad (4.7)$$

where $b_{L,R(\alpha)}^{ij}$ can be given in terms of the complex Yukawa couplings $\xi_{N,ij}^E$ for each scalar field. For $\alpha = h^0$, we have

$$b_{L(h^0)}^{ij} = \xi_{N,ji}^{E*}, \quad b_{R(h^0)}^{ij} = \xi_{N,ij}^E, \quad (4.8)$$

and for $\alpha = A^0$ we have

$$b_{L(A^0)}^{ij} = -i\xi_{N,ji}^{E*}, \quad b_{R(A^0)}^{ij} = i\xi_{N,ij}^E. \quad (4.9)$$

In calculating the amplitude for the decay, we further need to set the propagators for lepton and massive scalar particles. The propagator for massive scalar

particles S_α with momentum q is

$$D_{(\alpha)}(q) = \frac{i}{q^2 - m_\alpha^2}, \quad \alpha = h^0, A^0, \quad (4.10)$$

and the one for leptons with momentum q is

$$D_{ij}(q) = \frac{i(\not{q} + m_i)}{q^2 - m_i^2} \delta_{ij}, \quad i, j = e, \mu, \tau. \quad (4.11)$$

The one-loop amplitudes \mathcal{M}_k ($k = a, b, c, d$ corresponding to diagrams (a), (b), (c), (d) in Fig. (4.1), respectively) can now be worked out. Let us start calculating the self energy diagrams.

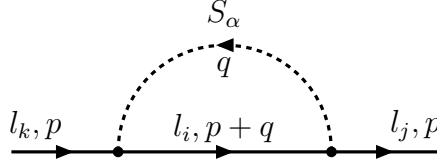


Figure 4.2: The leg including one loop of the self energy diagrams in Fig. (4.1).

To compute them the essential point is to calculate separately the upper leg of the diagram where there is a loop of diagram (a) in Fig. (4.1), depicted in Fig. (4.2). Then the amplitudes for the self energy diagrams can be readily calculated together with the help of the vertex factors in Eqs. (4.1), (4.1), and (4.1). The amplitude for the diagram in Fig. (4.2) is

$$\Sigma_{jk}^{(\alpha)}(p, q) = \sum_{i, m=e, \mu, \tau} V_{ji}^{(\alpha)\dagger} D_{im}(p+q) V_{mk}^{(\alpha)} D_{(\alpha)}(q). \quad (4.12)$$

where Then we write the one-loop amplitude, \mathcal{M}_a , for diagram (a) in Fig. (4.1) for $l_j \bar{l}_k$ final leptons

$$\mathcal{M}_{a,jk}^{(\alpha)} = \int \frac{d^4 q}{(2\pi)^4} \sum_{i, l=e, \mu, \tau} \left[\epsilon_\mu(Q) \bar{u}(p_1) \Sigma_{ji}^{(\alpha)}(p_1, q) D_{il}(p_1) V_{lk(Z)}^\mu u(p_2) \right], \quad (4.13)$$

where ϵ_μ being the boson polarization vector and Q is the 4-momentum of the on-shell Z boson. Similarly for diagram (b), we have

$$\mathcal{M}_{b,jk}^{(\alpha)} = \int \frac{d^4 q}{(2\pi)^4} \sum_{i, l=e, \mu, \tau} \left[\epsilon_\mu(Q) \bar{u}(p_1) V_{ji(Z)}^\mu D_{il}(p_2) \Sigma_{lk}^{(\alpha)}(p_2, q) u(p_2) \right]. \quad (4.14)$$

Total amplitude of the self energy diagrams for each scalar particles is then

$$\begin{aligned}\mathcal{M}_{ab,jk}^{(\alpha)} &= \mathcal{M}_a^{(\alpha)} + \mathcal{M}_b^{(\alpha)} \\ &= \epsilon_\mu(Q) \bar{u}(p_1) \left[\int \frac{d^4 q}{(2\pi)^4} \sum_{i,l=e,\mu,\tau} [\Sigma_{ji}^{(\alpha)}(p_1, q) D_{il}(p_1) V_{lk(Z)}^\mu \right. \\ &\quad \left. + V_{ji(Z)}^\mu D_{il}(p_2) \Sigma_{lk}^{(\alpha)}(p_2, q)] \right] u(p_2). \end{aligned} \quad (4.15)$$

Next we can write one-loop amplitude for diagram (c) depicted in Fig. (4.1)

$$\begin{aligned}\mathcal{M}_{c,jk}^{(\alpha)} &= \int \frac{d^4 q}{(2\pi)^4} \sum_{i,l,m,n=e,\mu,\tau} \left[\epsilon_\mu(Q) \bar{u}(p_1) (-V_{ji}^{(\alpha)}) D_{il}(p_1 + q) V_{lm(Z)}^\mu \right. \\ &\quad \left. D_{mn}(p_2 + q) V_{nk}^{(\alpha)} D_{(\alpha)}(q) u(p_2) \right]. \end{aligned} \quad (4.16)$$

Even though diagram (d) represents four separate contributions, only two of them give non-zero contribution due to absence of $Z - S_\alpha - S_\alpha$ type vertex. Then they are expressed as

$$\begin{aligned}\mathcal{M}_{d,jk}^{(\alpha\beta)} &= \int \frac{d^4 q}{(2\pi)^4} \sum_{i,l,m,n=e,\mu,\tau} \left[\epsilon_\mu(Q) \bar{u}(p_1) (-V_{ji}^{(\alpha)}) D_{il}(q) V_{lk}^{(\beta)} D_{(\beta)}(p_1 - q) \right. \\ &\quad \left. \times V_{\alpha Z \beta}^\mu D_{(\alpha)}(q - p_2) u(p_2) \right], \end{aligned} \quad (4.17)$$

where $\alpha \neq \beta$. Since for $\alpha = \beta$, $V_{\alpha Z \alpha}^\mu = 0$ from Eq. (4.1) ($\mathcal{M}_{d,jk}^{(\alpha\alpha)} = 0$). Total amplitude for the decay $Z \rightarrow l_j \bar{l}_k$ becomes

$$\begin{aligned}\mathcal{M}_{jk} &= \sum_{\alpha,\beta,i} (\mathcal{M}_{ab}^{(\alpha)} + \mathcal{M}_c^{(\alpha)} + \mathcal{M}_d^{(\alpha\beta)}) \\ &= \epsilon_\mu(Q) \bar{u}(p_1) \Gamma^\mu u(p_2), \end{aligned} \quad (4.18)$$

where $\Gamma^\mu = \Gamma_{ab}^\mu + \Gamma_{cd}^\mu$ is called the effective vertex function for the interaction of on-shell Z bosons with a fermionic current³ and $\Gamma_{ab}^\mu + \Gamma_{cd}^\mu$ are given as

$$\begin{aligned}\Gamma_{ab}^\mu &= \int \frac{d^4 q}{(2\pi)^4} \sum_\alpha \sum_{i,l} \left[\Sigma_{ji}^{(\alpha)}(p_1, q) D_{il}(p_1) V_{lk(Z)}^\mu + V_{ji(Z)}^\mu D_{il}(p_2) \Sigma_{lk}^{(\alpha)}(p_2, q) \right], \\ \Gamma_{cd}^\mu &= - \int \frac{d^4 q}{(2\pi)^4} \sum_{\alpha,\beta} \sum_{i,l,m,n} \left[V_{ji}^{(\alpha)} D_{il}(p_1 + q) V_{lm(Z)}^\mu D_{mn}(p_2 + q) V_{nk}^{(\alpha)} D_{(\alpha)}(q) \right. \\ &\quad \left. + V_{ji}^{(\alpha)} D_{il}(q) V_{lk}^{(\beta)} D_{(\beta)}(p_1 - q) V_{\alpha Z \beta}^\mu D_{(\alpha)}(q - p_2) \right]. \end{aligned} \quad (4.19)$$

³ We suppressed the j, k external lepton indices in the vertex function.

Having expressed the implicit form of the vertex function, our next job is to deal with the structures appearing in denominators coming from propagators. With the help of Feynman parametrization they can be put into quadratic forms in loop integral variable, which apparently simplifies the one-loop integrals. Details of Feynman parametrization and of putting the denominators of the vertex functions into quadratic form as an application are given in appendix C. Before dealing with the Dirac structures in the numerator of the vertex function Γ^μ , let us say a few words about the finiteness of the integral over internal momentum. Although the sum of the four diagrams in Fig. (4.1) is finite, each single diagram is divergent. To handle the divergent terms we will use a method known as dimensional regularization⁴[85]. More about dimensional regularization can be found in appendix D.

Let us turn our attention to structures in the numerators of Γ^μ . The possible form can be in fact narrowed down by appealing to some physical requirements such as Lorentz invariance, current conservation and any discrete symmetry if it is not violated. From the Lorentz invariance, Γ^μ should transform as a vector, which enables us to set the possible form a linear combination of the vectors (axial-vectors), $\gamma^\mu(\gamma^\mu\gamma_5)$ and $p_{1(2)}^\mu(p_{1(2)}^\mu\gamma_5)$. Therefore, using the combinations $p_1^\mu + p_2^\mu$ and $p_1^\mu - p_2^\mu$ for convenience, we have

$$\Gamma^\mu = \gamma^\mu(A + \gamma_5 A') + (p_1^\mu + p_2^\mu)(B + \gamma_5 B') + (p_1^\mu - p_2^\mu)(C - \gamma_5 C'), \quad (4.20)$$

where the unknown coefficients involve Dirac matrices dotted with vectors like \not{p}_1 , \not{p}_2 , \not{Q} and some Lorentz scalars p_1^2 , p_2^2 , Q^2 . Since Γ^μ is sandwiched between $\bar{u}(p_1)$ and $u(p_2)$, we may use the following on mass shell conditions,

$$\bar{u}(p_1)\not{p}_1 = m_1 \bar{u}(p_1), \quad \not{p}_2 u(p_2) = m_2 u(p_2), \quad \not{p}_{1(2)}^2 = p_{1(2)}^2 = m_{1(2)}^2. \quad (4.21)$$

After imposing the above conditions, the only non-trivial scalar variable available is Q^2 on which the coefficients depend. A further constraint is the Ward

⁴ In dimensional regularization nothing has been violated except that space-time is not four dimensional and thus all the physical requirements are preserved. The method leaves the theory Lorentz and gauge invariant [84].

identity, $Q_\mu \Gamma^\mu = 0$. This tells us that both C and C' should be zero. No further simplification can be done on general principles. It is conventional, however, to write the vertex function by means of the Gordon identity

$$\bar{u}(p_1) \gamma^\mu u(p_2) = \bar{u}(p_1) \left[\frac{p_1^\mu + p_2^\mu}{m_{l_1} + m_{l_2}} + i \frac{\sigma^{\mu\nu} Q_\nu}{m_{l_1} + m_{l_2}} \right] u(p_2), \quad (4.22)$$

together with a similar relation for terms involving γ_5

$$\bar{u}(p_1) \gamma^\mu \gamma_5 u(p_2) = \bar{u}(p_1) \left[\gamma_5 \frac{p_1^\mu + p_2^\mu}{m_{l_1} - m_{l_2}} - i \gamma_5 \frac{\sigma^{\mu\nu} Q_\nu}{m_{l_1} - m_{l_2}} \right] u(p_2). \quad (4.23)$$

These identities allow us to eliminate $(\gamma_5)(p_1 + p_2)^\mu$ terms in favor of $i(\gamma_5)\sigma^{\mu\nu}Q_\nu$. By using these identities and the mass shell conditions, we eventually get the general vertex for $Z \rightarrow l_j \bar{l}_k$ of the form

$$\Gamma^\mu = \gamma^\mu (f_V - \gamma_5 f_A) + \frac{i}{m_W} (f_M + \gamma_5 f_E) \sigma^{\mu\nu} Q_\nu, \quad (4.24)$$

where f_V (f_A) is the vector (axial-vector) coupling and f_M (f_E) is the magnetic (electric) dipole transitions of unlike fermions.

In calculating the couplings in Γ^μ , the one-loop momentum integrals can be calculated with the help of the d-dimensional integrals, which are given in appendix D. Taking into account of all the masses of internal and external leptons (anti-leptons) and following the procedure as stated, the explicit expressions, after lengthy calculations, for f_V , f_A , f_M and f_E can be expressed as

$$\begin{aligned} f_V = & \frac{g}{64 \pi^2 \cos \theta_W} \int_0^1 dx \frac{1}{m_{l_2^+}^2 - m_{l_1^-}^2} \left\{ c_V (m_{l_2^+} + m_{l_1^-}) \right. \\ & \left((-m_i \eta_i^+ + m_{l_1^-} (-1+x) \eta_i^V) \ln \frac{L_{1,h^0}^{self}}{\mu^2} \right. \\ & + (m_i \eta_i^+ - m_{l_2^+} (-1+x) \eta_i^V) \ln \frac{L_{2,h^0}^{self}}{\mu^2} \\ & + (m_i \eta_i^+ + m_{l_1^-} (-1+x) \eta_i^V) \ln \frac{L_{1,A^0}^{self}}{\mu^2} \\ & \left. \left. - (m_i \eta_i^+ + m_{l_2^+} (-1+x) \eta_i^V) \ln \frac{L_{2,A^0}^{self}}{\mu^2} \right) \right. \\ & \left. + c_A (m_{l_2^+} - m_{l_1^-}) \left((-m_i \eta_i^- + m_{l_1^-} (-1+x) \eta_i^A) \ln \frac{L_{1,h^0}^{self}}{\mu^2} \right. \right. \end{aligned}$$

$$\begin{aligned}
& + (m_i \eta_i^- + m_{l_2^+}(-1+x) \eta_i^A) \ln \frac{L_{2,h^0}^{self}}{\mu^2} \\
& + (m_i \eta_i^- + m_{l_1^-}(-1+x) \eta_i^A) \ln \frac{L_{1,A^0}^{self}}{\mu^2} \\
& + (-m_i \eta_i^- + m_{l_2^+}(-1+x) \eta_i^A) \ln \frac{L_{2,A^0}^{self}}{\mu^2} \Big) \Big\} \\
& - \frac{g}{64 \pi^2 \cos \theta_W} \int_0^1 dx \int_0^{1-x} dy \left\{ m_i^2 (c_A \eta_i^A - c_V \eta_i^V) \left(\frac{1}{L_{A^0}^{ver}} + \frac{1}{L_{h^0}^{ver}} \right) \right. \\
& - (1-x-y) m_i \left(c_A (m_{l_2^+} - m_{l_1^-}) \eta_i^- \left(\frac{1}{L_{h^0}^{ver}} - \frac{1}{L_{A^0}^{ver}} \right) \right. \\
& + c_V (m_{l_2^+} + m_{l_1^-}) \eta_i^+ \left(\frac{1}{L_{h^0}^{ver}} + \frac{1}{L_{A^0}^{ver}} \right) \Big) - (c_A \eta_i^A + c_V \eta_i^V) \\
& \left(-2 + (q^2 x y + m_{l_1^-} m_{l_2^+} (-1+x+y)^2) \left(\frac{1}{L_{h^0}^{ver}} + \frac{1}{L_{A^0}^{ver}} \right) - \ln \frac{L_{h^0}^{ver}}{\mu^2} \frac{L_{A^0}^{ver}}{\mu^2} \right) \\
& - (m_{l_2^+} + m_{l_1^-}) (1-x-y) \left(\frac{\eta_i^A (x m_{l_1^-} + y m_{l_2^+}) + m_i \eta_i^-}{2 L_{A^0 h^0}^{ver}} \right. \\
& + \left. \frac{\eta_i^A (x m_{l_1^-} + y m_{l_2^+}) - m_i \eta_i^-}{2 L_{h^0 A^0}^{ver}} \right) + \frac{1}{2} \eta_i^A \ln \frac{L_{A^0 h^0}^{ver}}{\mu^2} \frac{L_{h^0 A^0}^{ver}}{\mu^2} \Big\}, \\
f_A &= \frac{-g}{64 \pi^2 \cos \theta_W} \int_0^1 dx \frac{1}{m_{l_2^+}^2 - m_{l_1^-}^2} \left\{ c_V (m_{l_2^+} - m_{l_1^-}) \right. \\
& \left(m_i \eta_i^- + m_{l_1^-}(-1+x) \eta_i^A \right) \ln \frac{L_{1,A^0}^{self}}{\mu^2} \\
& + (-m_i \eta_i^- + m_{l_2^+}(-1+x) \eta_i^A) \ln \frac{L_{2,A^0}^{self}}{\mu^2} \\
& + (-m_i \eta_i^- + m_{l_1^-}(-1+x) \eta_i^A) \ln \frac{L_{1,h^0}^{self}}{\mu^2} \\
& + (m_i \eta_i^- + m_{l_2^+}(-1+x) \eta_i^A) \ln \frac{L_{2,h^0}^{self}}{\mu^2} \Big) \\
& + c_A (m_{l_2^+} + m_{l_1^-}) \left((m_i \eta_i^+ + m_{l_1^-}(-1+x) \eta_i^V) \ln \frac{L_{1,A^0}^{self}}{\mu^2} \right. \\
& - (m_i \eta_i^+ + m_{l_2^+}(-1+x) \eta_i^V) \ln \frac{L_{2,A^0}^{self}}{\mu^2} \\
& + (-m_i \eta_i^+ + m_{l_1^-}(-1+x) \eta_i^V) \ln \frac{L_{1,h^0}^{self}}{\mu^2} \\
& + (m_i \eta_i^+ - m_{l_2^+}(-1+x) \eta_i^V) \ln \frac{L_{2,h^0}^{self}}{\mu^2} \Big) \Big\}
\end{aligned}$$

$$\begin{aligned}
& + \frac{g}{64 \pi^2 \cos \theta_W} \int_0^1 dx \int_0^{1-x} dy \left\{ m_i^2 (c_V \eta_i^A - c_A \eta_i^V) \left(\frac{1}{L_{A^0}^{ver}} + \frac{1}{L_{h^0}^{ver}} \right) \right. \\
& - m_i (1-x-y) \left(c_V (m_{l_2^+} - m_{l_1^-}) \eta_i^- + c_A (m_{l_2^+} + m_{l_1^-}) \eta_i^+ \right) \left(\frac{1}{L_{h^0}^{ver}} - \frac{1}{L_{A^0}^{ver}} \right) \\
& + (c_V \eta_i^A + c_A \eta_i^V) \left(-2 + (q^2 x y - m_{l_1^-} m_{l_2^+} (-1+x+y)^2) \left(\frac{1}{L_{h^0}^{ver}} + \frac{1}{L_{A^0}^{ver}} \right) \right. \\
& - \ln \frac{L_{h^0}^{ver}}{\mu^2} \frac{L_{A^0}^{ver}}{\mu^2} \left. \right) - (m_{l_2^+} - m_{l_1^-}) (1-x-y) \left(\frac{\eta_i^V (x m_{l_1^-} - y m_{l_2^+}) + m_i \eta_i^+}{2 L_{A^0 h^0}^{ver}} \right. \\
& + \left. \frac{\eta_i^V (x m_{l_1^-} - y m_{l_2^+}) - m_i \eta_i^+}{2 L_{h^0 A^0}^{ver}} \right) - \frac{1}{2} \eta_i^V \ln \frac{L_{A^0 h^0}^{ver}}{\mu^2} \frac{L_{h^0 A^0}^{ver}}{\mu^2} \left. \right\}, \\
f_M &= - \frac{g m_W}{64 \pi^2 \cos \theta_W} \int_0^1 dx \int_0^{1-x} dy \left\{ \left((1-x-y) (c_V \eta_i^V + c_A \eta_i^A) \right. \right. \\
& \left. \left(x m_{l_1^-} + y m_{l_2^+} \right) + m_i (c_A (x-y) \eta_i^- + c_V \eta_i^+ (x+y)) \right) \frac{1}{L_{h^0}^{ver}} \\
& + \left((1-x-y) (c_V \eta_i^V + c_A \eta_i^A) (x m_{l_1^-} + y m_{l_2^+}) \right. \\
& - \left. m_i (c_A (x-y) \eta_i^- + c_V \eta_i^+ (x+y)) \right) \frac{1}{L_{A^0}^{ver}} \\
& - (1-x-y) \left(\frac{\eta_i^A (x m_{l_1^-} + y m_{l_2^+})}{2} \left(\frac{1}{L_{A^0 h^0}^{ver}} + \frac{1}{L_{h^0 A^0}^{ver}} \right) \right. \\
& + \left. \frac{m_i \eta_i^-}{2} \left(\frac{1}{L_{h^0 A^0}^{ver}} - \frac{1}{L_{A^0 h^0}^{ver}} \right) \right) \left. \right\}, \\
f_E &= - \frac{g m_W}{64 \pi^2 \cos \theta_W} \int_0^1 dx \int_0^{1-x} dy \left\{ \left((1-x-y) \left(- (c_V \eta_i^A + c_A \eta_i^V) \right. \right. \right. \\
& \left. \left(x m_{l_1^-} - y m_{l_2^+} \right) \right) - m_i (c_A (x-y) \eta_i^+ + c_V \eta_i^- (x+y)) \right) \frac{1}{L_{h^0}^{ver}} \\
& + \left((1-x-y) \left(- (c_V \eta_i^A + c_A \eta_i^V) (x m_{l_1^-} - y m_{l_2^+}) \right) \right. \\
& + \left. m_i (c_A (x-y) \eta_i^+ + c_V \eta_i^- (x+y)) \right) \frac{1}{L_{A^0}^{ver}} \\
& + (1-x-y) \left(\frac{\eta_i^V}{2} (m_{l_1^-} x - m_{l_2^+} y) \left(\frac{1}{L_{A^0 h^0}^{ver}} + \frac{1}{L_{h^0 A^0}^{ver}} \right) \right. \\
& + \left. \frac{m_i \eta_i^+}{2} \left(\frac{1}{L_{A^0 h^0}^{ver}} - \frac{1}{L_{h^0 A^0}^{ver}} \right) \right) \left. \right\}, \tag{4.25}
\end{aligned}$$

where

$$\begin{aligned}
L_{1, h^0}^{self} &= m_{h^0}^2 (1-x) + (m_i^2 - m_{l_1^-}^2 (1-x)) x, \\
L_{1, A^0}^{self} &= L_{1, h^0}^{self} (m_{h^0} \rightarrow m_{A^0}),
\end{aligned}$$

$$\begin{aligned}
L_{2,h^0}^{self} &= L_{1,h^0}^{self}(m_{l_1^-} \rightarrow m_{l_2^+}), \\
L_{2,A^0}^{self} &= L_{1,A^0}^{self}(m_{l_1^-} \rightarrow m_{l_2^+}), \\
L_{h^0}^{ver} &= m_{h^0}^2(1-x-y) + m_i^2(x+y) - q^2xy, \\
L_{h^0A^0}^{ver} &= m_{A^0}^2x + m_i^2(1-x-y) + (m_{h^0}^2 - q^2x)y, \\
L_{A^0}^{ver} &= L_{h^0}^{ver}(m_{h^0} \rightarrow m_{A^0}), \\
L_{A^0h^0}^{ver} &= L_{h^0A^0}^{ver}(m_{h^0} \rightarrow m_{A^0}),
\end{aligned} \tag{4.26}$$

and

$$\begin{aligned}
\eta_i^V &= \xi_{N,l_1i}^E \xi_{N,l_2}^{E*} + \xi_{N,l_1}^{E*} \xi_{N,l_2i}^E, \\
\eta_i^A &= \xi_{N,l_1i}^E \xi_{N,l_2}^{E*} - \xi_{N,l_1}^{E*} \xi_{N,l_2i}^E, \\
\eta_i^+ &= \xi_{N,l_1i}^{E*} \xi_{N,l_2}^{E*} + \xi_{N,l_1i}^E \xi_{N,l_2}^E, \\
\eta_i^- &= \xi_{N,l_1i}^{E*} \xi_{N,l_2}^{E*} - \xi_{N,l_1i}^E \xi_{N,l_2}^E.
\end{aligned} \tag{4.27}$$

The parameters c_V and c_A are $c_A = -\frac{1}{4}$ and $c_V = \frac{1}{4} - \sin^2 \theta_W$. In Eq. (4.27) the flavor changing couplings $\bar{\xi}_{N,l_ji}^D$ represent the effective interaction between the internal lepton i , ($i = e, \mu, \tau$) and outgoing (incoming) $j = 1$ ($j = 2$) one. Here we take $\bar{\xi}_{N,l_ji}^D$ complex in general and use the parametrization

$$\xi_{N,l_ji}^E = |\xi_{N,l_ji}^E| e^{i\theta_{ij}}, \tag{4.28}$$

where i, l_j denote the lepton flavors and θ_{ij} are CP violating parameters which are the sources of the lepton EDM.

The Br for the decay $Z \rightarrow l_1 \bar{l}_2$ can be formulated in terms of the above form factors. In calculating this we may use the partial width expression for this decay⁵,

$$\Gamma(Z \rightarrow l_1 \bar{l}_2) = \frac{1}{192\pi} \frac{1}{m_Z} |\mathcal{M}(Z \rightarrow l_1 \bar{l}_2)|^2. \tag{4.29}$$

Then Br is simply $Br(Z \rightarrow l_1 \bar{l}_2) = \Gamma(Z \rightarrow l_1 \bar{l}_2)/\Gamma_Z$, where Γ_Z is the total width for Z decay. By using the Eq. (4.18) together with Eq. (4.24) and neglecting the

⁵ In all our numerical analysis we will consider $l_1 \bar{l}_2 + \bar{l}_1 l_2$ as the final state instead of just taking $l_1 \bar{l}_2$.

mass of the final leptons, absolute square of the amplitude can be determined in terms of form factors as

$$|\mathcal{M}(Z \rightarrow l_1 \bar{l}_2)|^2 = 4m_Z^2 \left(|f_V|^2 + |f_A|^2 + \frac{1}{2\cos^2\theta_W} (|f_M|^2 + |f_E|^2) \right). \quad (4.30)$$

Thus the Br becomes

$$\begin{aligned} Br(Z \rightarrow l_1 \bar{l}_2) &= \frac{\Gamma(Z \rightarrow l_1 \bar{l}_2)}{\Gamma_Z} \\ &= \frac{1}{48\pi} \frac{m_Z}{\Gamma_Z} \left[|f_V|^2 + |f_A|^2 + \frac{1}{2\cos^2\theta_W} (|f_M|^2 + |f_E|^2) \right]. \end{aligned} \quad (4.31)$$

4.2 Numerical Analysis and Discussion

First of all we present the possible restrictions on the relevant free parameters $\bar{\xi}_{N,ij}^E, i, j = e, \mu, \tau$ coming from present and forthcoming experiments. At the first stage we can make two reasonable assumptions. The first is that $\bar{\xi}_{N,ij}^E, i, j = e, \mu$, are small compared to $\bar{\xi}_{N,\tau i}^E, i = e, \mu, \tau$ since the strength of these couplings are related with the masses of leptons denoted by the indices of them, similar to the Cheng-Sher scenario [87]. Second is that $\bar{\xi}_{N,ij}^E$ is symmetric with respect to interchange of the indices i and j .

Since we are dealing with the decay modes $Z \rightarrow e^\mp \mu^\pm, Z \rightarrow e^\mp \tau^\pm$ and $Z \rightarrow \mu^\mp \tau^\pm$, there are totaly nine number of free Yukawa couplings except the CP violating phases. Imposing the first assumption this number reduces to five. Further the second assumption makes this set smaller and leaves finally the set as $(\bar{\xi}_{N,e\tau}^E, \bar{\xi}_{N,\mu\tau}^E, \bar{\xi}_{N,\tau\tau}^E)$. There is in fact no experimental measurement, to be used for constraining the Yukawa coupling $\bar{\xi}_{N,\tau\tau}^E$.

Let us first consider possible constraints on $\bar{\xi}_{N,\mu\tau}^E$. This can be achieved by using the experimental limits of μ lepton EDM [88],

$$0.3 \times 10^{-19} \text{ e cm} < d_\mu < 7.1 \times 10^{-19} \text{ e cm}. \quad (4.32)$$

Following the [86], μ lepton EDM can be expressed in model III framework as

$$d_\mu = -\frac{iG_F}{\sqrt{2}} \frac{e}{32\pi^2} \frac{Q_\tau}{m_\tau} \left[(\bar{\xi}_{N,\mu\tau}^{E*})^2 - (\bar{\xi}_{N,\mu\tau}^E)^2 \right] \left[F(y_{h^0}) - F(y_{A^0}) \right], \quad (4.33)$$

where $y_\alpha = m_\tau^2/m_\alpha^2$ for $\alpha = h^0, A^0$, Q_μ is the charge of μ lepton and the function $F(y_\alpha)$ is

$$F(y_\alpha) = \frac{y_\alpha(3 - 4y_\alpha + y_\alpha^2 + 2 \ln y_\alpha)}{(-1 + y_\alpha)^3}. \quad (4.34)$$

Using the parametrization in Eq. (4.28), we may write, from Eq. (4.33), the following restricted region for $\bar{\xi}_{N,\mu\tau}^E$

$$\frac{d_\mu^{\min}}{C(\theta_{\mu\tau}, y_{h^0}, y_{A^0})} < |\bar{\xi}_{N,\mu\tau}^E|^2 < \frac{d_\mu^{\max}}{C(\theta_{\mu\tau}, y_{h^0}, y_{A^0})}, \quad (4.35)$$

where $C(\theta_{\mu\tau}, y_{h^0}, y_{A^0})$ is

$$C(\theta_{\mu\tau}, y_{h^0}, y_{A^0}) = \frac{G_F}{\sqrt{2}} \frac{e}{16\pi^2} \frac{Q_\tau}{m_\tau} \sin 2\theta_{\mu\tau} [F(y_{h^0}) - F(y_{A^0})]. \quad (4.36)$$

From Eq. (4.35) a possible physical region for $\bar{\xi}_{N,\mu\tau}^E$ is determined to be $(10^2 - 10^3)$, GeV by taking acceptable values for m_{h^0}, m_{A^0} and $\sin \theta_\mu$ and using the input values depicted in Table (4.1). There is indeed another way for the restriction of the coupling $\bar{\xi}_{N,\mu\tau}^D$, which involves the deviation of the anomalous magnetic moment (AMM) of muon over its SM prediction [89] due to the recent experimental result of muon AMM by g-2 Collaboration [90]. However, AMM of muon is possible in the model III even for vanishing complex Yukawa couplings. In the LFV $Z \rightarrow l_1 \bar{l}_2$ decay, the part which depends on the couplings η_i^A and η_i^- (see Eq. (4.27)) is non-vanishing when the complex Yukawa couplings are permitted in the model. Consequently, we choose EDM of muon since the restriction is also sensitive to complex phases, existing also in the $Z \rightarrow l_1 \bar{l}_2$ decay which is evident from Eq. (4.33).

The coupling $\bar{\xi}_{N,e\tau}^D$ is restricted using the experimental upper limit of the Br of the process $\mu \rightarrow e\gamma$ (1.2×10^{-11}) and the above constraint for $\bar{\xi}_{N,\mu\tau}^D$. From the discussion in [86] $\mu \rightarrow e\gamma$ decay can be used to fix the Yukawa combination $\bar{\xi}_{N,\mu\tau}^D \bar{\xi}_{N,e\tau}^D$ of the form

$$|\bar{\xi}_{N,\mu\tau}^E|^2 |\bar{\xi}_{N,e\tau}^E|^2 = \frac{1.2 \times 10^{-11} \Gamma_\mu}{B(y_{h^0}, y_{A^0})}, \quad (4.37)$$

where Γ_μ is the total width of the muon and the function $B(y_{h^0}, y_{A^0})$ is

$$B(y_{h^0}, y_{A^0}) = \frac{G_F^2 \alpha_{em} m_\mu^3}{2^{10} \pi^4} \frac{Q_\tau^2}{m_\tau^2} [F(y_{h^0}) - F(y_{A^0})]^2, \quad (4.38)$$

where α_{em} is the electromagnetic fine structure constant. Eq. (4.37), together with the use of limits for $\bar{\xi}_{N,e\tau}^E$, ensure us to determine the upper and lower limits of the coupling $\bar{\xi}_{N,e\tau}^D$. The values are at the order of magnitude of $(10^{-5} - 10^{-4})$. The maximum value of the $Br(Z \rightarrow \mu e)$ is calculated by taking the combination $\bar{\xi}_{N,\mu\tau}^D \bar{\xi}_{N,e\tau}^D$, which respects the upper bound of $\mu \rightarrow e\gamma$ decay. For the minimum value of $Br(Z \rightarrow \mu e)$, we use the combination $\bar{\xi}_{N,\mu\tau}^D \bar{\xi}_{N,e\tau}^D$ if each coupling is at its minimum value, even though this minimum value is artificial. Another way of restricting $\bar{\xi}_{N,e\tau}^D$ and getting the minimum value of $Br(Z \rightarrow \mu e)$ could be achieved by using the experimental result of the EDM of electron [91]. However, we expect that the experimental result of the EDM of electron is not more reliable than the one of the process $\mu \rightarrow e\gamma$. Let us finally emphasize that we take these constrained parameters complex in order to be able to describe the EDM which is possible in the case of CP violating interactions. Throughout our calculations we use the input values given in Table (4.1).

Table 4.1: The values of the input parameters used in the numerical calculations for the decay $Z \rightarrow l_1^- l_2^+$, $l_{1,2} = e, \mu, \tau$.

Parameter	Value
m_μ	0.106 (GeV)
m_τ	1.78 (GeV)
m_W	80.26 (GeV)
m_Z	91.19 (GeV)
G_F	$1.1663710^{-5} (GeV^{-2})$
Γ_Z	2.490 (GeV)
$\sin \theta_W$	$\sqrt{0.2325}$

Fig. (4.3) ((4.4)) represents $\sin \theta_{\tau e}$ dependence of the maximum (minimum) value of the $Br(Z \rightarrow \mu^\pm e^\pm)$ for $\sin \theta_{\tau\mu} = 0.5$, $m_{h^0} = 70 GeV$ and $m_{A^0} = 80 GeV$. Here the maximum and minimum values are predicted by taking upper and lower limits of μ lepton EDM into account. The maximum (minimum) value of the Br is 7×10^{-11} (10^{-13}) for small values of $\sin \theta_{\tau e}$ and its sensitivity to this parameter is weak. Br decreases at the order of the magnitude 15% for

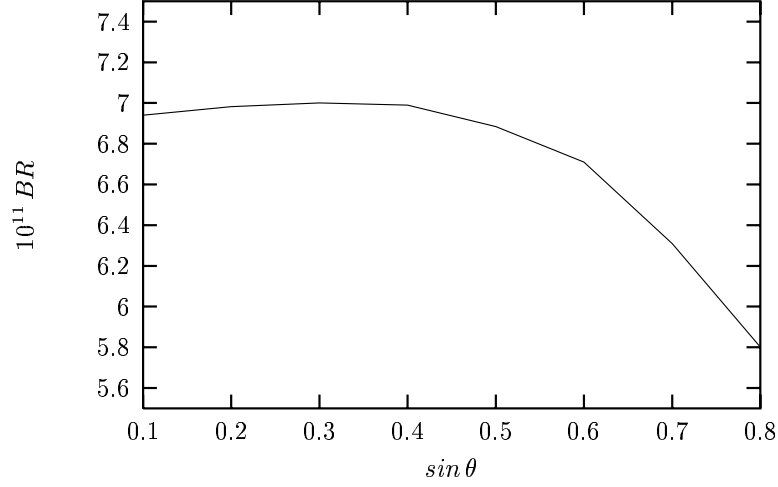


Figure 4.3: The maximum value of $Br(Z \rightarrow \mu^\pm e^\pm)$ as a function of $\sin\theta_{\tau e}$ for $\sin\theta_{\tau\mu} = 0.5$, $m_{h^0} = 70 \text{ GeV}$ and $m_{A^0} = 80 \text{ GeV}$.

$\sin\theta_{\tau e} \geq 0.5$ and it becomes more sensitive to $\sin\theta_{\tau e}$. $\sin\theta_{\tau\mu}$ dependence of the maximum (minimum) value of the $Br(Z \rightarrow \mu^\pm e^\pm)$ for $\sin\theta_{\tau e} = 0.5$, $m_{h^0} = 70 \text{ GeV}$ and $m_{A^0} = 80 \text{ GeV}$ almost the same as $\sin\theta_{\tau e}$ dependence of the Br under consideration. In Fig. (4.5) we present m_{A^0} dependence of the minimum value of the $Br(Z \rightarrow \mu^\pm e^\pm)$ for $\sin\theta_{\tau e} = 0.5$, $\sin\theta_{\tau\mu} = 0.5$ and $m_{h^0} = 70 \text{ GeV}$. The Br is strongly sensitive to m_{A^0} and decreases with increasing values of m_{A^0} . The same dependence appears for the maximum value of the Br . Fig. (4.6) ((4.7)) shows $\sin\theta_{\tau e}$ and $\sin\theta_{\tau\mu}$ dependence of the maximum (minimum) value of the $Br(Z \rightarrow \tau^\pm e^\pm)$ for $\sin\theta_{\tau\mu} = 0.5$ and $\sin\theta_{\tau e} = 0.5$ respectively. Here the coupling $\bar{\xi}_{N,\tau\tau}^D$ is taken as $\bar{\xi}_{N,\tau\tau}^D = 10^3 \text{ GeV}$. The maximum (minimum) value of the Br for this process is at the order of the magnitude of 10^{-11} (10^{-12}). Br increases with increasing values $\sin\theta_{\tau\mu}$, however this behavior appears in contrary to $\sin\theta_{\tau e}$ dependence. The sensitivity of $Br(Z \rightarrow \tau^\pm e^\pm)$ to both CP violating parameters, $\sin\theta_{\tau e}$ and $\sin\theta_{\tau\mu}$, is strong.

We present the coupling $\bar{\xi}_{N,\tau\tau}^D$ dependence of $Br(Z \rightarrow \tau^\pm e^\pm)$ in Figs. (4.8) and (4.9). These figures shows that the Br enormously increases with increasing values of the coupling $\bar{\xi}_{N,\tau\tau}^D$. Note that we take the coupling $\bar{\xi}_{N,\tau\tau}^D$ real in our calculations.

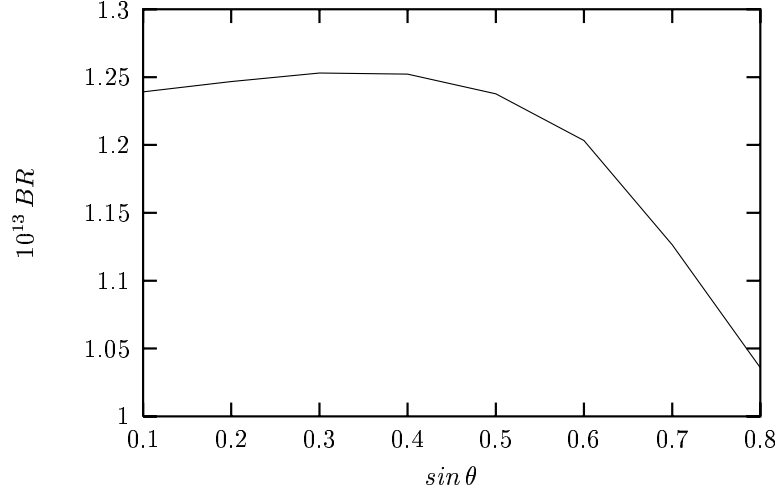


Figure 4.4: The minimum value of $Br(Z \rightarrow \mu^\pm e^\pm)$ as a function of $\sin\theta_{\tau e}$ for $\sin\theta_{\tau\mu} = 0.5$, $m_{h^0} = 70 \text{ GeV}$ and $m_{A^0} = 80 \text{ GeV}$.

To sum up, we study the $Z \rightarrow \mu^\pm \tau^\pm$ decay by taking τ lepton as an internal one similar to previous analysis. Here the experimental upper limit for $Br(Z \rightarrow \mu^\pm \tau^\pm)$ can be reached for the small values of $\bar{\xi}_{N,\tau\tau}^D$. Further, the theoretical calculations are consistent with this upper limit for the case where the mass differences of neutral Higgs bosons h^0 and A^0 are large, even for large values of the coupling $\bar{\xi}_{N,\tau\tau}^D$.

As a summary, we study the Br 's of the decays $Z \rightarrow e^\pm \mu^\pm$, $Z \rightarrow e^\pm \tau^\pm$ and $Z \rightarrow \mu^\pm \tau^\pm$ and observe that it is possible to reach the present experimental upper limits in the model III, playing with the model parameters in the restriction region. This result is important since the theoretical work in the SM shows that the branching rates are less than 10^{-54} and compared to this number large rates are expected with massive and mixing neutrinos. In our analysis, we predict that the Br for the $Z \rightarrow e^\pm \mu^\pm$ decay can reach to the values at the order of the magnitude 10^{-11} . Br for the process $Z \rightarrow e^\pm \tau^\pm$ depends strongly on the Yukawa coupling $\bar{\xi}_{N,\tau\tau}^D$ and for its large values such as $10^3 - 10^4 \text{ GeV}$, it can be in the range $10^{-10} - 10^{-9}$. The process $Z \rightarrow \mu^\pm \tau^\pm$ can have larger Br compared to the previous ones, since the Yukawa couplings entering in the expressions are $\bar{\xi}_{N,\mu\tau}^D$ and $\bar{\xi}_{N,\tau\tau}^D$. Furthermore, Br 's of the processes under consideration are sensitive

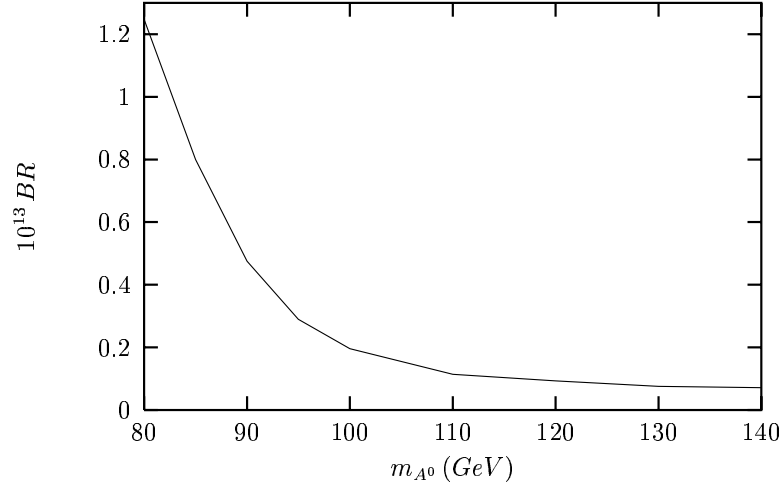


Figure 4.5: The minimum value of $Br(Z \rightarrow \mu^\pm e^\pm)$ as a function of m_{A^0} for $\sin\theta_{\tau\mu} = 0.5$, $\sin\theta_{\tau e} = 0.5$ and $m_{h^0} = 70 \text{ GeV}$.

to the CP -violating parameters since the source of the parts which depend on couplings η_i^A and η_i^- are the non-vanishing complex Yukawa couplings, in the model III.

In future, with the reliable experimental result of upper limits of the Br 's of above processes it would be possible to test models beyond the SM and free parameters of these models

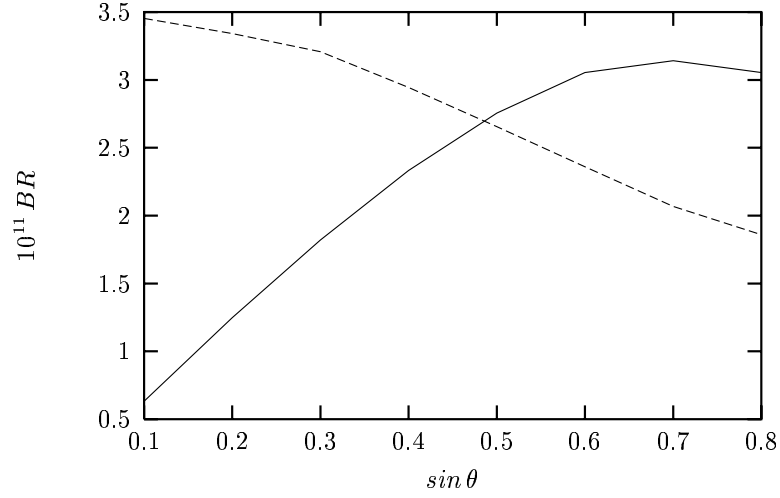


Figure 4.6: The maximum value of $Br(Z \rightarrow \tau^\pm e^\pm)$ as a function of $\sin\theta$ for $\bar{\xi}_{N,\tau\tau}^D = 10^3 \text{ GeV}$, $m_{h^0} = 70 \text{ GeV}$ and $m_{A^0} = 80 \text{ GeV}$. Here solid line represents the dependence with respect to $\sin\theta_{\tau\mu}$ for $\sin\theta_{\tau e} = 0.5$ and dashed line to $\sin\theta_{\tau e}$ for $\sin\theta_{\tau\mu} = 0.5$.

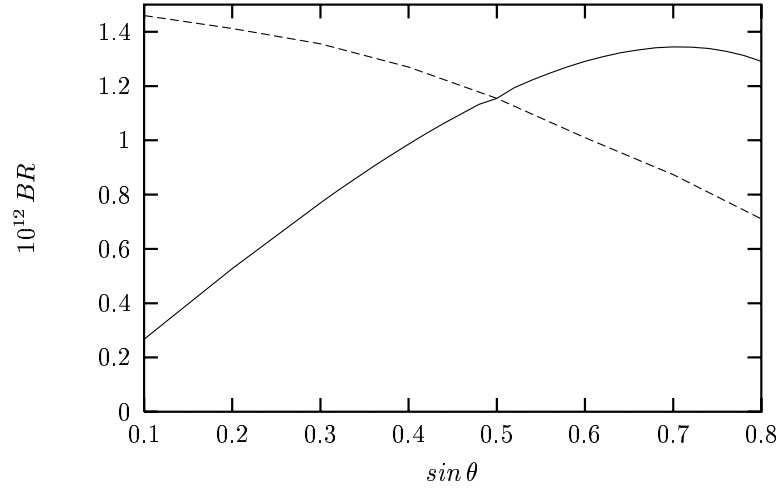


Figure 4.7: The minimum value of $Br(Z \rightarrow \tau^\pm e^\pm)$ as a function of $\sin\theta$ for $\bar{\xi}_{N,\tau\tau}^D = 10^3 \text{ GeV}$, $m_{h^0} = 70 \text{ GeV}$ and $m_{A^0} = 80 \text{ GeV}$. Here solid line represents the dependence with respect to $\sin\theta_{\tau\mu}$ for $\sin\theta_{\tau e} = 0.5$ and dashed line to $\sin\theta_{\tau e}$ for $\sin\theta_{\tau\mu} = 0.5$.

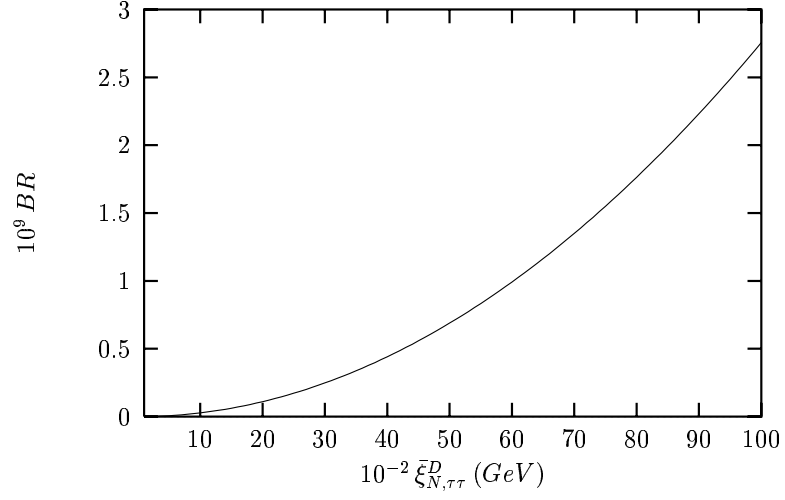


Figure 4.8: The maximum value of $Br(Z \rightarrow \tau^\pm e^\pm)$ as a function of $\bar{\xi}_{N,\tau\tau}^D$ for $\sin\theta_{\tau\mu} = 0.5$, $\sin\theta_{\tau e} = 0.5$, $m_{h^0} = 70 \text{ GeV}$ and $m_{A^0} = 80 \text{ GeV}$.

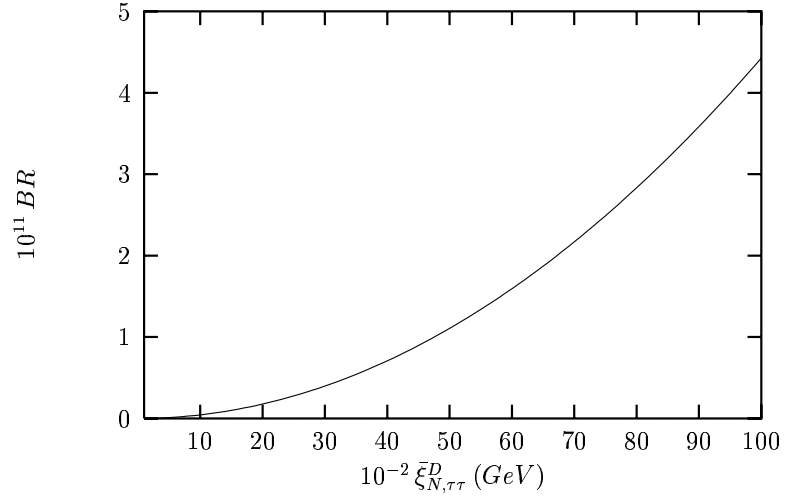


Figure 4.9: The minimum value of $Br(Z \rightarrow \tau^\pm e^\pm)$ as a function of $\bar{\xi}_{N,\tau\tau}^D$ for $\sin\theta_{\tau\mu} = 0.5$, $\sin\theta_{\tau e} = 0.5$, $m_{h^0} = 70 \text{ GeV}$ and $m_{A^0} = 80 \text{ GeV}$.

CHAPTER 5

THE FLAVOR CHANGING $t \rightarrow cl_1^-l_2^+$ IN MODEL III

Rare decays of heavy quarks have long been a subject of intense theoretical and experimental study. The main argument for this is the fact that loop processes are an invaluable test for the short-distance structure of the theory. Furthermore, many such decays are sensitive to parameters in the SM and are excellent probes for getting some clues about the effects of new physics such as supersymmetry, an extended Higgs sector and charged Higgs bosons and heavier fermion families.

There are special reasons for studying rare decays of t quark both in the SM and beyond, as it is by far largest fermion mass and therefore physicists give a special role to the top quark. As such, richness of the decay products stimulates one to study its decays to be a useful quantitative reference point for comparing the SM to experiment. The rare decay of top quark have been studied in the literature in the framework of the SM and beyond [92]–[100]; the one-loop flavor changing transitions, sensitive to possible effects from new physics, $t \rightarrow c(\gamma, Z, g)$ in [95, 97] and $t \rightarrow cH^0$ in [93, 97, 98, 99, 100]. The reason for the special interest in these decays is again that observation of a single event of this kind in near future colliders would imply evidence of new physics which could be related with the Higgs sector of the theory.

In the framework of the SM these processes are in general quite suppressed due to the Glashow–Iliopoulos–Maiani (GIM) mechanism [2] controlled by the light masses of the b, s, d quarks circulating in the loop. The corresponding Br 's are additionally decreased by the large total decay width Γ_T of the top quark. Thus the Br 's of the rare decays of the top quark into gauge bosons (γ, Z, g)

plus c-quark are too much small. With the current experimental value of the top quark mass, the predicted values of the Br of the process $t \rightarrow c\gamma$ is of the order of $\sim 5 \times 10^{-13}$, for the Z boson $\sim 1 \times 10^{-13}$, for the gluon $\sim 4 \times 10^{-13}$ [93], the Br for $t \rightarrow cH^0$ is at the order of the magnitude of $10^{-14} - 10^{-13}$, in the SM [98]. Apparently these numbers are so tiny that it is not possible to measure them even at the highest luminosity accelerators.

Some of this undesirable features can change with physics beyond the SM. As has already been mentioned, for one or more additional scalar Higgs doublets to the SM, the flavor changing neutral couplings could indeed be generated at tree level unless *ad hoc* discrete symmetries imposed [22]. Then it is possible to enhance the Br for the rare top quark decays in different kinds of models which include new physics. As an example $t \rightarrow cH^0$ decay has been studied in one of this kind of models, model III [100] and it has been found that the Br of this process could reach to the values of the order 10^{-6} , varying the free parameters of the model III, respecting the existing experimental restrictions. The predicted Br is in fact almost seven orders larger compared to the one in the SM, which is indeed a strong enhancement.

In this chapter, we study the analysis of the flavor changing (FC) $t \rightarrow c(l_1^- l_2^+ + l_1^+ l_2^-)$ decay in the framework of the general two Higgs doublet model (model III). This decay occurs at tree level since the FC transitions in the quark and leptonic sector are permitted in the model III. Here, the Yukawa couplings for $t - c$ and $l_1^- - l_2^+$ transitions play the main role and they take place by means of the internal neutral Higgs bosons, h^0 and A^0 . In the process, it is possible to get h^0 and A^0 resonances since the kinematical region is large enough and this difficulty can be solved by choosing the appropriate propagator for h^0 and A^0 bosons (see the next section). We are able to get the Br of the $t \rightarrow c(l_1^- l_2^+ + l_1^+ l_2^-)$ for $l_1 = \tau$ and $l_2 = \mu$ at the tree level at the order of magnitude $10^{-8} - 10^{-7}$, which is a measurable quantity in the accelerators and we further calculate the one loop effects related with the interactions due to the internal mediating charged Higgs boson (see Fig. (5.1): (b), (c), (d)) and observe that their contribution to the Br of the decay

$t \rightarrow c l_1^- l_2^+$ are negligible. They are of the order of $10^{-11} - 10^{-10}$.

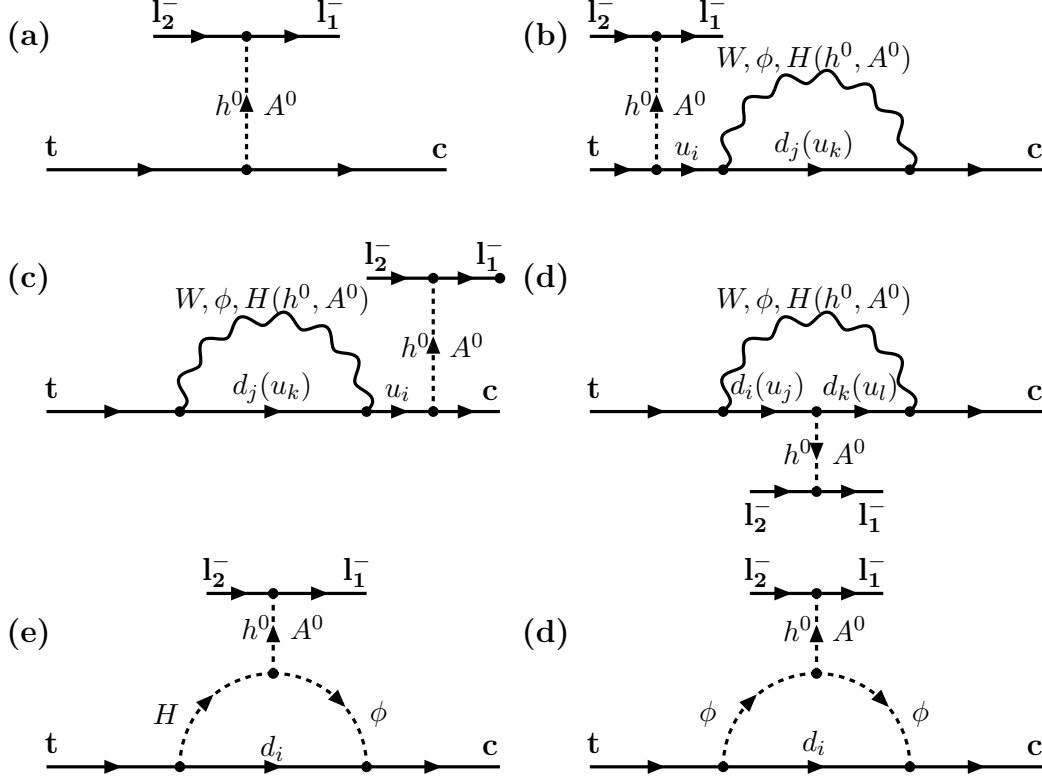


Figure 5.1: Tree level and one loop level diagrams contributing to the decay $t \rightarrow c l_1^- l_2^+$. The dashed lines represent the Higgs bosons h^0, A^0 . In Figs. (b), (c), (d) the wavy lines represent both W^\pm, ϕ^\pm, H^\pm and h^0, A^0 at the same time.

We will present, in the next section, the Br of the decay $t \rightarrow c(l_1^- l_2^+ + l_1^+ l_2^-)$ in the framework of model III and the last section contains numerical analysis and our conclusions.

5.1 $t \rightarrow c(l_1^- l_2^+ + l_1^+ l_2^-)$ in Model III

The flavor changing transition $t \rightarrow c l_1^- l_2^+$ is forbidden in the SM. Such transitions would be possible in the case that the Higgs sector of the model is extended and FCNCs in the tree level are permitted unless the *ad hoc* discrete symmetries are invoked, which is indeed related to the fact that no phenomenological need

to do this as long as the couplings of the scalars to the light quarks are taken to be small. This section contains the calculation of the Br of the decay under consideration, in the model III. In this model, there are various new parameters, such as complex Yukawa couplings, masses of new Higgs bosons, etc. and they should of course be constrained by using the present experimental outputs.

The $t \rightarrow cl_1^- l_2^+$ process is controlled by the Yukawa interaction given by Eq. (2.12). The part representing the FC interactions was readily be obtained in chapter 3 (see Eq. (4.3)). Furthermore throughout our calculations we will use the dimensional Yukawa couplings $\bar{\xi}_N^{U,D,E}$ instead of original $\xi^{U,D,E}$. As is obvious from the construction of the model III the $t \rightarrow cl_1^- l_2^+$ decay process occurs at the tree level, which gets occurred with the help of the neutral Higgs bosons h^0 and A^0 enabling non-zero $t - c(l_1^- - l_2^+)$ transition amplitude. For completeness, we also take the one loop contributions into account (see Fig. (5.1)) and use the on-shell renormalization scheme to get rid of the existing divergences from the vertex function.

In getting renormalized $t \rightarrow ch^{0*}(A^{0*})$ transition vertex functions defined as

$$\begin{aligned}\Gamma_{REN}^{h^{0*}} &= \Gamma_0^{h^{0*}} + \Gamma_C^{h^0}, \\ \Gamma_{REN}^{A^{0*}} &= \Gamma_0^{A^{0*}} + \Gamma_C^{A^0},\end{aligned}\tag{5.1}$$

our strategy is to use the following on-shell conditions

$$\begin{aligned}\Gamma_{REN}^{h^0}|_{onshell} &= \frac{i}{2\sqrt{2}} \left((\xi_{N,ct}^U + \xi_{N,tc}^{U*}) + (\xi_{N,ct}^U - \xi_{N,tc}^{U*})\gamma_5 \right), \\ \Gamma_{REN}^{A^0}|_{onshell} &= -\frac{1}{2\sqrt{2}} \left((\xi_{N,ct}^U - \xi_{N,tc}^{U*}) + (\xi_{N,ct}^U + \xi_{N,tc}^{U*})\gamma_5 \right),\end{aligned}\tag{5.2}$$

and to extract the counter term by evaluating vertex functions in Eq. (5.1) at on-shell point as

$$\begin{aligned}\Gamma_C^{h^0} &= \Gamma_{REN}^{h^0}|_{onshell} - \Gamma_0^{h^0}|_{onshell}, \\ \Gamma_C^{A^0} &= \Gamma_{REN}^{A^0}|_{onshell} - \Gamma_0^{A^0}|_{onshell}.\end{aligned}\tag{5.3}$$

where $\Gamma_0^{h^0}$ denotes the bare vertex function. Depicted in Fig. (5.1) is the loop diagrams including H^\pm intermediate Higgs boson for FC interaction (Fig. (5.1);

b, c, d) at the quark level. As already stated $\xi_{N,bb}^D$ and $\xi_{N,tt}^U$ are dominant couplings in the loop effects. Therefore, we neglect all the Yukawa couplings except $\xi_{N,bb}^D$ and $\xi_{N,tt}^D$ in the loop contributions. Notice that the self energy diagrams do not give any contribution in the on-shell renormalization scheme. As is obvious from the chosen on-shell renormalization scheme that none of the self energy diagrams give any nonzero contributions.

The renormalized vertex function is connected to the $l_1^- l_2^+$ out going leptons by intermediate neutral h^0 and A^0 bosons as shown in the Fig. (5.1) and for the matrix element square of the process $t \rightarrow c (l_1^- l_2^+ + l_1^+ l_2^-)$ we eventually get

$$\begin{aligned} |\mathcal{M}|^2 = & 8 m_t^2 (1-s) \sum_{S=h^0, A^0} |p_S|^2 \left(|a_S^{(q)}|^2 + |a_S'^{(q)}|^2 \right) \\ & \left((s m_t^2 - (m_{l_1^-} - m_{l_2^+})^2) |a_S^{(l)}|^2 + (s m_t^2 - (m_{l_1^-} + m_{l_2^+})^2) |a_S'^{(l)}|^2 \right) \\ & + 16 m_t^2 (1-s) \left((s m_t^2 - (m_{l_1^-} - m_{l_2^+})^2) \text{Re}[p_{h^0} p_{A^0}^* a_{h^0}^{(l)} a_{A^0}^{*(l)} (a_{h^0}^{(q)} a_{A^0}^{*(q)} \right. \\ & + a_{h^0}'^{(q)} a_{A^0}'^{*(q)})] + (s m_t^2 - (m_{l_1^-} + m_{l_2^+})^2) \text{Re}[p_{h^0} p_{A^0}^* a_{h^0}'^{(l)} a_{A^0}'^{*(l)} (a_{h^0}^{(q)} a_{A^0}^{*(q)} \\ & + a_{h^0}'^{(q)} a_{A^0}'^{*(q)})] \Big), \end{aligned} \quad (5.4)$$

where p_S is defined as

$$p_S = \frac{i}{s m_t^2 - m_S^2 + i m_S \Gamma_{tot}^S}, \quad (5.5)$$

with the help of the Breit–Wigner prescription and Γ_{tot}^S is the total decay width of S boson, for $S = h^0, A^0$. Here, the parameter s is $s = q^2/m_t^2$, and q^2 is the intermediate S boson momentum square. In Eq. (5.4) the functions $a_{h^0, A^0}^{(l)}, a_{h^0, A^0}'^{(l)}$ which includes merely Yukawa couplings for leptons have tree level contributions and $a_{h^0, A^0}^{(q)}, a_{h^0, A^0}'^{(q)}$ including Yukawa couplings for quarks are the combinations of tree level and one-loop level contributions and they can be nominated as,

$$\begin{aligned} a_{h^0, A^0}^{(l)} &= a_{h^0, A^0}^{Tree(l)}, \\ a_{h^0, A^0}^{(q)} &= a_{h^0, A^0}^{Tree(q)} + a_{h^0, A^0}^{Loop(q)}, \\ a_{h^0, A^0}'^{(l)} &= a_{h^0, A^0}'^{Tree(l)}, \\ a_{h^0, A^0}'^{(q)} &= a_{h^0, A^0}'^{Tree(q)} + a_{h^0, A^0}'^{Loop(q)}, \end{aligned} \quad (5.6)$$

and we give the explicit form of above terms as a long series of equations written below

$$\begin{aligned}
a_{h^0}^{Tree(l)} &= -\frac{i}{2\sqrt{2}} (\xi_{N,l_1 l_2}^D + \xi_{N,l_2 l_1}^{*D}), \\
a_{A^0}^{Tree(l)} &= \frac{1}{2\sqrt{2}} (\xi_{N,l_1 l_2}^D - \xi_{N,l_2 l_1}^{*D}), \\
a_{h^0}'^{Tree(l)} &= -\frac{i}{2\sqrt{2}} (\xi_{N,l_1 l_2}^D - \xi_{N,l_2 l_1}^{*D}), \\
a_{A^0}'^{Tree(l)} &= \frac{1}{2\sqrt{2}} (\xi_{N,l_1 l_2}^D + \xi_{N,l_2 l_1}^{*D}), \\
a_{h^0}^{Tree(q)} &= \frac{i}{2\sqrt{2}} (\xi_{N,ct}^U + \xi_{N,tc}^{*U}), \\
a_{A^0}^{Tree(q)} &= -\frac{1}{2\sqrt{2}} (\xi_{N,ct}^U - \xi_{N,tc}^{*U}), \\
a_{h^0}'^{Tree(q)} &= \frac{i}{2\sqrt{2}} (\xi_{N,ct}^D - \xi_{N,tc}^{*D}), \\
a_{A^0}'^{Tree(q)} &= -\frac{1}{2\sqrt{2}} (\xi_{N,ct}^D + \xi_{N,tc}^{*D}), \\
a_{h^0}^{Loop(q)} &= -\frac{i}{32\sqrt{2}\pi^2} V_{cb} V_{tb}^* \xi_{N,bb}^D \left(m_b^2 \xi_{N,bb}^D \xi_{N,tt}^{U*} \int_0^1 dx \int_0^{1-x} dy f_1^{h^0}(x, y) \right. \\
&\quad + m_b m_t (\xi_{N,bb}^{D*})^2 \int_0^1 dx \int_0^{1-x} dy \left((1-x-y) f_1^{h^0}(x, y) \right) \\
&\quad - m_b m_t |\xi_{N,bb}^D|^2 \int_0^1 dx \int_0^{1-x} dy \left((x+y) f_1^{h^0}(x, y) \right) \\
&\quad \left. - \xi_{N,bb}^{D*} \xi_{N,tt}^{U*} \int_0^1 dx \int_0^{1-x} dy f_2^{h^0}(x, y) \right), \\
a_{A^0}^{Loop(q)} &= \frac{1}{32\sqrt{2}\pi^2} V_{cb} V_{tb}^* \xi_{N,bb}^D \left(m_b^2 \xi_{N,bb}^D \xi_{N,tt}^{U*} \int_0^1 dx \int_0^{1-x} dy f_1^{A^0}(x, y) \right. \\
&\quad - m_b m_t (\xi_{N,bb}^{D*})^2 \int_0^1 dx \int_0^{1-x} dy \left((1-x-y) f_1^{A^0}(x, y) \right) \\
&\quad - m_b m_t |\xi_{N,bb}^D|^2 \int_0^1 dx \int_0^{1-x} dy \left((x+y) f_1^{A^0}(x, y) \right) \\
&\quad \left. + \xi_{N,bb}^{D*} \xi_{N,tt}^{U*} \int_0^1 dx \int_0^{1-x} dy f_2^{A^0}(x, y) \right), \\
a_{h^0}'^{Loop(q)} &= a_{h^0}^{Loop(q)}, \\
a_{A^0}'^{Loop(q)} &= a_{A^0}^{Loop(q)}, \tag{5.7}
\end{aligned}$$

where

$$f_1^S = \frac{1}{L^S(m_S)} - \frac{1}{L^S(s)},$$

$$f_2^S = (1 - x - y) \left(\frac{m_t^2 x + m_S^2 y}{L^S(m_S)} - \frac{m_t^2 (x + s y)}{L^S(s)} \right) + 2 \ln \frac{L^S(s)}{L^S(m_S)}, \quad (5.8)$$

with

$$\begin{aligned} L^S(s) &= m_b^2 (x - 1) + m_{H^\pm}^2 x + m_t^2 (-1 + x + y) (x + s y), \\ L^S(m_S) &= m_b^2 (x - 1) + m_{H^\pm}^2 x + (-1 + x + y) (m_t^2 x + m_S^2 y). \end{aligned} \quad (5.9)$$

In further studying, numerically, the differential decay width (dDw) $\frac{d\Gamma}{ds}(t \rightarrow c(l_1^- l_2^+ + l_1^+ l_2^-))$, it gets reformulated in the rest frame of top quark here as

$$\frac{d\Gamma}{ds} = \frac{1}{256 N_c \pi^3} \lambda |\mathcal{M}|^2, \quad (5.10)$$

where λ is defined as

$$\begin{aligned} \lambda = \frac{1}{2 m_t^2 s} &\left[(m_t^2 (s - 1)^2 - 4 m_c^2) (m_c^4 + m_{l_1}^4 + (m_{l_2}^2 - m_t^2 s)^2 \right. \\ &\left. - 2 m_c^2 (m_{l_1}^2 + m_{l_2}^2 - m_t^2 s) - 2 m_{l_1}^2 (m_{l_2}^2 + m_t^2 s)) \right]^{1/2}, \end{aligned}$$

and boundary values for the variable s in physically allowed region can be determined by applying kinematical limits and we get

$$\frac{(m_{l_1} + m_{l_2})^2}{m_t^2} \leq s \leq \frac{(m_t - m_c)^2}{m_t^2}.$$

5.2 Numerical Analysis and Discussion

From the experimental point of view, in order to make analysis of the differential Br (dBr), $A_{CP}(s)$, Br and A_{CP} of the decay $t \rightarrow c(l_1^- l_2^+ + l_1^+ l_2^-)$ within the framework of the model III, the Yukawa couplings $\xi_{N,tc}^U$ and $\xi_{N,l_1 l_2}^E$ play the crucial role at tree level and if one goes to loop level new Yukawa couplings, particularly $\bar{\xi}_{N,bb}^D$ and $\bar{\xi}_{N,tt}^U$, appear and become significant. In analyzing above-mentioned physical quantities of this decay we need to restrict these couplings with the help of relevant experimental measurements since they are free parameters of the model used. Therefore our next task is trying to restrict these parameters within current experimental results. In numerical calculations the following parametrization of

the Yukawa couplings appearing in the leptonic sector, $\xi_{N,l_1 l_2}^E = |\xi_{N,l_1 l_2}^E| e^{i\theta_{l_1 l_2}}$, is used.

Along this line, first note that, related to the quark sector, we use the constraint region by restricting the Wilson coefficient C_7^{eff} , which is indeed the effective coefficient of the operator $O_7 = (e/16\pi^2)\bar{s}_\alpha\sigma_{\mu\nu}(m_b R + m_s L)b_\alpha\mathcal{F}^{\mu\nu}$ (see [61] and references therein), in the region $0.257 \leq |C_7^{eff}| \leq 0.439$. These were in fact discussed in details in the last section of chapter 3 within the light of the CLEO measurement [101]

$$BR(B \rightarrow X_s \gamma) = (3.15 \pm 0.35 \pm 0.32) \times 10^{-4}, \quad (5.11)$$

and all possible uncertainties in the calculation of C_7^{eff} [61]. Second point is that, related to the leptonic sector, we can use some experimental results such as anomalous magnetic moment of muon, dipole moments of leptons, rare leptonic decays to restrict the couplings $\xi_{N,l_1 l_2}^E$.

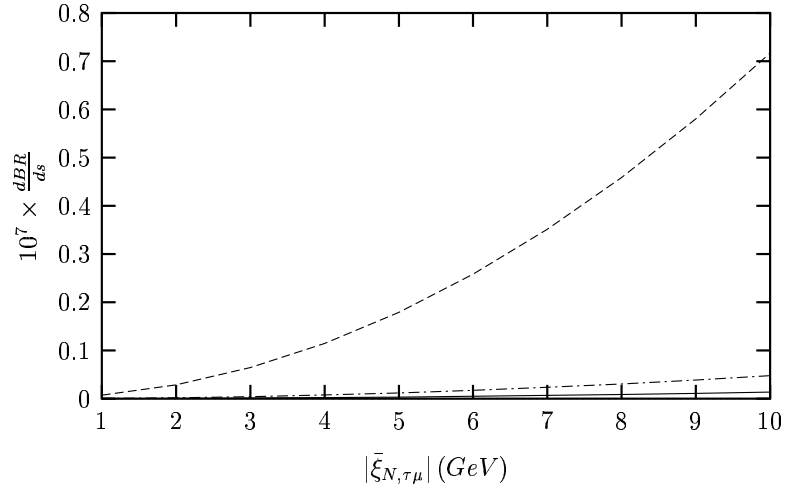


Figure 5.2: $dBr(t \rightarrow c(\tau^-\mu^+ + \tau^+\mu^-))$ as a function of $|\bar{\xi}_{N,\tau\mu}^E|$ for $\sin\theta_{\tau\mu} = 0.5$, real $\bar{\xi}_{N,tc}^D$ and $\Gamma_{tot}^{h^0} = \Gamma_{tot}^{A^0} = 0.1 \text{ GeV}$. The solid (dashed, dash-dotted) line represents the case for $s = (10/175)^2, (50/175)^2, (150/175)^2$.

Let us turn our attention to the usage of the above experimental outputs. As already noted in chapter 3 the upper and lower limits for the couplings $\xi_{N,bb}^D$, $\xi_{N,tt}^U$ and also for $\xi_{N,tc}^U$ get determined by directly using the above restriction related to

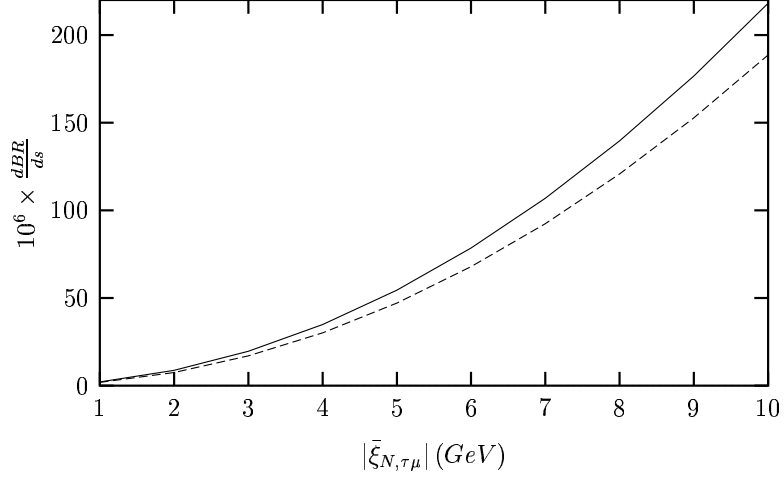


Figure 5.3: $d\text{Br}(t \rightarrow c(\tau^- \mu^+ + \tau^+ \mu^-))$ as a function of $|\bar{\xi}_{N,\tau\mu}^E|$ for $\sin \theta_{\tau\mu} = 0.5$, real $\bar{\xi}_{N,tc}^D$ and $\Gamma_{tot}^{h^0} = \Gamma_{tot}^{A^0} = 0.1 \text{ GeV}$. The solid (dashed) line represents the case for $s = (80/175)^2((90/175)^2)$.

the quark sector. In our numerical analysis we choose the upper limits for those couplings and take $\xi_{N,tc}^U \sim 0.01 \xi_{N,tt}^U$, respecting the constraints mentioned. For the Yukawa couplings in the leptonic part, furthermore, the measured anomalous magnetic moment of muon [102] enables us to choose the upper bound of $\xi_{N,l_1 l_2}^E$ for $l_1 = \tau$ and $l_2 = \mu$. For $l_1 = \tau$ and $l_2 = e$, we use the numerical result obtained for the couplings $\xi_{N,\tau e}^E$ in [103], based on the experimental measurement of the leptonic process $\mu \rightarrow e\gamma$ [104], of which is $Br(\mu \rightarrow e\gamma) = \Gamma(\mu \rightarrow e\gamma)/\Gamma(\mu \rightarrow e\nu\bar{\nu}) < 1.2 \times 10^{-11}$. Although the total decay widths of h^0 and A^0 are unknown parameters, we expect that they are of the same order of magnitude $\Gamma_{tot}^{H^0} \sim (0.1 - 1.0) \text{ GeV}$, where H^0 is the SM Higgs boson. Notice that, in further analysis, we take the value of the total decay width $\Gamma_T \sim \Gamma(t \rightarrow bW)$ as $\Gamma_T = 1.55 \text{ GeV}$ and choose the numerical values $m_{h^0} = 80 \text{ GeV}$ and $m_{A^0} = 90 \text{ GeV}$, for the calculation of the Br .

We present our results for the $d\text{Br}$ and Br of the decay $t \rightarrow c(l_1^- l_2^+ + l_1^+ l_2^-)$ for $l_1 = \tau$ and $l_2 = \mu$ in a series of figures, from Fig. (5.2) to Fig. (5.5). Depicted in Fig. (5.2) is the plot of the $d\text{Br}$ for the $t \rightarrow c(\tau^- \mu^+ + \tau^+ \mu^-)$

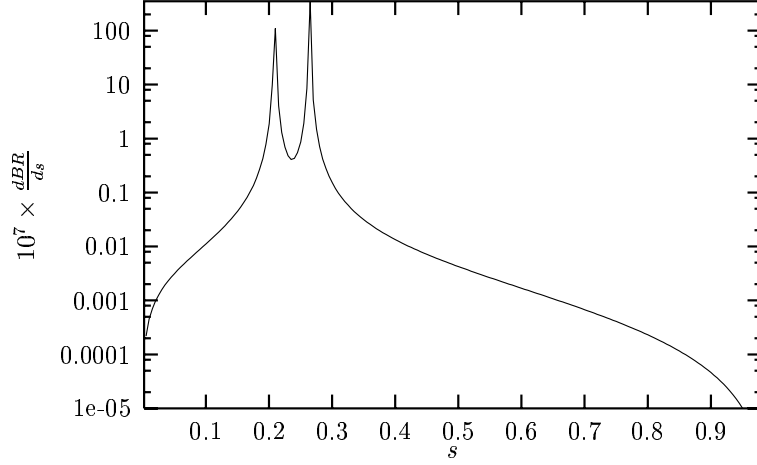


Figure 5.4: $dBr(t \rightarrow c(\tau^- \mu^+ + \tau^+ \mu^-))$ as a function of s for $|\bar{\xi}_{N,\tau\mu}^E| = 10 \text{ GeV}$, $\sin \theta_{\tau\mu} = 0.5$, real $\bar{\xi}_{N,tc}^D$ and $\Gamma_{tot}^{h^0} = \Gamma_{tot}^{A^0} = 0.1 \text{ GeV}$.

decay with respect to $|\bar{\xi}_{N,\tau\mu}^E|$ for $\sin \theta_{\tau\mu} = 0.5$, at different s values¹, namely $(10/175)^2$, $(50/175)^2$, and $(150/175)^2$. In plotting these, we choose $\bar{\xi}_{N,tc}^U$ real and set $\Gamma_{tot}^{h^0} = \Gamma_{tot}^{A^0} = 0.1 \text{ GeV}$. The solid (dashed, dash-dotted) line represents the case for $s = (10/175)^2$ ($(50/175)^2$, $(150/175)^2$). As is obvious from the figure dBr is of the order of the magnitude 10^{-8} for $s = (50/175)^2$ and $|\bar{\xi}_{N,\tau\mu}^E| \sim 5 \text{ GeV}$. However, dBr is less than 10^{-8} for $s = (10/175)^2$ and $s = (150/175)^2$ and it, in fact, reaches extremely small values for $|\bar{\xi}_{N,\tau\mu}^E| \leq 1 \text{ GeV}$. Increasing $|\bar{\xi}_{N,\tau\mu}^E|$ causes to enhance the dBr of the decay, as expected. Fig. (5.3) is devoted to the same dependence for $s = (80/175)^2$ (solid line), $(90/175)^2$ (dashed line), where the values of s are taken at the h^0 and A^0 resonances. The dBr is of the order of the magnitude 10^{-6} for the small values of the coupling $|\bar{\xi}_{N,\tau\mu}^E|$ and increases extremely with the increasing values of this coupling.

In Fig. (5.4), what we present is the dBr as a function of the parameter s , for $|\bar{\xi}_{N,\tau\mu}^E| = 10 \text{ GeV}$, $\sin \theta_{\tau\mu} = 0.5$ and $\Gamma_{tot}^{h^0} = \Gamma_{tot}^{A^0} = 0.1 \text{ GeV}$. It is observed that dBr has a strong s dependence and there appear two sharp peaks for s values of corresponding h^0 and A^0 resonances.

Finally, in Fig. (5.5) the Br for the process $t \rightarrow c(\tau^- \mu^+ + \tau^+ \mu^-)$ as a function

¹ We in fact choose these s values which are away from the resonances.

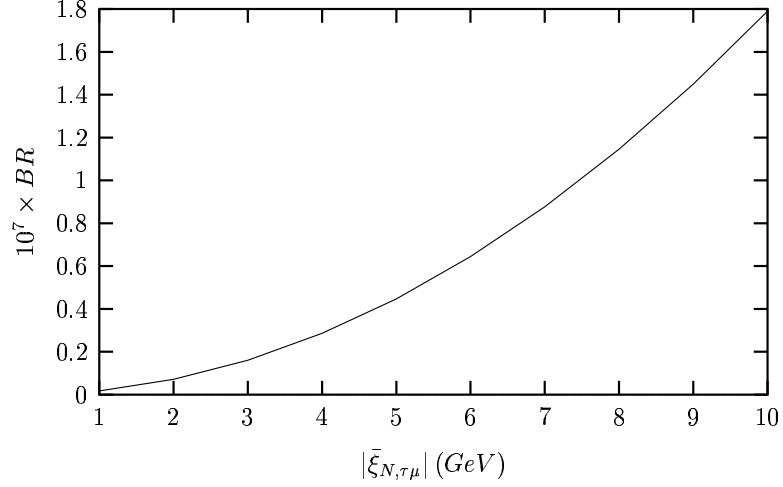


Figure 5.5: BR ($t \rightarrow c(\tau^- \mu^+ + \tau^+ \mu^-)$) as a function of $|\bar{\xi}_{N,\tau\mu}^E|$ for $\sin \theta_{\tau\mu} = 0.5$, real $\bar{\xi}_{N,tc}^D$ and $\Gamma_{tot}^{h^0} = \Gamma_{tot}^{A^0} = 0.1 \text{ GeV}$.

of $|\bar{\xi}_{N,\tau\mu}^E|$ at $\sin \theta_{\tau\mu} = 0.5$ and $\Gamma_{tot}^{h^0} = \Gamma_{tot}^{A^0} = 0.1 \text{ GeV}$ is depicted. The Br is of the order of the magnitude 10^{-8} for $|\bar{\xi}_{N,\tau\mu}^E| \sim 2 \text{ GeV}$ and increases to the values 10^{-7} with increasing $|\bar{\xi}_{N,\tau\mu}^E|$. Notice that the one loop effects are of the order of the magnitude 0.1 % of the tree level result and therefore their contribution can be neglected.

In the case of outgoing τ and e leptons, the Br is predicted of the order of the magnitude $10^{-14} - 10^{-15}$, respecting the numerical values of the coupling $|\bar{\xi}_{N,\tau\mu}^E| = (10^{-4} - 10^{-3}) \text{ GeV}$, obtained in [103], based on the experimental measurement of the leptonic process $\mu \rightarrow e\gamma$. For the case of the outgoing μ and e leptons, we believe that the Br is indeed extremely small, too difficult to be measured.

To sum up, our results can be briefly summarized as follows. The Br of the flavor changing process $t \rightarrow c(l_1^- l_2^+ + l_1^+ l_2^-)$ is forbidden in the SM and in the framework of the SM with the extended Higgs sector it is possible to bring considerable contribution at tree level, of the order of the magnitude $10^{-8} - 10^{-7}$, for $l_1 = \tau$ and $l_1 = \mu$. This physical parameter can be measured in the future experiments and it gives a strong clue about the new physics beyond the SM. Furthermore, the Br is sensitive to Yukawa coupling $\xi_{N,l_1 l_2}^E$ and this results in

smaller Br 's of $t \rightarrow c(l_1^- l_2^+ + l_1^+ l_2^-)$, for $l_1 = \tau, l_2 = e$ and $l_1 = \mu, l_2 = e$. Notice that the loop effects are negligibly small. Before finalizing the chapter let us say a few words about the experimental feasibility of this decay mode. Due to efficiency problems in measuring the τ final lepton and in identifying the c -quark jet, there is a difficulty in the Br measurement of the decay. Then kinematical cuts are needed in order to isolate the signal from a possibly large background. These cuts further make the signal demoted. On the other hand, the possible enhancement of the Br of the decay considered in model III, at least, motivates us to search new models to get a measurable Br on theoretical side. Thus, both experimental and theoretical investigations of the decay $t \rightarrow c(l_1^- l_2^+ + l_1^+ l_2^-)$, especially for $l_1 = \tau, l_2 = \mu$, would play an important role for the determination of the physics beyond the SM.

CHAPTER 6

CONCLUSION

We have examined within the framework of model III version of the 2HDM, the rare $B \rightarrow K^* \tau^+ \tau^-$ decay including neutral Higgs Boson effects, the lepton flavor violation through the leptonic Z decay modes $Z \rightarrow l_1^\pm l_2^\mp$ and the rare top decay $t \rightarrow c l_1^\pm l_2^\mp$. These decays have a common feature in a sense that they are basically related to the flavor part of the SM, which is known as “flavor physics”. Even though flavor physics can be regarded as the least tested part of the SM, experimental situation concerning it is drastically changing. Since the decay modes considered are forbidden at the tree level and usually suppressed in the loop level in the framework of the SM, they are good candidates to search the physics beyond the SM. For this purpose we considered the possibility of the existence of a non-minimal Higgs sector and take the next to minimal Higgs sector consisting of two Higgs doublets. Motivation for exploring those scenarios, especially for the one with two Higgs doublets, are summarized as follows:

- So far, the Higgs sector of the SM is totally unknown and the simplest way to fulfill the requirement that the ρ -parameter at the tree level should be unity is to have two $SU(2)$ Higgs doublets.
- Some models with larger symmetries, as in the case of supersymmetric ones, end up at low energies in a non-minimal scalar sector.
- There is a possibility of generating additional sources for either spontaneous or explicit CP violation in an extended SM through its scalar sector.

- They enable us to generate flavor changing neutral currents, inspired by the increasing evidence on neutrino oscillations, and lepton flavor violation supported by the atmospheric and the solar neutrino experiments.

The 2HDM predicts the existence of five Higgs particles, two CP -even Higgs bosons h^0 and H^0 , one CP -odd one A^0 , and two charged Higgs particles H^\pm . The charged and CP -odd Higgs particles are peculiar to the 2HDM and the experimental discoveries would become a clear signature for the presence of a non-minimal Higgs sector and the physics beyond the SM. In our calculations, we used one of the suitable parametrization of the 2HDM type III in a sense that only one of the doublets acquires nonzero VEV.

Within the context of the model III we have analyzed the processes with FCNCs and dealt with them both in the quark and the lepton sectors. Since there are several B physics experiments running at the moment and being started operating in the upcoming years, these will undoubtedly prove the flavor sector of the SM with precision and may reveal new physics effects. Therefore we first concentrate on the exclusive $B \rightarrow K^* \tau^+ \tau^-$ decay including the NHB effects.

Based on the constraints coming from the experimental measurements, the physical parameters of the decay $B \rightarrow K^* \tau^+ \tau^-$ such as the forward-backward asymmetry of the dilepton (A_{FB}), CP violating asymmetry (A_{CP}), and the CP asymmetry in the forward-backward asymmetry ($A_{CP}(A_{FB})$), are found to be of the order of 10^{-2} in the restricted region. For the parameters A_{FB} and A_{CP} , the NHB effects decreases their magnitude by 30% and 50% for $C_7^{eff} > 0$, respectively. The sensitivity of A_{FB} on the parameters $\sin \theta$, $\bar{\xi}_{N,\tau\tau}^D$ and $\frac{m_{h^0}}{m_{A^0}}$ is strong especially for the case $C_7^{eff} > 0$. A_{CP} has similar behavior with respect to those parameters except the mass ratio m_{h^0}/m_{A^0} whose effect is weak. Only the parameters $\bar{\xi}_{N,\tau\tau}^D$ and m_{h^0}/m_{A^0} the sensitivity of $A_{CP}(A_{FB})$ is strong for positive C_7^{eff} values. Undoubtedly the experimental investigation of these physical parameters provides us not only a crucial test for new physics effects beyond the SM but also a criteria for the sign of C_7^{eff} which is still unknown.

We next worked out the Br 's of the lepton flavor violating Z decays, $Z \rightarrow e^\pm \mu^\mp$, $Z \rightarrow e^\pm \tau^\mp$, and $Z \rightarrow \mu^\pm \tau^\mp$. Their importance in fact lies in the huge discrepancies between the SM prediction for the Br 's ($10^{-60} - 10^{-54}$) and the sensitive measurements ($10^{-9} - 10^{-8}$). In our analysis we predicted in the model III that the Br for the $Z \rightarrow e^\pm \mu^\mp$ decay can reach the values of the order of 10^{-11} in the restricted region. For another decay mode $Z \rightarrow e^\pm \tau^\mp$ the Br depends strongly on the Yukawa coupling $\bar{\xi}_{N,\tau\tau}^D$ and takes the values of the order of $10^{-10} - 10^{-9}$ for $\bar{\xi}_{N,\tau\tau}^D$ values in the range $10^3 - 10^4$ GeV. The third and last decay mode $Z \rightarrow \mu^\pm \tau^\mp$ has the largest Br among them due to contributions from both $\bar{\xi}_{N,\mu\tau}^D$ and $\bar{\xi}_{N,\tau\tau}^D$. We also found that the Br 's calculated are sensitive to the CP violating parameters stemming from complex Yukawa couplings. It is worth mentioning that results of future experiments concerning the Br 's of these processes constrain the couplings.

In addition to these the rare top decay $t \rightarrow c l_1^\pm l_2^\mp$ involving flavor changing vertices both in the quark and the lepton sector were discussed in the context of the model III. We reported that the Br of the decay which is forbidden in the SM and, in model III, it takes values of the order of $10^{-8} - 10^{-7}$ for $l_{1,2} = \tau, \mu$ at tree level. It was observed that loop effects are negligibly small. For the lepton pairs $l_{1,2} = \tau, e$ and $l_{1,2} = \mu, e$ the Br 's for the corresponding decays are smaller and too difficult to be observed in near future. There are indeed two additional free parameters which are the total decay widths of the Higgs bosons, $\Gamma_{tot}^{h^0}$ and $\Gamma_{tot}^{A^0}$ entering into the expressions because of the fact that there is enough kinematical region which permits to get h^0 and A^0 resonances. What comes out from all these discussions that especially for the lepton pair $l_{1,2} = \tau, \mu$ the future experimental search for the rare decay process $t \rightarrow c l_1^\pm l_2^\mp$ will play an effective role in the determination of the physics beyond the SM.

REFERENCES

- [1] S. L. Glashow, *Nucl. Phys.* **B22** (1961) 579; S. Weinberg, *Phys. Rev. Lett.* **19** (1967) 1264; A. Salam, in: *Proceedings of the 8th Nobel symposium*, p. 367, ed. N. Svartholm, Almqvist and Wiksell, Stockholm 1968.
- [2] S. L. Glashow, I. Iliopoulos, L. Maiani, *Phys. Rev.* **D2** (1970) 1285.
- [3] N. Cabbibo, *Phys. Rev. Lett.* **10** (1963) 531; M. Kobayashi, K. Maskawa, *Prog. Theor. Phys.* **49** (1973) 652.
- [4] H. Y. Han, Y. Nambu, *Phys. Rev.* **139** (1965) 1006; C. Bouchiat, I. Iliopoulos, Ph. Meyer, *Phys. Lett.* **B138** (1972) 652.
- [5] E. O. İltan, G. Turan, İ. Turan, *J. Phys.* **G28** (2002) 307.
- [6] E. O. İltan, İ. Turan, *Phys. Rev.* **D65** (2002) 013001.
- [7] E. O. İltan, İ. Turan, *Phys. Rev.* **D67** (2003) 015004.
- [8] M. Gell-Mann, *Phys. Rev.* **92** (1953) 833; K. Nishijima and T. Nakano, *Prog. Theor. Phys.* **10** (1953) 581.
- [9] Y. Nambu, *Phys. Rev. Lett.* **4** (1960) 380; J. Goldstone, *Nuovo Cimento* **19** (1961) 154; J. Goldstone, A. Salam and S. Weinberg, *Phys. Rev.* **127** (1962) 965.
- [10] For an introduction to symmetry breaking sector of the Electroweak theory see, 'Introduction to the Symmetry Breaking Sector', M. Herrero, Proceedings of the XXIII international Meeting on Fundamental Physics, Comillas, Santander, Spain, May 1995, eds. T. Rodrigo and A. Ruiz, World Sci. Pub. Co (1996) p. 87.
- [11] UA1 Collaboration, G. Armson et.al., *Phys. Lett.* **B122** (1983) 103; UA2 Collaboration, M. Banner et.al., *Phys. Lett.* **B122** (1983) 476.
- [12] P. W. Higgs, *Phys. Lett.* **12** (1964) 132; F. Englert and R. Brout, *Phys. Rev. Lett.* (1964) 321; G. S. Gurallnik, C. R. Hagen and T. W. B. Kibble, *Phys. Rev. Lett.* **13** (1964) 585; P. W. Higgs, *Phys. Rev.* **145** (1966) 1156; T. W. B. Kibble, *Phys. Rev.* **155** (1967) 1554.

- [13] J. E. Kim, P. Langacker, M. Levine and H. H. Williams, *Rev. Mod. Phys.* **53** (1981) 211.
- [14] P. Langacker, *Phys. Rep.* **72** (1981) 185.
- [15] P. Fayet, *Nucl. Phys.* **B90** (1975) 104; E. Witten, *Nucl. Phys.* **B231** (1984) 419; S. Dimopoulos and H. Georgi, *Nucl. Phys.* **B193** (1981) 150; N. Sakati, *Z. Phys.* **C11** (1981) 153; K. Inoue, A. Komatsu and S. Takeshita, *Prog. Theor. Phys.* **67** (1982) 927 [Erratum: **70** (1983) 330]; **71** (1984) 413.
- [16] J. E. Kim, *Phys. Rep.* **150** (1987) 1.
- [17] R. D. Peccei and H. R. Quinn, *Phys. Rev. Lett.* **38** (1997) 1440; R. D. Peccei and H. R. Quinn, *Phys. Rev.* **D16** (1977) 1791.
- [18] T. D. Lee, *Phys. Rev.* **D8** (1973) 1226.
- [19] S. Weinberg, *Phys. Rev. Lett.* **37** (1976) 657.
- [20] G. C. Branco and M. N. Rebelo, *Phys. Lett.* **B160** (1985) 117.
- [21] M. Sher, *Phys. Rept.* **179** (1989) 273; D. V. Nanopoulos and K. Tamvakis, *Phys. Lett. B* **110** (1982) 449.
- [22] S. L. Glashow and S. Weinberg, *Phys. Rev.* **D15** (1977) 1958.
- [23] D. Atwood, L. Reina and A. Soni, *Phys. Rev.* **D55** (1997) 3156.
- [24] H. Georgi, *Hadr. Journ. of Phys.* **1** (1978) 155.
- [25] J. L. Hewett, in Proc. of the 21st Annual SLAC Summer Institute, ed. L. De Porcel and C. Dunwoode, SLAC-PUB-6521 (1994)
- [26] C. Anway-Wiese, **CDF** Colloboration, in Proc. of the 8th Meeting of the Division of Particle and Fields of The American Physical Society, Albuquerque, New Mexico, 1994, ed. S. Seidel (World Scientific, Singapoure, 1995).
- [27] W. S. Hou, R. S. Willey and A. Soni, *Phys. Rev. Lett.* **58** (1987) 1608.
- [28] N. G. Deshpande and J. Trampetic, *Phys. Rev. Lett.* **60** (1988) 2583.
- [29] C. S. Lim, T. Morozumi and A. I. Sanda, *Phys. Lett.* **B218** (1989) 343.
- [30] B. Grinstein, M. J. Savage and M. B. Wise, *Nucl. Phys.* **B319** (1989) 271.
- [31] C. Dominguez, N. Paver and Riazuddin, *Phys. Lett.* **B214** (1988) 459.
- [32] N. G. Deshpande, J. Trampetic and K. Ponose, *Phys. Rev.* **D39** (1989) 1461.

- [33] P. J. O'Donnell and H. K. Tung, *Phys. Rev.* **D43** (1991) 2067.
- [34] N. Paver and Riazuddin, *Phys. Rev.* **D45** (1992) 978.
- [35] A. Ali, T. Mannel and T. Morozumi, *Phys. Lett.* **B273** (1991) 505.
- [36] A. Ali, G. F. Giudice and T. Mannel, *Z. Phys.* **C67** (1995) 417.
- [37] C. Greub, A. Ioannissian and D. Wyler, *Phys. Lett.* **B346** (1995) 145; D. Liu *Phys. Lett.* **B346** (1995) 355; G. Burdman, *Phys. Rev.* **D52** (1995) 6400; Y. Okada, Y. Shimizu and M. Tanaka *Phys. Lett.* **B405** (1997) 297.
- [38] A. J. Buras and M. Münz, *Phys. Rev.* **D52** (1995) 186.
- [39] N. G. Deshpande, X. -G. He and J. Trampetic, *Phys. Lett.* **B367** (1996) 362.
- [40] W. Jaus and D. Wyler, *Phys. Rev.* **D41** (1990) 3405.
- [41] Y. B. Dai, C. S. Huang and H. W. Huang, *Phys. Lett.* **B390** (1997) 257, C. S. Huang, L. Wei, Q. S. Yan and S. H. Zhu, *Phys. Rev.* **D63** (2001) 114021.
- [42] H. E. Logan and U. Nierste, *Nucl. Phys.* **B586** (2000) 39.
- [43] E. Iltan and G. Turan, *Phys. Rev.* **D63** (2001) 115007.
- [44] R. Casalbuoni, A. Deandra, N. Di Bartolemo, R. Gatto and G. Nardulli, *Phys. Lett.* **B312** (1993) 315.
- [45] P. Colangelo, F. De Fazio, P. Santorelli and E. Scrimieri, *Phys. Rev.* **D53** (1996) 3672.
- [46] W. Roberts, *Phys. Rev.* **D54** (1996) 863.
- [47] T. M. Aliev, A. Özpıneci and M. Savcı, *Phys. Rev.* **D56** (1997) 4260.
- [48] P. Ball and V. Braun, *Phys. Rev.* **D57** (1998) 4260.
- [49] T. Affolder, et.al. , *Phys. Rev. Lett.* **83** (1999) 3378.
- [50] T. M. Aliev, E. Iltan, *Phys. Lett.* **B451** (1999) 175.
- [51] E. Iltan, *Phys. Rev.* **D60** (1999) 034023.
- [52] E. Iltan, *Phys. Rev.* **D61** (1999) 054001.
- [53] T. M. Aliev, C. S. Kim, Y. G. Kim, *Phys. Rev.* **D62** (2000) 0140264.
- [54] T. M. Aliev, D. A. Demir, M. Savcı, *Phys. Rev.* **D62** (2000) 074016.
- [55] T. M. Aliev, M. Savcı, *Phys. Lett.* **B481** (2000) 275.

- [56] T. M. Aliev, M. K. Cakmak, M. Savci, *Nucl. Phys.* **B607** (2001) 305.
- [57] T. M. Aliev, A. Ozpineci, M. Savci *Nucl.Phys.* **B585** (2000) 275.
- [58] C. S. Huang, *Nucl.Phys.Proc.Suppl.* **93** (2001) 73.
- [59] T. M. Aliev, M. K. Cakmak, A. Ozpineci, M. Savci, *Phys. Rev.* **D64** (2001) 055007.
- [60] T. M. Aliev, A. Ozpineci, M. Savci, *Phys. Lett.* **B511** (2001) 49.
- [61] T. M. Aliev, E. Iltan, *J. Phys. G: Nucl. Part. Phys.* **25** (1999) 989.
- [62] B. Grinstein, R. Springer, and M. Wise, *Nuc. Phys.* **B339** (1990) 269; R. Grigjanis, P.J. O'Donnell, M. Sutherland and H. Navelet, *Phys. Lett.* **B213** (1988) 355; *Phys. Lett.* **B286** (1992) E, 413; G. Cella, G. Curci, G. Ricciardi and A. Viceré, *Phys. Lett.* **B325** (1994) 227, *Nucl. Phys.* **B431** (1994) 417.
- [63] M. Misiak, *Nucl. Phys.* **B393** (1993) 23 [Erratum: **B439** (1995) 461].
- [64] T. M. Aliev, and E. Iltan, *Phys. Rev.* **D58** (1998) 095014.
- [65] T. M. Aliev, E. O. Iltan, *Phys.Lett.* **B451** (1999) 175.
- [66] M. Ciuchini, G. Degrossi, P. Gambino and G. I. Giudice, *Nucl. Phys.* **B527** (1998) 21.
- [67] F. M. Borzumati and C. Greub, *Phys. Rev.* **D58** (1998) 074004.
- [68] G. Buchalla, G. Isidori and S. J. Rey, *Nucl. Phys.* **B511** (1998) 594.
- [69] M. S. Alam Collaboration, to appear in ICHEP98 Conference (1998).
- [70] Y. Fukuda, et.al., *Phys. Rev. Lett.* **81**, (1998) 1562.
- [71] R. Hawkings and K. Mönig, *Eur. Phys. J. direct* **C8** (1999) 1.
- [72] Particle Data Group Collaboration, C. Caso *et al.*, *Eur. Phys. J.* **C3** (1998) 1.
- [73] OPAL Collaboration, R. Akers *et al.*, *Z. Phys.* **C67** (1995) 555.
- [74] L3 Collaboration, O. Adriani *et al.*, *Phys. Lett.* **B316** (1993) 427.
- [75] DELPHI Collaboration, P. Abreu *et al.*, *Z. Phys.* **C73** (1997) 243.
- [76] G. Wilson, “Neutrino oscillations: are lepton-flavor violating Z decays observable with the CDR detector?” and “Update on experimental aspects of lepton-flavour violation”, talks at DESY-ECFA LC Workshops held at Frascati, Nov 1998 and at Oxford, March 1999, transparencies obtainable at <http://wwwsis.lnf.infn.it/talkshow/> and at http://hepnts1.rl.ac.uk/ECFA_DESY_OXFORD/scans/0025_wilson.pdf.

- [77] B. Pontecorvo, *Zh. Exsp. Theor. Fiz.* **33** (1957) 549; Z. Maki, M. Nakagawa and S. Sakata, *Prog. Theor. Phys.* **28** (1962) 870; B. Pontecorvo, *Sov. Phys. JETP* **26** (1968) 984.
- [78] T. Riemann and G. Mann, “Nondiagonal Z decay: $Z \rightarrow e\mu$ ”, in *Proc. of the Int. Conf. Neutrino’82, 14-19 June 1982, Balatonfüred, Hungary* (A. Frenkel and E. Jenik, eds), Vol II, pp. 58-, Budapest, 1982, scanned copy at <http://www.ifh.de/~riemann>; V. Ganapathi, T. Weiler, E. Laermann, I. Schmitt, and P. Zerwas, *Phys. Rev. D* **27** (1983) 570; G. Mann and T. Riemann, *Annalen Phys.* **40** (1984) 334.
- [79] V. Ganapathi, T. Weiler, E. Laermann, I. Schmitt, and P. Zerwas, *Phys. Rev.* **D27** (1983) 579; M. Clements, C. Footman, A. Kronfeld, S. Narasimhan, and D. Photiadis, *Phys. Rev.* **D27** (1983) 570.
- [80] J. I. Illana, M. Jack and T. Riemann, Contribution to Proc. of 2nd joint ECFA/DESY Workshop on Physics studies for a future linear collider, DESY 99-165 (2000), J. I. Illana, and T. Riemann, *Phys. Rev.* **D63** 053004 (2001).
- [81] E. Witten, *Nucl. Phys.* **B268** (1986) 79, R. N. Mohapatra and J. W. F. Valle, *Phys. Rev.* **D34** (1986) 1642, J. L. Hewett and T. G. Rizzo, *Phys. Rept.* **183** (1989) 193.
- [82] P. Langacker, *Phys. Rept.* **72** (1981) 185.
- [83] A. Ghosal, Y. Koide and H. Fusaoka, *Phys. Rev.* **D64** (2001) 053012.
- [84] G. ’t Hooft and M. J. G. Veltman, *Nucl. Phys.* **B44** (1972) 189.
- [85] C. G. Bollini and J. J. Giambiagi, *Phys. Lett.* **40B**, (1972) 566, C. G. Bollini and J. J. Giambiagi, *Nuovo Cim.* **12B**, (1972) 20, J. F. Ashmore, *Lett. Nuovo Cim.* **4**, (1972) 289, G. M. Cicuta and E. Montaldi, *Lett. Nuovo Cim.* **4**, (1972) 329.
- [86] E. Iltan, *Phys. Rev.* **D64** (2001) 013013.
- [87] T. P. Cheng and M. Sher, *Phys. Rev.* **D35**, (1987) 3383.
- [88] K. Abdullah et.al, *Phys. Rev. Lett.* **65**, (1990) 2347.
- [89] A. Czarnecki and W. J. Marciano, *Phys. Rev.* **D64**, (2001) 013014.
- [90] H. N. Brown et.al, Muon g-2 Collaboration, *Phys. Rev. Lett.* **86**, (2001) 2227.
- [91] E. D. Commins et.al, *Phys. Rev. A* **50**, (1994) 2960.

- [92] G. Mahlon and S. Parke, *Phys. Lett.* **B347** (1995) 394; E. Jenkins, *Phys. Rev.* **D56** (1997) 458; D. Atwood and M. Sher, *Phys. Lett.* **B411** (1997) 306.
- [93] J. L. Diaz-Cruz, et. al., *Phys. Rev.* **D41** (1990) 891; G. Eilam, J. L. Hewett and A. Soni, *Phys. Rev.* **D44** (1991) 1473 [Erratum *Phys. Rev.* **D59** 039901 (1999)].
- [94] C. S. Li, R. J. Oakes and J. M. Yang, *Phys. Rev.* **D49** (1994) 293; J. M. Yang and C. S. Li, *Phys. Rev.* **D49** (1994) 3412; G. Couture, C. Hamzaoui and H. König, *Phys. Rev.* **D52** (1995) 171; J. L. Lopez, D. V. Nanopoulos and R. Rangarajan, *Phys. Rev.* **D56** (1997) 3100; G. Couture, M. Frank and H. König, *Phys. Rev.* **D56** (1997) 4213; G. M. de Divitiis, R. Petronzio, L. Silvestrini, *Nucl. Phys.* **B504** (1997) 45.
- [95] C. Yue, G. Lu, G. Liu and Q. Xu, *Phys. Rev.* **D64** (1995) 095004; T. Han, R. D. Peccei, and X. Zhang, *Nucl. Phys.* **B454** (1995) 527; T. Han, R. D. Peccei, and X. Zhang, *Nucl. Phys.* **B454** (1995) 527; T. Han, K. Whisnant, B.-L. Young, and X. Zhang, *Phys. Rev.* **D55** (1997) 7241; *Phys. Lett.* **B385** (1996) 311; M. Hosch, K. Whisnant, and B. -L. Young, *Phys. Rev.* **D56** (1997) 5725; E. Malkawi and T. Tait, *Phys. Rev.* **D54** (1996) 5758; T. Tait and C. P. Yuan, *Phys. Rev.* **D55** (1997) 7300; T. Han, M. Hosch, K. Whisnant, B. -L. Young and X. Zhang, *Phys. Rev.* **D58** (1998) 073008; F. del Aguila and J. A. Aguilar-Saavedra, *Phys. Lett.* **B462** (1999) 310; J. L. Diaz-Cruz, M. A. Perez, G. Tavares-Velasco, J. J. Toscano, *Phys. Rev.* **D60** (1999) 115014; F. del Aguila and J. A. Aguilar-Saavedra, *Nucl. Phys.* **B576** (2000) 56; C. Yue, G. Lu, Q. Xu, *Phys. Lett.* **B508** (2001) 290.
- [96] W. S. Hou, *Phys. Lett.* **B296** (1992) 179; K. Agashe, M. Graesser, *Phys. Rev.* **D54** (1996) 4445; M. Hosch, K. Whisnant, B. L. Young, *Phys. Rev.* **D56** (1997) 5725; J. Guasch, hep-ph/9710267; L. T. Handoko and J. Hashida, *Phys. Rev.* **D58** (1998) 094008.
- [97] G. Eilam, B. Haeri and A. Soni, *Phys. Rev.* **D41** (1990) 875.
- [98] B. Mele, S. Petrarca and A. Soddu, *Phys. Lett.* **B435**, (1998) 401.
- [99] T. Han and Jing Jiang, B. Mele, *Phys. Lett.* **B516**, (2001) 337.
- [100] E. Iltan, *Phys. Rev.* **D65**, (2002) 075017.
- [101] S. Chen, et. al., CLEO Collaboration, *Phys. Rev. Lett.* **87** (2001) 251807.
- [102] E. Iltan, H. Sundu, *Acta. Phys. Slov.* **53** (2003) 17.
- [103] E. Iltan, *Phys. Rev.* **D64** (2001) 013013.
- [104] MEGA Collaboration, M.L. Brooks et.al., *Phys. Rev. Lett.* **83** (1999) 1521.

- [105] A. Antaramian, L. J. Hall and A. Rasin, *Phys. Rev. Lett.* **69** (1992) 187; L. J. Hall and S. Weinberg, *Phys. Rev.* **D48** (1993) R979; M. J. Savage, *Phys. Lett.* **B266** (1991) 135; L. Wolfe and Y. L. Wu, *Phys. Rev. Lett.* **73** (1994) 2809; F. J. Botella and J. P. Silva, *Phys. Rev.* **D51** (1995) 3870
- [106] S. Bertolini, *Nucl. Phys.* **B272** (1986) 77.
- [107] T. Muta, *Foundations of Quantum Chromodynamics* (World Scientific, Singapore, 1987).
- [108] M. E. Peskin and D. V. Schroeder, *An Introduction to Quantum Field Theory* (Addison-Wesley Publishing Company, the United States of America, 1995).

APPENDIX A

MINIMA CONDITIONS OF THE POTENTIAL AND THE PHYSICAL EIGENSTATES

The purpose of this appendix is to drive the minima conditions of the potential and is to get the physical eigenstates in terms of gauge eigenstates. Subject to a Z_2 symmetry given in the Eq. (2.17) which is implemented to avoid FCNC at three level, the most general gauge invariant potential can be written as

$$\begin{aligned}
V(\Phi_1, \Phi_2) = & \mu_1^2 \Phi_1^\dagger \Phi_1 + \mu_2^2 \Phi_2^\dagger \Phi_2 + \lambda_1 (\Phi_1^\dagger \Phi_1)^2 + \lambda_2 (\Phi_2^\dagger \Phi_2)^2 \\
& + \lambda_3 (\Phi_1^\dagger \Phi_1) (\Phi_2^\dagger \Phi_2) + \lambda_4 (\Phi_1^\dagger \Phi_2) (\Phi_2^\dagger \Phi_1) \\
& + \frac{1}{2} [\lambda_5 (\Phi_1^\dagger \Phi_2)^2 + h.c.].
\end{aligned} \tag{A.1}$$

From hermicity requirement all the coupling constants are taken to be real with the exception of λ_5 . However, there is still a freedom, the phase of Φ_2 , which can be chosen such a way that the last term in (A.1) becomes $\frac{1}{2} \lambda_5 [(\Phi_1^\dagger \Phi_2)^2 + h.c.]$. In all our calculations throughout the thesis in order to concentrate on the effects of the flavor changing Yukawa couplings we assume that the scalar potential is CP conserved. In fact, the Higgs potential in 2HDM which is not enforced to satisfy any discrete symmetry may be in general CP conserved or CP violated [24], [105]. Within this assumption the new source of CP violation is merely from the Yukawa couplings.

Let us now study the physical particle (mass eigenvalues and eigenstates) contents of the scalar doublets using (A.1) The method of analysis is somehow similar to that found in [106].

For convenience let us use the following parametrization for the doublets

$$\Phi_1 = \begin{pmatrix} \phi_1 + i\phi_2 \\ \phi_3 + i\phi_4 \end{pmatrix}; \quad \Phi_2 = \begin{pmatrix} \phi_5 + i\phi_6 \\ \phi_7 + i\phi_8 \end{pmatrix}. \quad (\text{A.2})$$

Along our strategy in computing minimum conditions of the potential in (A.1), we consider the potential to be a function of the variables $\{\phi_1, \phi_2, \dots, \phi_8\}$ with coefficients depending on the parameters $\mu_1^2, \mu_2^2, \lambda_i, i = 1, 2, \dots, 5$. The minimum conditions are

$$T_i = \left. \frac{\partial V}{\partial \phi_i} \right|_{\min} = 0, \quad (\text{A.3})$$

where $i = 1, 2, \dots, 8$ and “min” means $\langle \phi_3 \rangle = v_1/\sqrt{2}; \langle \phi_7 \rangle = v_2/\sqrt{2}$ and $\langle \phi_j \rangle = 0$ for $j = 1, 2, 4, 5, 6, 8$. From (A.3) we get the following nonzero conditions

$$\begin{aligned} T_3 &= v_1(\mu_1^2 + \lambda_1 v_1 + \lambda_{345} v_2^2) = 0, \\ T_7 &= v_2(\mu_1^2 + \lambda_1 v_1 + \lambda_{345} v_1^2) = 0, \end{aligned} \quad (\text{A.4})$$

where $\lambda_{345} \equiv 2(\lambda_3 + \lambda_4 + \lambda_5)$. There are two independent set of solutions

- Case a) $v_1^2 = v_2^2 \neq 0$

The solutions for v_1^2 and v_2^2 of (A.4) are

$$v_1^2 = \frac{\lambda_{345}\mu_2^2 - \lambda_2\mu_1^2}{\lambda_1\lambda_2 - \lambda_{345}^2}, \quad v_2^2 = \frac{\lambda\mu_1^2 - \lambda_1\mu_2^2}{\lambda_1\lambda_2 - \lambda_{345}^2}. \quad (\text{A.5})$$

- Case b) $v_2^2 = 0, v_1^2 \neq 0$

$$v_1 = -\frac{\mu_1^2}{\lambda_1}. \quad (\text{A.6})$$

After constructing the mass squared matrix and getting the physical spectrum of the charged and the neutral sectors, two linearly independent solutions of the Eq. (A.4) are discussed separately. Therefore, the next task is to evaluate the second derivative of the potential (getting quadratic terms in (A.1)) about its minimum and to get the mass squared matrix defined as

$$M_{ij}^2 = \frac{1}{2} \left. \frac{\partial^2 V}{\partial \phi_i \partial \phi_j} \right|_{\phi_3=v_1/\sqrt{2}, \phi_7=v_2/\sqrt{2}}. \quad (\text{A.7})$$

Using (A.1), (A.4), and (A.7) the 8×8 mass squared matrix becomes

$$\begin{pmatrix} M_{11}^2 & 0 & 0 & 0 & M_{15}^2 & 0 & 0 & 0 \\ 0 & M_{22}^2 & 0 & 0 & 0 & M_{26}^2 & 0 & 0 \\ 0 & 0 & M_{33}^2 & 0 & 0 & 0 & M_{37}^2 & 0 \\ 0 & 0 & 0 & M_{44}^2 & 0 & 0 & 0 & M_{48}^2 \\ M_{15}^2 & 0 & 0 & 0 & M_{55}^2 & 0 & 0 & 0 \\ 0 & M_{26}^2 & 0 & 0 & 0 & M_{66}^2 & 0 & 0 \\ 0 & 0 & M_{37}^2 & 0 & 0 & 0 & M_{77}^2 & 0 \\ 0 & 0 & 0 & M_{48}^2 & 0 & 0 & 0 & M_{88}^2 \end{pmatrix}, \quad (\text{A.8})$$

where the mass squared elements are given as

$$\begin{aligned} M_{11}^2 &= -v_2^2 \lambda_{45} = M_{22}^2, \\ M_{15}^2 &= \lambda_{45} v_1 v_2 = M_{26}^2, \\ M_{33}^2 &= 2\lambda_1 v_1^2, \\ M_{37}^2 &= 2\lambda_{345} v_1 v_2, \\ M_{44}^2 &= -\lambda_5 v_2^2, \\ M_{48}^2 &= \lambda_5 v_1 v_2, \\ M_{55}^2 &= -\lambda_{45} v_1^2 = M_{66}^2, \\ M_{77}^2 &= 2\lambda_2 v_2^2, \\ M_{88}^2 &= -\lambda_5 v_1^2, \end{aligned} \quad (\text{A.9})$$

where $\lambda_{345} \equiv 2(\lambda_3 + \lambda_4 + \lambda_5)$ and $\lambda_{45} \equiv 2(\lambda_4 + \lambda_5)$.

From the computational point of view one can put the above 8×8 symmetric matrix into block diagonal form, which allows us to diagonalize each of these sub-matrices separately. This is since that one can simply relabel the scalar fields without any effect on the physical spectra of the mass squared matrix. So recalling the positions of the fields as $1 \rightarrow 1, 2 \rightarrow 3, 3 \rightarrow 5, 4 \rightarrow 7, 5 \rightarrow 2, 6 \rightarrow 4, 7 \rightarrow 6$ and

$8 \rightarrow 8$, the mass squared matrix turns into

$$\begin{pmatrix} M_{11}^2 & M_{15}^2 & 0 & 0 & 0 & 0 & 0 & 0 \\ M_{15}^2 & M_{55}^2 & 0 & 0 & 0 & 0 & 0 & 0 \\ 0 & 0 & M_{22}^2 & M_{26}^2 & 0 & 0 & 0 & 0 \\ 0 & 0 & M_{26}^2 & M_{66}^2 & 0 & 0 & 0 & 0 \\ 0 & 0 & 0 & 0 & M_{33}^2 & M_{37}^2 & 0 & 0 \\ 0 & 0 & 0 & 0 & M_{37}^2 & M_{77}^2 & 0 & 0 \\ 0 & 0 & 0 & 0 & 0 & 0 & M_{44}^2 & M_{48}^2 \\ 0 & 0 & 0 & 0 & 0 & 0 & M_{48}^2 & M_{88}^2 \end{pmatrix}, \quad (\text{A.10})$$

where the first two sub-matrices of the part formed by the components $\{\phi_1, \phi_2, \phi_5, \phi_6\}$ are indeed identical ($M_{11}^2 = M_{22}^2, M_{15}^2 = M_{26}^2, M_{55}^2 = M_{66}^2$). After performing diagonalization procedure these correspond to the masses of the four charged scalars (2 charged Goldstone bosons and 2 charged physical Higgs). The rest in the $\{\phi_3, \phi_4, \phi_7, \phi_8\}$ space corresponds to the neutral scalars (one neutral Goldstone boson, 2 neutral scalars and one neutral pseudoscalar). In diagonalizing the mass squared matrix (A.10), the following further decomposition is useful

$$\begin{pmatrix} M_{11}^2 & M_{15}^2 & 0 & 0 \\ M_{15}^2 & M_{55}^2 & 0 & 0 \\ 0 & 0 & M_{22}^2 & M_{26}^2 \\ 0 & 0 & M_{26}^2 & M_{66}^2 \end{pmatrix} \oplus \begin{pmatrix} M_{33}^2 & M_{37}^2 \\ M_{37}^2 & M_{77}^2 \end{pmatrix} \oplus \begin{pmatrix} M_{44}^2 & M_{48}^2 \\ M_{48}^2 & M_{88}^2 \end{pmatrix}, \quad (\text{A.11})$$

where $M_{11}^2 = M_{22}^2, M_{15}^2 = M_{26}^2, M_{55}^2 = M_{66}^2$. Having decomposed the mass squared matrix into the above form, we may analyze the charged and the neutral sectors separately.

A.1 The Charged Scalar Sector

Let us concentrate on the part in (A.11) spanned by the $\{\phi_1, \phi_2, \phi_5, \phi_6\}$ elements. Since the upper 2×2 sub-matrix is identical to lower 2×2 part, it can be further decomposed and this results in decoupling the positive and negative

states. The identical mass squared matrices is of the form

$$\begin{pmatrix} -\lambda_{45}v_2^2 & \lambda_{45}v_1v_2 \\ \lambda_{45}v_1v_2 & -\lambda_{45}v_2^2 \end{pmatrix}, \quad (\text{A.12})$$

whose diagonalization is straightforward. The eigenvalues corresponding to the masses of the four charged states (denoted as χ^\pm and H^\pm) are obtained

$$\{m_{\chi^\pm}, m_{H^\pm}\} = \{0, -(v_1^2 + v_2^2)\lambda_{45}\}. \quad (\text{A.13})$$

Then the associated normalized charged eigenstates in the matrix form can be parametrized as

$$u(m_{\chi^\pm}) = \begin{pmatrix} \cos \beta \\ \sin \beta \end{pmatrix}, \quad u(m_{H^\pm}) = \begin{pmatrix} -\sin \beta \\ \cos \beta \end{pmatrix}. \quad (\text{A.14})$$

From the above eigenstates a unitary matrix P is formed as

$$P = \begin{pmatrix} u^T(\chi^\pm) \\ u^T(H^\pm) \end{pmatrix} = \begin{pmatrix} \cos \beta & \sin \beta \\ -\sin \beta & \cos \beta \end{pmatrix}. \quad (\text{A.15})$$

The physical eigenstates are related to the initially defined fields as from $(|)_{mass} = P(|)_{gauge}$

$$\begin{pmatrix} \chi^+ \\ H^+ \end{pmatrix} = \begin{pmatrix} \cos \beta & \sin \beta \\ -\sin \beta & \cos \beta \end{pmatrix} \begin{pmatrix} \phi_1 \\ \phi_5 \end{pmatrix},$$

$$\begin{pmatrix} \chi^- \\ H^- \end{pmatrix} = \begin{pmatrix} \cos \beta & \sin \beta \\ -\sin \beta & \cos \beta \end{pmatrix} \begin{pmatrix} \phi_2 \\ \phi_6 \end{pmatrix}, \quad (\text{A.16})$$

with masses given in (A.13).

A.2 The Neutral Scalar Sector

We now first focus on the part in (A.11) spanned by $\{\phi_4, \phi_8\}$. The eigenvalues can easily read from (A.13) by replacing λ_{45} with λ_5 , which is obvious from (A.9) that $M_{44}^2 = M_{88}^2 = M_{11}^2(\lambda_{45} \rightarrow \lambda_5)$ and $M_{48}^2 = M_{15}^2(\lambda_{45} \rightarrow \lambda_5)$. Consequently the

eigenvalues (the mass squared of one neutral Goldstone boson denoted as χ^0 and that of one neutral pseudoscalar Higgs boson denoted as A^0) are

$$\{m_{\chi^0}, m_{A^0}\} = \{0, -(v_1^2 + v_2^2)\lambda_5\}. \quad (\text{A.17})$$

The eigenvectors (and the corresponding unitary matrix P) for the eigenstates χ^0 and A^0 are the same as those in the charged sector ((A.14) and (A.15)). Thus they read

$$\begin{pmatrix} \chi^0 \\ A^0 \end{pmatrix} = \begin{pmatrix} \cos \beta & \sin \beta \\ -\sin \beta & \cos \beta \end{pmatrix} \begin{pmatrix} \phi_4 \\ \phi_8 \end{pmatrix}. \quad (\text{A.18})$$

The only remaining part is the sub-matrix in $\{\phi_3, \phi_7\}$ space which is responsible for the CP -even neutral Higgs sector. From (A.9) and (A.11) the sub-matrix is

$$\begin{pmatrix} 2\lambda_1 v_1^2 & 2\lambda_{345} v_1 v_2 \\ 2\lambda_{345} v_1 v_2 & 2\lambda_2 v_2^2 \end{pmatrix}. \quad (\text{A.19})$$

Following the same procedure the eigenvalues corresponding to the masses squared of the CP -even neutral scalars denoted as H^0 and h^0 are obtained

$$m_{H^0, h^0}^2 = A + B \pm \sqrt{(A - B)^2 + C^2}, \quad (\text{A.20})$$

where

$$A \equiv \lambda_1 v_1^2, \quad B \equiv \lambda_2 v_2^2, \quad C \equiv 2\lambda_{345} v_1 v_2, \quad (\text{A.21})$$

and the sub-indices (H^0, h^0) refer respectively to $(+, -)$ ($m_{H^0} \geq m_{h^0}$). The corresponding eigenvectors are given from (A.19) and (A.20)

$$u(m_{H^0}) = \begin{pmatrix} \cos \alpha \\ \sin \alpha \end{pmatrix}, \quad u(m_{h^0}) = \begin{pmatrix} -\sin \alpha \\ \cos \alpha \end{pmatrix}, \quad (\text{A.22})$$

where

$$\tan 2\alpha = \frac{C}{(A - B)} = \frac{2\lambda_{345} v_1 v_2}{\lambda_1 v_1^2 - \lambda_2 v_2^2}. \quad (\text{A.23})$$

Constructing the matrix P from (A.22) the physical eigenstates are

$$\begin{pmatrix} H^0 \\ h^0 \end{pmatrix} = \begin{pmatrix} \cos \alpha & \sin \alpha \\ -\sin \alpha & \cos \alpha \end{pmatrix} \begin{pmatrix} \sqrt{2}\phi_3 - v_1 \\ \sqrt{2}\phi_7 - v_2 \end{pmatrix}. \quad (\text{A.24})$$

The constraints on the parameters of the scalar potential can be determined from the argument that all masses are positive. The conditions are from (A.13), (A.17), and (A.20)

$$\lambda_5 < 0, \quad \lambda_{45} < 0, \quad \text{and} \quad |C| \leq 2\sqrt{AB}. \quad (\text{A.25})$$

A.3 For Case a) Set of Solutions

For Case a) in which both doublets have nonzero VEVs, the eigenvalues and the eigenvectors can be rewritten from (A.4), (A.16), (A.17), (A.20) and (A.23)

$$\{m_{\chi^\pm}, m_{H^\pm}\} = \{0, -(v_1^2 + v_2^2)\lambda_{45}\},$$

$$\begin{pmatrix} \chi^{+(-)} \\ H^{+(-)} \end{pmatrix} = \begin{pmatrix} \cos \beta & \sin \beta \\ -\sin \beta & \cos \beta \end{pmatrix} \begin{pmatrix} \phi_{1(2)} \\ \phi_{5(6)} \end{pmatrix},$$

$$\{m_{\chi^0}, m_{A^0}\} = \{0, -(v_1^2 + v_2^2)\lambda_5\},$$

$$\begin{pmatrix} \chi^0 \\ A^0 \end{pmatrix} = \begin{pmatrix} \cos \beta & \sin \beta \\ -\sin \beta & \cos \beta \end{pmatrix} \begin{pmatrix} \phi_4 \\ \phi_8 \end{pmatrix},$$

$$m_{H^0, h^0}^2 = \lambda_1 v_1^2 + \lambda_2^2 \pm \sqrt{(\lambda_1 v_1^2 - \lambda_2 v_2^2)^2 + 4v_1^2 v_2^2 \lambda_{345}^2},$$

$$\begin{pmatrix} H^0 \\ h^0 \end{pmatrix} = \begin{pmatrix} \cos \alpha & \sin \alpha \\ -\sin \alpha & \cos \alpha \end{pmatrix} \begin{pmatrix} \sqrt{2}\phi_3 - v_1 \\ \sqrt{2}\phi_7 - v_2 \end{pmatrix}, \quad (\text{A.26})$$

where $\tan 2\alpha = 2v_1 v_2 \lambda_{345} / (\lambda_1 v_1^2 - \lambda_2 v_2^2)$ and $\tan \beta = v_2 / v_1$.

A.4 For Case b) Set of Solutions

For Case b) where only one of the scalar doublets has nonzero VEV. We indeed use this second set of solutions in all our calculations, because the interpretation of the fields can easily be done. A more general case will be discussed in Appendix B without assuming that v_2 vanishes. The crucial difference between them is that in the latter case there is an additional mixing in the CP -even neutral sector.

Since the Case b) is relevant to all our calculations, let us discuss it separately. So, the rest of this appendix is devoted to the case in which v_2 vanishes. The mass squared matrix from (A.3), (A.7), and (A.6) is

$$\begin{pmatrix} 0 & 0 & 0 & 0 & 0 & 0 & 0 & 0 \\ 0 & 0 & 0 & 0 & 0 & 0 & 0 & 0 \\ 0 & 0 & M_{33}^2 & 0 & 0 & 0 & 0 & 0 \\ 0 & 0 & 0 & 0 & 0 & 0 & 0 & 0 \\ 0 & 0 & 0 & 0 & M_{55}^2 & 0 & 0 & 0 \\ 0 & 0 & 0 & 0 & 0 & M_{66}^2 & 0 & 0 \\ 0 & 0 & 0 & 0 & 0 & 0 & M_{77}^2 & 0 \\ 0 & 0 & 0 & 0 & 0 & 0 & 0 & M_{88}^2 \end{pmatrix}, \quad (\text{A.27})$$

where the nonzero entries are

$$\begin{aligned} M_{33}^2 &= 2\lambda_1 v_1^2, \\ M_{55}^2 &= \mu_2^2 + \frac{\lambda_3}{2} v_1^2 = M_{66}^2, \\ M_{77}^2 &= \mu_2^2 + \lambda_{345} v_1^2, \\ M_{88}^2 &= \mu_2^2 + (\lambda_{345} - \lambda_5) v_1^2. \end{aligned} \quad (\text{A.28})$$

We clearly see that the mass squared matrix is already diagonal and it is expected that all fields defined originally coincide with the physical (mass) eigenstates. Therefore no mixing angle appears ($\alpha = 0, \beta = 0$).

For the charged sector formed by the fields $\{\phi_1, \phi_2, \phi_5, \phi_6\}$ the sub-diagonal

4×4 mass matrix squared is

$$\begin{pmatrix} 0 & 0 & 0 & 0 \\ 0 & 0 & 0 & 0 \\ 0 & 0 & \mu_2^2 + \frac{\lambda_3}{2}v_1^2 & 0 \\ 0 & 0 & 0 & \mu_2^2 + \frac{\lambda_3}{2}v_1^2 \end{pmatrix}. \quad (\text{A.29})$$

The corresponding eigenvalues are

$$\{m_{\chi^\pm}, m_{H^\pm}\} = \{0, \mu_2^2 + \frac{\lambda_3}{2}v_1^2\}, \quad (\text{A.30})$$

and the eigenvectors are

$$\begin{aligned} u(\chi^\pm) &= \{(1, 0, 0, 0)^T, (0, 1, 0, 0)^T\}, \\ u(H^\pm) &= \{(0, 0, 1, 0)^T, (0, 0, 0, 1)^T\}. \end{aligned} \quad (\text{A.31})$$

Thus the eigenstates are simply

$$\begin{pmatrix} \chi_1 \\ \chi_2 \\ H^1 \\ H^2 \end{pmatrix} = \begin{pmatrix} 1 & 0 & 0 & 0 \\ 0 & 1 & 0 & 0 \\ 0 & 0 & 1 & 0 \\ 0 & 0 & 0 & 1 \end{pmatrix} \begin{pmatrix} \phi_1 \\ \phi_2 \\ \phi_3 \\ \phi_4 \end{pmatrix}, \quad (\text{A.32})$$

such that $\chi^\pm \equiv \chi_1 \pm i\chi_2 = \phi_1 \pm i\phi_2$ and $H^\pm \equiv H^1 \pm iH^2 = \phi_3 \pm i\phi_4$.

For the neutral sector the sub-matrix spanned by $\{\phi_4, \phi_8\}$ is

$$\begin{pmatrix} 0 & 0 \\ 0 & \mu_2^2 + (\lambda_{345} - \lambda_5)v_1^2 \end{pmatrix}. \quad (\text{A.33})$$

The eigenvalues corresponding to the masses of χ^0 and A^0 are simply

$$\{m_{\chi^0}, m_{A^0}\} = \{0, \mu_2^2 + (\lambda_{345} - \lambda_5)v_1^2\}, \quad (\text{A.34})$$

with mass eigenstates

$$\begin{pmatrix} \chi^0 \\ A^0 \end{pmatrix} = \begin{pmatrix} 1 & 0 \\ 0 & 1 \end{pmatrix} \begin{pmatrix} \phi_4 \\ \phi_8 \end{pmatrix}. \quad (\text{A.35})$$

Finally for the part formed by $\{\phi_3, \phi_7\}$, the masses and mass eigenstates are

$$\{m_{H^0}, m_{h^0}\} = \{2\lambda_1 v_1^2, \mu_2^2 + \lambda_{345} v_1^2\},$$

$$\begin{pmatrix} H^0 \\ h^0 \end{pmatrix} = \begin{pmatrix} 1 & 0 \\ 0 & 1 \end{pmatrix} \begin{pmatrix} \sqrt{\phi_3} - v_1 \\ \phi_7 \end{pmatrix}. \quad (\text{A.36})$$

A few words about this particular choice of solution are in order. With this choice all new particles are collected in the second doublet and then ϕ_1 corresponds to the scalar doublet of the SM. H^0 corresponds to SM Higgs field and it does not interact with h^0 and A^0 , since no mixing exists between CP -even neutral Higgs fields. Therefore new physics effects are more apparent in this framework. As already noted this is a special case of the result derived in Appendix B where v_2 is assumed to be nonzero.

APPENDIX B

AN EQUIVALENT NEW PARAMETRIZATION OF THE DOUBLETS AND THE YUKAWA LAGRANGIAN IN THE QUARK MASS BASIS

In this appendix we describe the transition from the representation of the scalar doublets in which they both have non-zero VEVs to an equivalent one where only one of them acquires a non-zero VEV. We will call the former one as Case a) and the latter one as Case b). In the latter we express the Yukawa Lagrangian in the quark mass basis in order to get the rotated Yukawa couplings in terms of the original ones.

For the sake of simplicity, let us consider only the quark sector of the Yukawa Lagrangian (lepton sector can also be included without much afford) for Case a) from Eq. (2.16)

$$\begin{aligned}\mathcal{L}_Y &= \eta_{ij}^{a,U} \bar{Q}_{iL} \tilde{\Phi}_1^a U_{jR} + \eta_{ij}^{a,D} \bar{Q}_{iL} \Phi_1^a D_{jR} + \xi_{ij}^{a,U\dagger} \bar{Q}_{iL} \tilde{\Phi}_2^a U_{jR} \\ &+ \xi_{ij}^{a,D} \bar{Q}_{iL} \Phi_2^a D_{jR} + h.c.\end{aligned}\tag{B.1}$$

where

$$\Phi_{1(2)}^a = \begin{pmatrix} \phi_{1(2)}^{a+} \\ \phi_{1(2)}^{a0} \end{pmatrix}; \quad \langle \Phi_{1(2)}^a \rangle = v_{1(2)},\tag{B.2}$$

and the superscript “a” denotes Case a). Since we argue that these two representations of the scalar doublets are physically equivalent, there must be an orthogonal transformation which transforms one into other. Thus we have

$$\Phi^b = \Lambda_\theta \Phi^a,\tag{B.3}$$

where

$$\Phi^{a(b)} = \begin{pmatrix} \Phi_1^{a(b)} \\ \Phi_2^{a(b)} \end{pmatrix}, \quad \Lambda_\theta \equiv \begin{pmatrix} \cos \theta & \sin \theta \\ -\sin \theta & \cos \theta \end{pmatrix}. \quad (\text{B.4})$$

For the sake of simplicity let us write (B.1) in the form

$$\mathcal{L}_Y = \bar{Q}_{iL} [f_{ij}^{a,U T} \tilde{\Phi}^a] U_{jR} + \bar{Q}_{iL} [f_{ij}^{a,D T} \Phi^a] D_{jR} + h.c., \quad (\text{B.5})$$

where

$$f^{a,U(D)} \equiv \begin{pmatrix} \eta_{ij}^{a,U(D)} \\ \xi_{ij}^{a,U(D)} \end{pmatrix}, \quad (\text{B.6})$$

and "T" stands for transposition. From (B.4) we transform (B.5) into the form in terms of the weak eigenstates for Case b)

$$\begin{aligned} \mathcal{L}_Y &= \bar{Q}_{iL} [f_{ij}^{a,U T} \Lambda_\theta^T \tilde{\Phi}^b] U_{jR} + \bar{Q}_{iL} [f_{ij}^{a,D T} \Lambda_\theta^T \Phi^a] D_{jR} + h.c. \\ &\equiv \bar{Q}_{iL} [f_{ij}^{b,U T} \tilde{\Phi}^b] U_{jR} + \bar{Q}_{iL} [f_{ij}^{b,D T} \Phi^a] D_{jR} + h.c., \end{aligned} \quad (\text{B.7})$$

where we have defined

$$f_{ij}^{b,U(D)} \equiv \Lambda_\theta f_{ij}^{a,U(D)}. \quad (\text{B.8})$$

Therefore both Lagrangians, (B.5) and (B.7), are "equivalent", thus under the transformations (B.3) and (B.8) physics becomes invariant. So there is a freedom to use any of these bases which are related to each other with the parameter θ which is completely arbitrary. One can then set $\theta = \beta$ and from (B.2) and (B.3) the VEV of Φ^b takes the following form

$$\begin{aligned} \langle \Phi^b \rangle &= \Lambda_\beta \langle \Phi^a \rangle, \\ \begin{pmatrix} \langle \Phi_1^b \rangle \\ \langle \Phi_2^b \rangle \end{pmatrix} &= \begin{pmatrix} \cos \beta & \sin \beta \\ -\sin \beta & \cos \beta \end{pmatrix} \begin{pmatrix} \langle \Phi_1^a \rangle \\ \langle \Phi_2^a \rangle \end{pmatrix}, \\ &= \begin{pmatrix} \cos \beta \langle \Phi_1^a \rangle + \sin \beta \langle \Phi_2^a \rangle \\ -\sin \beta \langle \Phi_1^a \rangle + \cos \beta \langle \Phi_2^a \rangle \end{pmatrix}, \\ &= \begin{pmatrix} \cos \beta v_1 + \sin \beta v_2 \\ -\sin \beta v_1 + \cos \beta v_2 \end{pmatrix}, \end{aligned}$$

$$= \begin{pmatrix} v \\ 0 \end{pmatrix}, \quad (\text{B.9})$$

where $v = \sqrt{v_1^2 + v_2^2}$ and $\tan \beta = v_2/v_1$ are used. Thus, having started with two scalar doublets whose VEVs are non-zero and by means of a transformation we reach a system in which only one of the transformed doublets acquires non-zero VEV ($\langle \Phi_1^b \rangle = v$).

Our next task is to express the gauge (weak) fields of the doublets $\Phi_{1(2)}^b$ in terms of mass eigenstates. To achieve this, first it is more convenient to get the relations between the gauge fields in Case b) and those in Case a). Then getting the gauge fields of the doublets $\Phi_{1(2)}^b$ as a function of mass fields is straightforward. The following parametrization of the doublets is more suitable

$$\begin{aligned} \langle \Phi_{1(2)}^a \rangle &= \frac{1}{\sqrt{2}} \begin{pmatrix} \sqrt{2}\phi_{1(2)}^{a+} \\ v_{1(2)} + y_{1(2)}^a + iz_{1(2)}^a \end{pmatrix}, \\ \langle \Phi_{1(2)}^b \rangle &= \frac{1}{\sqrt{2}} \begin{pmatrix} \sqrt{2}\phi_{1(2)}^{b+} \\ v(0) + y_{1(2)}^b + iz_{1(2)}^b \end{pmatrix}. \end{aligned} \quad (\text{B.10})$$

Using the transformation (B.3) with $\theta = \beta$ and from (B.10) we have

$$\begin{aligned} \Phi_1^b &= \cos \beta \Phi_1^a + \sin \beta \Phi_2^a, \\ &= \frac{1}{\sqrt{2}} \begin{pmatrix} \sqrt{2}(\cos \beta \phi_1^{a+} + \sin \beta \phi_2^{a+}) \\ v + \cos \beta y_1^a + \sin \beta y_2^a + i(\cos \beta z_1^a + \sin \beta z_2^a) \end{pmatrix}, \end{aligned} \quad (\text{B.11})$$

and

$$\begin{aligned} \Phi_2^b &= -\sin \beta \Phi_1^a + \cos \beta \Phi_2^a, \\ &= \frac{1}{\sqrt{2}} \begin{pmatrix} \sqrt{2}(-\sin \beta \phi_1^{a+} + \cos \beta \phi_2^{a+}) \\ -\sin \beta y_1^a + \cos \beta y_2^a + i(-\sin \beta z_1^a + \cos \beta z_2^a) \end{pmatrix}. \end{aligned} \quad (\text{B.12})$$

From the comparison of (B.11) and (B.12) with (B.10) the following relations read

$$\phi^{b+} = \Lambda_\beta \phi^{a+}, \quad y^b = \Lambda_\beta y^a, \quad z^b = \Lambda_\beta z^a, \quad (\text{B.13})$$

where $\phi^{a(b)} = \begin{pmatrix} \phi_1^{a(b)+} \\ \phi_2^{a(b)+} \end{pmatrix}$ and similar definitions for y and z .

Having obtained the relations among gauge eigenstates defined in both cases, our next step is to express the gauge eigenstates $\{\phi^b, y^b, z^b\}$ in terms of the mass eigenstates $\{\chi^\pm, H^\pm, \chi^0, A^0, H^0, h^0\}$ defined in appendix A. One can simply read the relation between $\{\phi^a, y^a, z^a\}$ and mass eigenstates from appendix A by just making the replacements $\sqrt{2}\phi_3 - v_1 \rightarrow y_1^a, \sqrt{2}\phi_7 - v_2 \rightarrow y_2^a, \phi_4 \rightarrow z_1^a, \phi_8 \rightarrow z_2^a$ (see (A.16), (A.18), and (A.24)). We then have

$$\phi^{a+} = \Lambda_\beta^{-1} \begin{pmatrix} \chi^+ \\ H^+ \end{pmatrix}, \quad y^a = \Lambda_\alpha^{-1} \begin{pmatrix} H^0 \\ h^0 \end{pmatrix}, \quad z^a = \Lambda_\beta^{-1} \begin{pmatrix} \chi^0 \\ A^0 \end{pmatrix}, \quad (\text{B.14})$$

where

$$\Lambda_\beta^{-1} = \begin{pmatrix} \cos \beta & -\sin \beta \\ \sin \beta & \cos \beta \end{pmatrix}, \quad \Lambda_\alpha^{-1} = \begin{pmatrix} \cos \alpha & -\sin \alpha \\ \sin \alpha & \cos \alpha \end{pmatrix}. \quad (\text{B.15})$$

Therefore from (B.13), (B.14), and (B.15) we get

$$\begin{aligned} \phi^{b+} &= \Lambda_\beta \Lambda_\beta^{-1} \begin{pmatrix} \chi^+ \\ H^+ \end{pmatrix} = \begin{pmatrix} \chi^+ \\ H^+ \end{pmatrix}, \\ z^b &= \Lambda_\beta \Lambda_\beta^{-1} \begin{pmatrix} \chi^0 \\ A^0 \end{pmatrix} = \begin{pmatrix} \chi^0 \\ A^0 \end{pmatrix}, \\ y^b &= \Lambda_\beta \Lambda_\alpha^{-1} \begin{pmatrix} H^0 \\ h^0 \end{pmatrix}, \\ &= \begin{pmatrix} \cos \beta & \sin \beta \\ -\sin \beta & \cos \beta \end{pmatrix} \begin{pmatrix} \cos \alpha & -\sin \alpha \\ \sin \alpha & \cos \alpha \end{pmatrix} \begin{pmatrix} \chi^0 \\ A^0 \end{pmatrix}, \\ &= \begin{pmatrix} \cos(\alpha - \beta) & -\sin(\alpha - \beta) \\ \sin(\alpha - \beta) & \cos(\alpha - \beta) \end{pmatrix} \begin{pmatrix} \chi^0 \\ A^0 \end{pmatrix}. \end{aligned} \quad (\text{B.16})$$

Forming the doublets $\Phi_{1(2)}^b$ from above relations they read

$$\Phi_1^b = \frac{1}{\sqrt{2}} \begin{pmatrix} \sqrt{2}\chi^+ \\ v + \bar{H}^0 + i\chi^0 \end{pmatrix},$$

$$\Phi_2^b = \frac{1}{\sqrt{2}} \begin{pmatrix} \sqrt{2}H^+ \\ H_1 + iH_2 \end{pmatrix}, \quad (\text{B.17})$$

where

$$\begin{aligned} \bar{H}^0 &= \cos(\alpha - \beta)H^0 - \sin(\alpha - \beta)h^0, \\ H_1 &= \sin(\alpha - \beta)H^0 + \cos(\alpha - \beta)h^0, \\ H_2 &= A^0, \end{aligned} \quad (\text{B.18})$$

and H^0, h^0, A^0 are the mass eigenstates (there is a mixing between H^0 and h^0). Since the scalar kinetic term is invariant under such rotation given in (B.3), we may identify the doublet Φ_1^b with the usual Higgs doublet of the SM. Then all fermions acquire mass by the doublet Φ_1^b through the symmetry breaking. Further the linear combination of the physical scalar fields (H^0, h^0) represented as \bar{H}^0 is equivalent to the SM Higgs particle (its couplings to vector bosons are the exact analogue of those of the SM's one and it has always flavor diagonal Yukawa couplings independent of the type of the model). As a consequence Φ_2^b is irrelevant for the symmetry breaking and responsible only for new interactions (all new scalar fields belong to the Φ_2^b doublet).

Note that the case $v_2 = 0$ is a valid solution for the minima conditions of the scalar potential and with this choice, the mixing angles vanish, $\beta = 0, \alpha = 0$. Then from (B.18) $\bar{H}^0 = H^0, H_1 = h^0$ and from (B.17) we have

$$\begin{aligned} \Phi_1^b &= \frac{1}{\sqrt{2}} \begin{pmatrix} \sqrt{2}\chi^+ \\ v + H^0 + i\chi^0 \end{pmatrix}, \\ \Phi_2^b &= \frac{1}{\sqrt{2}} \begin{pmatrix} \sqrt{2}H^+ \\ h^0 + iA^0 \end{pmatrix}, \end{aligned} \quad (\text{B.19})$$

where the mixing between the CP -even neutral scalars H^0 and h^0 disappears.

Final part of this appendix is devoted to expressing the Yukawa couplings in the quark mass basis in terms of those defined originally. Since, in this thesis, the relevant parametrization of the scalar doublets are those given in (B.19),

let us consider the Yukawa Lagrangian for Case b) as our starting point with additionally setting $v_2 = 0$ ¹

$$\begin{aligned}\mathcal{L}_Y &= \eta_{ij}^U \bar{Q}_{iL} \tilde{\Phi}_1 U_{jR} + \eta_{ij}^D \bar{Q}_{iL} \Phi_1 D_{jR} + \xi_{ij}^{U\dagger} \bar{Q}_{iL} \tilde{\Phi}_2 U_{jR} \\ &+ \xi_{ij}^D \bar{Q}_{iL} \Phi_2 D_{jR} + h.c.\end{aligned}\quad (\text{B.20})$$

With this choices of the doublets, as is stated earlier, Φ_b is responsible for generating the quark masses, thus the couplings $\eta_{ij}^{U,D}$ are only involved in this generation process. Then in the quark mass basis only the rotated couplings, denoted as $\hat{\eta}_{ij}^{U,D}$, are diagonal, while the additional rotated couplings $\hat{\xi}_{ij}^{U,D}$ are in general not.

Transition to the quark mass basis is implemented by biunitary transformations involving unitary matrices $V_{L,R}^U$ and $V_{L,R}^D$ ². The quark fields transform as

$$\begin{aligned}U_{L,R} &\rightarrow \hat{U}_{L,R} = V_{L,R}^U U_{L,R}, \\ D_{L,R} &\rightarrow \hat{D}_{L,R} = V_{L,R}^D D_{L,R}.\end{aligned}\quad (\text{B.21})$$

After the transformation defined in (B.21) FC part of the Lagrangian (B.20) becomes (since Φ_1 is identical to the SM doublet)

$$\mathcal{L}_Y^{FC} = \xi_{ij}^{U\dagger} \bar{Q}_{iL} \tilde{\Phi}_2 U_{jR} + \xi_{ij}^D \bar{Q}_{iL} \Phi_2 D_{jR} + h.c. \quad (\text{B.22})$$

Expressing (B.22) in terms of quark mass fields from (B.21) we get

$$\begin{aligned}\mathcal{L}_Y^{FC} &= \frac{1}{\sqrt{2}} \xi^{U\dagger} \left(\overline{V_L^{U\dagger} \hat{U}_L} \quad \overline{V_L^{D\dagger} \hat{D}_L} \right) \begin{pmatrix} h^0 - iA^0 \\ \sqrt{2} H^- \end{pmatrix} V_R^{U\dagger} \hat{U}_R \\ &+ \frac{1}{\sqrt{2}} \xi^D \left(\overline{V_L^{U\dagger} \hat{U}_L} \quad \overline{V_L^{D\dagger} \hat{D}_L} \right) \begin{pmatrix} \sqrt{2} H^+ \\ h^0 + iA^0 \end{pmatrix} V_R^{D\dagger} \hat{D}_R + h.c., \\ &= \frac{1}{\sqrt{2}} \{ \overline{\hat{U}_L} [V_L^U \xi^{U\dagger} V_R^{U\dagger}] \hat{U}_R (h^0 - iA^0) \\ &+ \overline{\hat{D}_L} [V_L^D \xi^D V_R^{D\dagger}] \hat{D}_R (h^0 + iA^0) \} + \overline{\hat{D}_L} [V_L^D \xi^{U\dagger} V_R^{U\dagger}] \hat{U}_R H^- \\ &+ \overline{\hat{U}_L} [V_L^U \xi^D V_R^{D\dagger}] \hat{D}_R H^+ + h.c., \\ &\equiv \mathcal{L}_{Y,Neutral}^{FC} + \mathcal{L}_{Y,Charged}^{FC},\end{aligned}\quad (\text{B.23})$$

¹ Here we drop all the superscript "b" in all terms for simplicity.

² $V_{L,R}^U$ and $V_{L,R}^D$ are defined to be the rotation matrices acting on the up-type and down-type quarks with left or right chirality respectively. They further satisfy $V_{L,R}^{U(D)} V_{L,R}^{U(D)\dagger} = I$.

where

$$\begin{aligned}
\mathcal{L}_{Y,Neutral}^{FC} &= \frac{1}{\sqrt{2}} \{ \widehat{U}_L \xi_{Neutral}^{U\dagger} \widehat{U}_R (h^0 - iA^0) \\
&\quad + \widehat{D}_L \xi_{Neutral}^D \widehat{D}_R (h^0 + iA^0) \} + h.c., \\
\mathcal{L}_{Y,Charged}^{FC} &= \widehat{D}_L \xi_{Charged}^{U\dagger} \widehat{U}_R H^- + \widehat{U}_L \xi_{Charged}^D \widehat{D}_R H^+ + h.c. \quad (B.24)
\end{aligned}$$

with

$$\begin{aligned}
\xi_{Neutral}^{U\dagger} &= V_L^U \xi^{U\dagger} V_R^{U\dagger}, \quad \xi_{Neutral}^D = V_L^D \xi^D V_R^{D\dagger}, \\
\xi_{Charged}^{U\dagger} &= V_L^D \xi^{U\dagger} V_R^{U\dagger}, \quad \xi_{Charged}^D = V_L^U \xi^D V_R^{D\dagger}. \quad (B.25)
\end{aligned}$$

Then the charged couplings can also be express in terms of neutral ones of the form

$$\begin{aligned}
\xi_{Charged}^D &= V_L^U \xi^D V_R^{D\dagger}, \\
&= V_L^U (V_L^{D\dagger} V_L^D) \xi^D V_R^{D\dagger}, \\
&= (V_L^U V_L^{D\dagger}) V_L^D \xi^D V_R^{D\dagger}, \\
&= V_{CKM} (V_L^D \xi^D V_R^{D\dagger}), \\
&= V_{CKM} \xi_{Neutral}^D, \\
(\xi_{Charged}^{U\dagger})^\dagger &= (V_L^D \xi^{U\dagger} V_R^{U\dagger})^\dagger, \\
\xi_{Charged}^U &= V_R^U \xi^U V_L^{D\dagger}, \\
&= V_R^U \xi^U (V_L^{U\dagger} V_L^U) V_L^{D\dagger}, \\
&= V_R^U \xi^U V_L^{U\dagger} (V_L^U V_L^{D\dagger}), \\
&= (V_R^U \xi^U V_L^{U\dagger}) V_{CKM}, \\
&= \xi_{Neutral}^U V_{CKM}, \quad (B.26)
\end{aligned}$$

where $V_{CKM} \equiv V_L^U V_L^{D\dagger}$ is the CKM mixing matrix.

APPENDIX C

THE FEYNMAN PARAMETRIZATION

In calculating loop integrals the Feynman parametrization is usually very useful. The idea is to put the denominator factors of a vertex function into a single quadratic polynomial in loop integral variable by introducing some auxiliary parameters to be integrated over. Let us first present the most general form of the Feynman parametrization,

$$\prod_{i=1}^n \frac{1}{A_i^{\beta_i}} = \frac{\Gamma(\beta)}{\prod_{i=1}^n \Gamma(\beta_i)} \int_0^1 \left[\prod_{i=1}^n dx_i x_i^{\beta_i-1} \right] \frac{\delta(1-x)}{[\sum_{i=1}^n x_i A_i]^\beta}, \quad (\text{C.1})$$

where $\Gamma(\beta_i)$ is the gamma function, $\beta_i, i = 1, 2, \dots, n$ are arbitrary complex numbers, and $\beta \equiv \sum_{i=1}^n \beta_i$ and $x \equiv \sum_{i=1}^n x_i$. It is now useful to give two simpler cases of two and three factors in denominator of any vertex function appearing in all loop calculations, since up to one loop level they are the only structures encountered in calculations. They read from (C.1) for $n = 2$ and $n = 3$ respectively

$$\begin{aligned} \frac{1}{AB} &= \int_0^1 dx \frac{1}{[xA + (1-x)B]^2}, \\ \frac{1}{ABC} &= 2 \int_0^1 dx \int_0^{1-x} dy \frac{1}{[xA + yB + (1-x-y)C]^3}. \end{aligned} \quad (\text{C.2})$$

As an application some specific examples can be given here. To this aim, let us apply the method to the calculation of the effective vertex function for the decay $Z \rightarrow l_1^- l_2^+$ considered in chapter 4 (see Eq. (4.24)). If one looks the terms in the denominator of Γ_{ab}^μ , the form is

$$\frac{1}{[(p_{1(2)} + q)^2 - m_i^2](q^2 - m_\alpha^2)}, \quad (\text{C.3})$$

where $i = e, \mu, \tau$. For this piece the integral with only $n = 2$ case is relevant and by setting $A \equiv (p_{1(2)} + q)^2 - m_i^2$ and $B \equiv q^2 - m_\alpha^2$ we have

$$\frac{1}{[(p_{1(2)} + q)^2 - m_i^2](q^2 - m_\alpha^2)} = \int_0^1 \frac{dx}{[x((p_{1(2)} + q)^2 - m_i^2) + (1-x)(q^2 - m_\alpha^2)]^2}. \quad (\text{C.4})$$

Then the common expression in the denominator of Γ_{ab}^μ becomes

$$\begin{aligned} D_{1(2)}^{self} &\equiv x(p_{1(2)}^2 + q^2 - 2q \cdot p_{1(2)} - m_i^2) + (1-x)q^2 - m_\alpha^2(1-x) \\ &= (q - xp_{1(2)})^2 - m_{l_{1(2)}}^2 x^2 + (m_{l_{1(2)}}^2 - m_i^2)x - m_\alpha^2(1-x), \end{aligned} \quad (\text{C.5})$$

where the on-shell condition for external leptons, $p_{1(2)}^2 = m_{l_{1(2)}}^2$, was used. Now by shifting q to complete the square as $k_{1(2)} \equiv q - xp_{1(2)}$ we get

$$D_{1(2)}^{self} = k_{1(2)}^2 - L_{1(2),\alpha}^{self}, \quad (\text{C.6})$$

with

$$L_{1(2),\alpha}^{self} \equiv m_\alpha^2(1-x) + [m_i^2 - m_{l_{1(2)}}^2(1-x)]x. \quad (\text{C.7})$$

If one looks the structures in the denominator of Γ_{cd}^μ (see Eq. (4.24)), there are three factors which can be again combined by using integral over Feynman parameters ($n = 3$). For the term coming from triangular diagram (c) in Fig. (4.1), with setting $A \equiv (p_1 + q)^2 - m_i^2$, $B \equiv (p_2 + q)^2 - m_i^2$ and $C \equiv q^2 - m_\alpha^2$, the denominator, called $D_{c(\alpha)}^{ver}$, can be formed as

$$\begin{aligned} D_{c(\alpha)}^{ver} &= xA + yB + (1-x-y)C, \\ &= x(q^2 + 2q \cdot p_1 + m_{l_1}^2 - m_i^2) + y(q^2 + 2q \cdot p_2 + m_{l_2}^2 - m_i^2) \\ &+ (1-x-y)(q^2 - m_\alpha^2), \\ &= k_c^2 - L_{c(\alpha)}^{ver}, \end{aligned} \quad (\text{C.8})$$

where we set $k_c \equiv q + xp_1 + yp_2$ and $L_\alpha^{ver} \equiv m_\alpha^2(1-x-y) + m_i^2(x+y) - Q^2xy$ with the assumption that mass squares of the final leptons are negligible. Here $Q^2 = (p_1 - p_2)^2$ is the momentum transfer squared. Finally the denominator belonging to diagram (d) in Fig. (4.1) is

$$D_{(\alpha\beta)}^{ver} = k_d^2 - L_{d(\alpha\beta)}^{ver}, \quad (\text{C.9})$$

where in this case $k_d \equiv q - xp_1 - yp_2$ and $L_{\alpha\beta}^{ver} \equiv m_\beta^2 x + m_i^2 (1 - x - y) - (m_\alpha^2 - Q^2 x)y$.

Now all the bracket quantities in the denominators turn into a quadratic function of the shifted integration variables as of the form $(k^2 - L)^n$, $n = 2, 3$. Then it is much easier to evaluate the remaining spherically symmetric integral without difficulty.

APPENDIX D

DIMENSIONAL REGULARIZATION

In this appendix we present some basics of one of the regularization methods, so called *dimensional regularization* due to 't Hooft and Veltman [?]. Even though one can make any physical quantity divergent free by means of any suitable renormalization program, we still need to deal with some divergent integrals at any intermediate state. Any mathematical prescription introduced in order to render the divergent Feynman integrals finite is generically called regularization. It is a purely mathematical tool and has no physical consequences. Thus any physical result should be independent of the regularization scheme chosen.

Several schemes have been devised. Among them, one of the most conservative ones is dimensional regularization¹. The basic idea of dimensional regularization is simply to state that we compute the Feynman diagram as an analytic function of the dimensionality of space-time d lower than four and any loop-momentum integral will converge for sufficiently small d . The final expression for any observable should have a well defined limit as $d \rightarrow 4$. In fact, to make the behavior of the result of the loop integral evident, a new parameter $\epsilon = 4 - d$ is defined and the expressions are expanded in ϵ , keeping only pole and finite parts separately. Once adding all possible diagrams contributing to the observable quantity, the ϵ -pole has to cancel. For a review see [107]. It is better to stress that some care has to be given to the algebra in d -dimensions and let us note the following

¹ What we mean by calling 'conservative' for a regularization scheme is that after applying the regularization scheme the theory should preserve as many physical laws as possible. In dimensional regularization none of the physical requirements has been violated except that space-time has a dimension d lower than 4.

remarks. All the space-time index μ in this case runs from 0 to $d - 1$ so that components of a momentum vector k^μ are

$$k^\mu = (k^0, k^1, \dots, k^{d-1}), \quad (\text{D.1})$$

and the trace of the metric tensor is now

$$g^\mu_\mu = g_{\mu\nu} g^{\mu\nu} = d. \quad (\text{D.2})$$

The Dirac algebra in d -dimensions is unchanged except the modification in (D.2). Thus we can simply write the followings

$$\begin{aligned} \{\gamma^\mu, \gamma^\nu\} &= 2g^{\mu\nu}, \\ \gamma_\mu \gamma^\mu &= d, \\ \gamma_\mu \gamma_\nu \gamma^\mu &= (2 - d) \gamma_\nu. \end{aligned} \quad (\text{D.3})$$

Since there are more than one way to generalize identities to d dimensional space-time, we need to fix our convention. Throughout in all calculations the following convention was used

- The metric in d-dimension is $g^{\mu\nu} = \{+, -, \dots, -\}$.
- The integral measure is chosen as $\int \frac{d^d k}{(2\pi)^d}$.
- The trace of the γ matrices is normalized to $\text{Tr}[\gamma_\mu \gamma_\nu] = 4 g_{\mu\nu}$.
- γ_5 is an object² satisfying $\{\gamma^\mu, \gamma_5\} = 0$, $\gamma_5^2 = 1$, $\gamma_5^\dagger = \gamma_5$.

Having expressed any vertex function including loop contributions, with the help of the Feynman parametrization method discussed in appendix C, the factors in denominator of the function will take a quadratic form in the integration variable k'^μ . This term can be a complete square by redefining the integral variable and call k^μ . The denominator eventually takes the form $(k^2 - L)^n$ where n

² Since there is no mathematically consistent generalization of γ_5 in arbitrary dimensions, instead of trying to drive an explicit formula for γ_5 we rather require the existence of such quantity which satisfies the requirements given above.

is an integer. Then from the fact that in dimensional regularization we break none of the symmetries of space-time, any integral of an odd function in k vanishes,

$$\int d^d k k_\mu f(k^2) = 0, \quad (\text{D.4})$$

where $f(k^2)$ is an integrable function of k^2 . Further, unbroken symmetries allows one to replace the following identities

$$\begin{aligned} k^\mu k^\nu &\rightarrow \frac{1}{d} k^2 g^{\mu\nu}, \\ k^\mu k^\nu k^\alpha k^\beta &\rightarrow \frac{1}{d(d+2)} (k^2)^2 [g^{\mu\nu} g^{\alpha\beta} + g^{\mu\alpha} g^{\nu\beta} + g^{\mu\beta} g^{\nu\alpha}]. \end{aligned} \quad (\text{D.5})$$

Then one-loop momentum integrals can easily be computed with the help of the following d -dimensional integrals in Minkowski space, quoted from the reference [108]:

$$\begin{aligned} \int \frac{d^d k}{(2\pi)^d} \frac{1}{(k^2 - L)^n} &= \frac{(-1)^n i}{(4\pi)^{d/2}} \frac{\Gamma(n - \frac{d}{2})}{\Gamma(n)} \left(\frac{1}{L}\right)^{n - \frac{d}{2}}, \\ \int \frac{d^d k}{(2\pi)^d} \frac{k^2}{(k^2 - L)^n} &= \frac{(-1)^{n-1} i}{(4\pi)^{d/2}} \frac{d}{2} \frac{\Gamma(n - \frac{d}{2} - 1)}{\Gamma(n)} \left(\frac{1}{L}\right)^{n - \frac{d}{2} - 1}, \\ \int \frac{d^d k}{(2\pi)^d} \frac{k^\mu k^\nu}{(k^2 - L)^n} &= \frac{(-1)^{n-1} i}{(4\pi)^{d/2}} \frac{g^{\mu\nu}}{2} \frac{\Gamma(n - \frac{d}{2} - 1)}{\Gamma(n)} \left(\frac{1}{L}\right)^{n - \frac{d}{2} - 1}, \\ \int \frac{d^d k}{(2\pi)^d} \frac{(k^2)^2}{(k^2 - L)^n} &= \frac{(-1)^n i}{(4\pi)^{d/2}} \frac{d(d+2)}{4} \frac{\Gamma(n - \frac{d}{2} - 1)}{\Gamma(n)} \left(\frac{1}{L}\right)^{n - \frac{d}{2} - 2}, \\ \int \frac{d^d k}{(2\pi)^d} \frac{k^\mu k^\nu k^\alpha k^\beta}{(k^2 - L)^n} &= \frac{(-1)^n i}{(4\pi)^{d/2}} \frac{\Gamma(n - \frac{d}{2} - 2)}{\Gamma(n)} \left(\frac{1}{L}\right)^{n - \frac{d}{2} - 2} \\ &\quad \times \frac{1}{4} (g^{\mu\nu} g^{\alpha\beta} + g^{\mu\alpha} g^{\nu\beta} + g^{\mu\beta} g^{\nu\alpha}), \end{aligned} \quad (\text{D.6})$$

where $\Gamma(n)$ is the Gamma function. Since $n = 2$ and 3 cases have been encountered commonly, it is better to give expansion of the terms (D.6) as $d \rightarrow 4$. The behavior near $d=4$ can be readily extracted by expanding the factors in the right hand side of (D.6) as

$$\begin{aligned} \left(\frac{1}{L}\right)^{2 - \frac{d}{2}} &= 1 - \frac{\epsilon}{2} \ln L + \dots, \\ \Gamma\left(2 - \frac{d}{2}\right) &= \frac{2}{\epsilon} - \gamma + \mathcal{O}(\epsilon), \quad \text{as } \epsilon \rightarrow 0, \end{aligned} \quad (\text{D.7})$$

where $\epsilon \equiv 4-d$ and γ is the Euler–Mascheroni constant, $\gamma = 0.5772$. Then the combination of these factors gives

$$\frac{\Gamma(2 - \frac{d}{2})}{(4\pi)^{d/2}} \left(\frac{1}{L}\right)^{2 - \frac{d}{2}} = \frac{2}{\epsilon} - (\ln L + \gamma - \ln 4\pi) + \mathcal{O}(\epsilon) \quad (\text{D.8})$$

where it apparently reflects its singular nature as $\epsilon \rightarrow 0$ ($d \rightarrow 4$). However addition of all possible diagrams contributing the process considered make the coefficient of $1/\epsilon$ zero.

VITA

İsmail Turan was born in 1975 in Gölpazarı, Bilecik. He graduated with a Bachelor of Science degree in Physics from the Middle East Technical University in 1997. He acquired his M.S. degree in High Energy Physics in 1999 at METU. His master thesis title is *The Faddeev-Jackiw Quantization of the $U(1)$ Gauged $SU(2)$ WZW Model*. Presently, he works as a research assistant in the Physics Department, METU, Ankara.